NASA CR-374

FINAL REPORT FOR A BRUSHLESS D. C. TORQUE MOTOR

By W. W. Yates and R. E. Skamfer

Prepared under Contract No. NAS 5-3934 by
WESTINGHOUSE ELECTRIC CORPORATION
Lima, Ohio

for Goddard Space Flight Center

NATIONAL AERONAUTICS AND SPACE ADMINISTRATION

For sale by the Clearinghouse for Federal Scientific and Technical Information
Springfield, Virginia 22151 – Price $4.00

ABSTRACT

16089

The object of this report is to provide a comprehensive record of the work performed on NASA Contract NAS 5-3934. This contract covered the development of a brushless d-c torque motor having characteristics similar to a conventional permanent magnet torque motor for operation in a vacuum.

The approach used in the design utilized a permanent magnet rotor and a 3-phase winding in a stationary armature. Magnetic pickup windings in an auxiliary reluctance switch sensed rotor position. The output of these sensing windings was used to drive transistors which provided power to the armature.

The test results indicated very good agreement with calculations except for ripple torque and weight. The motor weighed approximately 10 percent higher than the calculated weight. The ripple torque could be improved considerably in future designs.

Author

TABLE OF CONTENTS

LIST OF FIGURES

LIST OF TABLES

I. INTRODUCTION

This report provides a comprehensive record of the work performed on NASA Contract NAS5-3934 - Brushless D.C. Torque Motor. It covers the period from June 25, 1964 to June 25, 1965, the completion date of the contract.

The purpose of this research effort as stated in NASA Specification #63-135 dated November 15, 1963, is to design and develop a brushless d-c torque motor having performance characteristics similar to those of a conventional permanent-magnet d-c torque motor. The developed motor was to be designed for high torqueing sensitivity, high no-load running efficiency, and minimum size and weight. The motor must be capable of operating in a vacuum at 1×10^{-9} mm Hg for one year in an ambient range of -10°C to +70°C. A 50 g, 2 msec shock and 5 minutes of random vibration from 20 to 2000 cycles per second at 15 g's rms in each of three mutually perpendicular directions must be withstood. It is also desirable that the commutator be sufficiently versatile to permit shaft position control and speed control using both excitation level and pulse modulation systems. Two engineering models were to be built and shipped to NASA.

The torque motor may properly be divided into three systems which form separate design entities although interrelated in function and interdependent in operation. These are the permanent-magnet motor itself, the rotor-position-sensing device, and the electronic control. The permanent-magnet motor consists of a rotating permanent-magnet field and a stationary armature. The position of the rotating field magnet in relation to its armature field is sensed by the rotor-position-sensing device. This device transmits the position information to the electronic control. The control uses transistor switches to change the position of the armature field in order to maintain torque as the position of the rotating field changes. The details of these three systems will be covered in the discussion.

As of the end of the reporting period, work on the contract has been completed and the two engineering models have been shipped. Tests are complete and the results are recorded in this report. The results show a high level of agreement with calculated data. Unequal voltages from the reluctance switch secondaries caused higher ripple torque than calculated. Circuit modifications in future designs would lower the ripple torque considerably.

II. DISCUSSION

A. General Approach

Various types of brushless d-c motors were considered for this application. One type was an extremely slow speed synchronous (reluctance or permanent-magnet) motor excited from an inverter. This motor would exhibit a high ripple torque and would be subject to pulling out of step if pull-out torque is exceeded. Another approach considered was the use of an induction motor with an inverter combined with the motor stator. The performance of this motor would have the characteristic of an a-c motor.

In order to duplicate the characteristics of a conventional permanent-magnet d-c torque motor with a brushless d-c motor, it is necessary to sense rotor position. A true d-c characteristic is obtained by sensing the rotor position and switching stationary armature circuits in proper relation to a moving permanent-magnet field. The function of the commutator and brushes can be duplicated in a motor by a solid state, electronic switching system. The result is a brushless d-c motor without the deficiencies of a mechanical commutator. A schematic representation of this approach is shown in Figure 1.a. A photograph of the actual motor and control constructed is shown in Figure 1.b.

The brushless motor uses a permanent-magnet rotor for field excitation and a slotted stator with a conventional three-phase induction motor winding for the armature field. The current in the armature is switched by a solid state three-phase bridge switching network. Switching logic and rotor position sensing for the commutation process is accomplished by using a reluctance switch. The drive power for the reluctance switch is obtained from an oscillator which is powered from a constant 28 volt d-c source. A second reluctance switch is provided to obtain reverse rotation.

By using an element (reluctance switch rotor) which continuously detects the angular position of a permanent-magnet torque rotor with respect to its stator poles, a torque motor can be developed which has complete angular freedom. Thus, the shaft can furnish torque in appreciable magnitude while rotating or while in a locked position.

The variation in magnitude of the output signal obtained from the reluctance switch occurs over a period of time which is comparatively lengthy as contrasted to the high speed switching capability of semiconductor devices. It is therefore necessary in this application to provide a circuit that will detect the output voltage level and provide a digital response at a predetermined value. This will insure that the power transistors do not operate in a partially "on" state and improve the circuit efficiency.

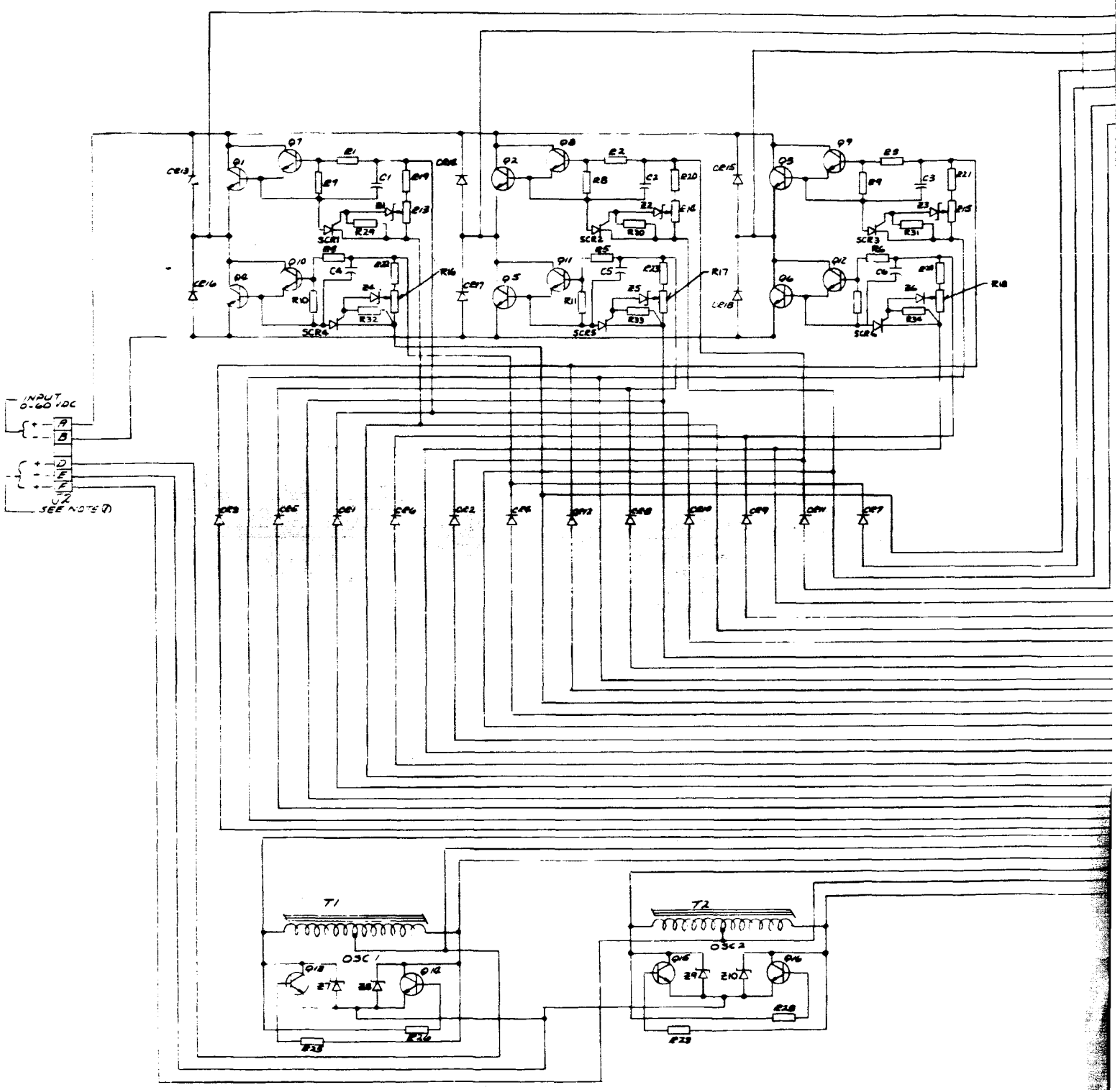

FIGURE 1.a. Schematic Diagram - Torque Motor and Commutator

#1

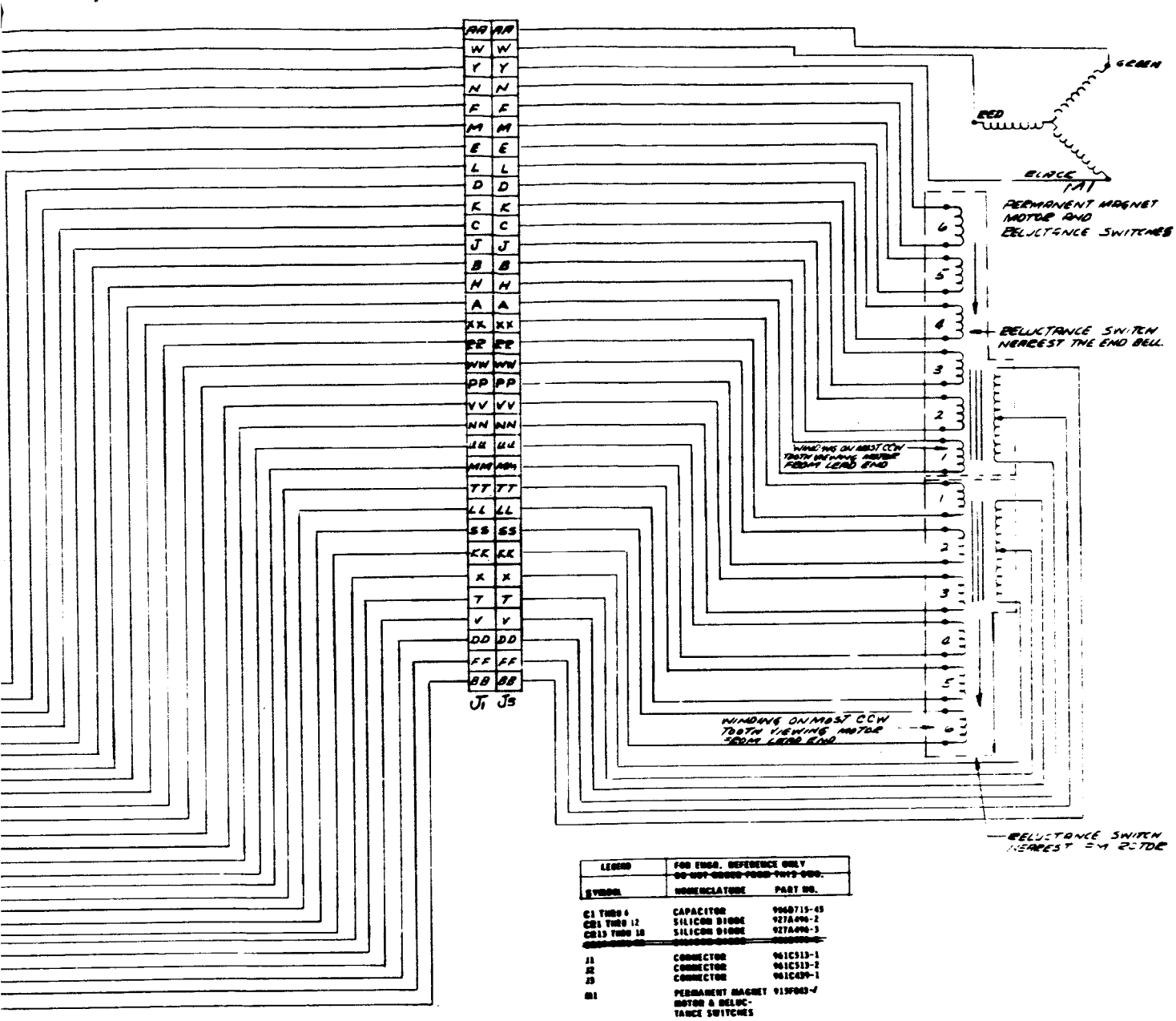

LEGEND	FOR ENGR. REFERENCE ONLY DO NOT CHANGE FROM THIS DWG.	
SYMBOL	NOMENCLATURE	PART NO.
C1 THRU 6	CAPACITOR	9960715-45
CR1 THRU 12	SILICON DIODE	927A496-2
CR13 THRU 18	SILICON DIODE	927A496-3
J1	CONNECTOR	961C513-1
J2	CONNECTOR	961C513-2
J3	CONNECTOR	961C439-1
M1	PERMANENT MAGNET MOTOR & RELUCTANCE SWITCHES	915F043-1
Q1 THRU 6	TRANSISTOR	9216091-1
Q7 THRU 16	TRANSISTOR	914F290-1
R1 THRU 6	RESISTOR	914F240-17
R7 THRU 12, R19 THRU 24	RESISTOR	920A736-17
R13 THRU 18	POTENTIOMETER	9960949-10
R25 THRU 28	RESISTOR	P10CT598-52
SCR1 THRU 6	SILICON CONTROLLED RECTIFIER	9870957-7
T1, 2	TRANSFORMER	9618080-1
Z1 THRU 6	ZENER DIODE	939D464-22
Z7 THRU 10	ZENER DIODE	939D464-23
R29 THRU 34	RESISTOR	P18D3546-12

NOTE 2) APPLY A 28VDC SIGNAL BETWEEN PINS D AND E OR PINS F AND E TO OBTAIN FORWARD AND REVERSE ROTATION -- CAUTION: DO NOT APPLY VOLTAGE TO BOTH SETS OF TERMINALS AT THE SAME TIME.

#2

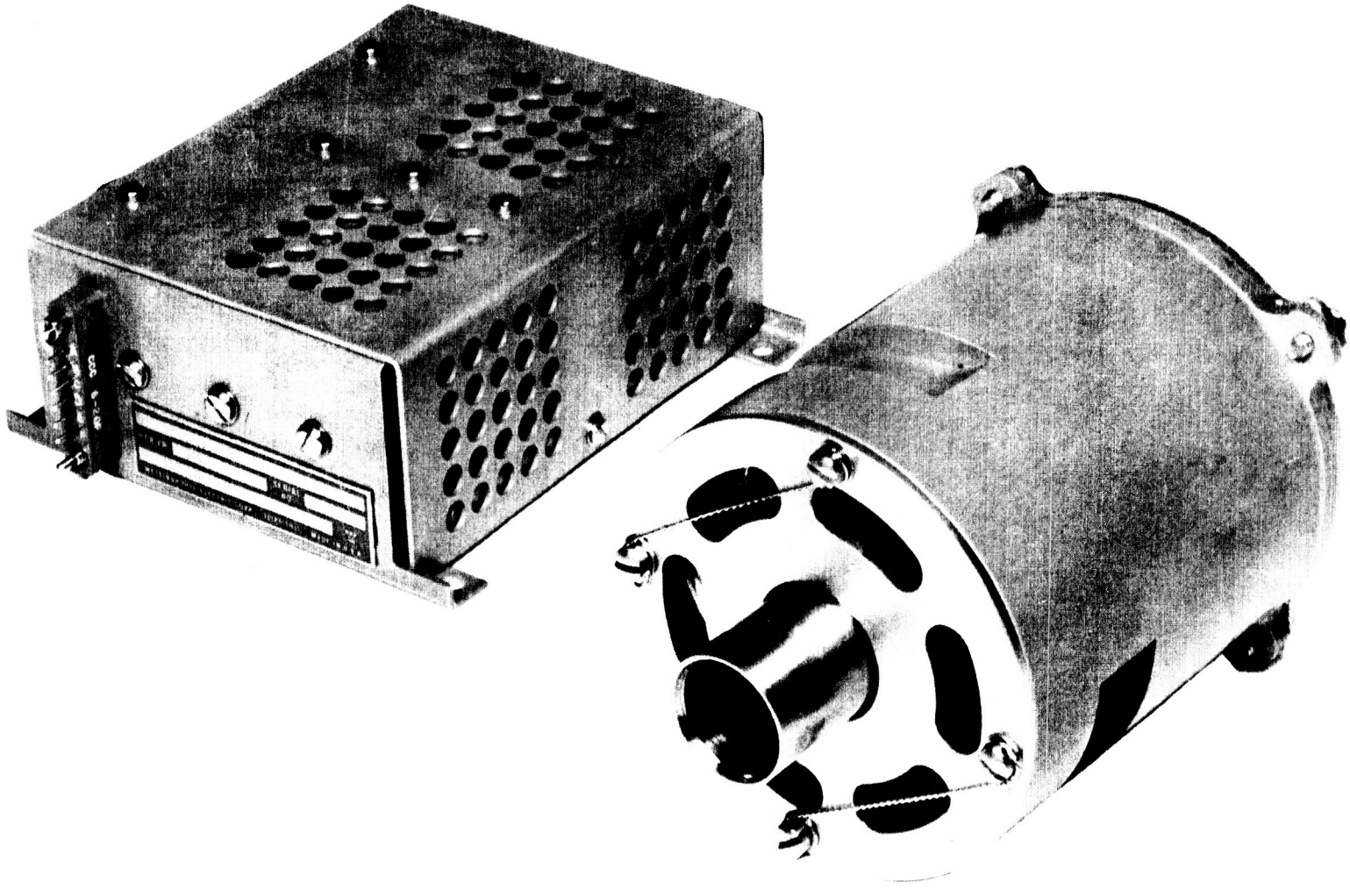

FIGURE 1.b. Motor and Control Photograph

B. Specific Design

1. Electrical Design of PM Torque Motor

a. General

The following items of NASA Specification #63-135 were considered in the electrical design of the permanent-magnet motor.

(1) The torque motor must be as small and as light-weight as possible, not to exceed 3.5 inches in diameter and 2 pounds weight (exclusive of commutating circuitry). (The preliminary design indicated that the combined motor and reluctance switches would weigh approximately 2.7 pounds. The final design weight was 3.1 pounds.)

(2) The torque motor must develop the maximum possible shaft torque, not to be less than 100 in-oz at 40 VDC excitation.

(3) The torque motor must not draw more than 1 ampere of current at a stall torque of 100 in-oz.

Since the requested weight would obviously be exceeded, it was felt that the stall torque requirement of 100 in-oz at 40 VDC and 1 ampere should be taken as nominal (calculated performance rather than minimum performance. In the design, the size of the motor was increased until, with a calculated 1 ampere flowing at 40 VDC, the calculated stall torque was 100 in-oz. The calculation accuracy can not be ascertained until the unit is built and tested.

(4) The torque motor must be capable of continuous operation at speeds up to 100 RPM.

(5) The no-load speed of the torque motor must be approximately 30 RPM with 3 VDC excitation at the armature terminals.

Since the speed at 3 VDC would depend to a large extent on the bearing friction (which is not accurately known) the no-load speed must be determined by test. No attempt was made to calculate this condition.

(6) The torque motor no-load running losses must be as small as possible, not to exceed 0.5 watts at 30 RPM.

(7) The peak-to-peak ripple torque at constant armature voltage, as a function of rotor angular position, must be as low as possible, not to exceed 10 percent of the average torque or 0.5 in-oz, whichever is larger.

There is a large inherent ripple in the three-segment winding chosen for the armature because of the alternate use of two and three legs of the winding. It is difficult to obtain a value for ripple torque analytically. A graphical procedure was used which gave a value of 11.8 percent.

(8) The torque motor static friction torque must be as small as possible, not to exceed 0.5 in-oz for any position of the torquer.

This also is a parameter which cannot be determined except by test. The bearings to be used are solid lubricant bearings to be fabricated by the Westinghouse Research Laboratories using relatively new lubricating materials.

(9) The torque motor and drive circuitry must be able to withstand continuous stall current at 60 VDC excitation without damage or deterioration of performance.

(10) The torque motor and commutator must be capable of operating in a vacuum of 1×10^{-9} mm Hg for a 1 year period.

(11) The torque motor and commutator must operate properly over an ambient temperature range of -10°C to +70°C.

b. Consideration of Ripple Torque and Effective Conductors

The circuit of the armature is identical to a Y-connected, 3-phase, induction motor. A delta connection could be used, but the only difference would be that more turns per coil of a smaller wire size would have to be used. The switching is such that the three phases of the winding are alternately connected as shown in Figure 2, having for the first connection one phase connected in series with the other two in parallel. The second connection has two phases connected in series with the third phase disconnected.

The standard formula for torque of ordinary DC motors is

$$\text{Torque (oz-in)} = \frac{(22.6)(p)(\phi)(Z)(I_a)}{(pp)} \; 10^{-8}$$

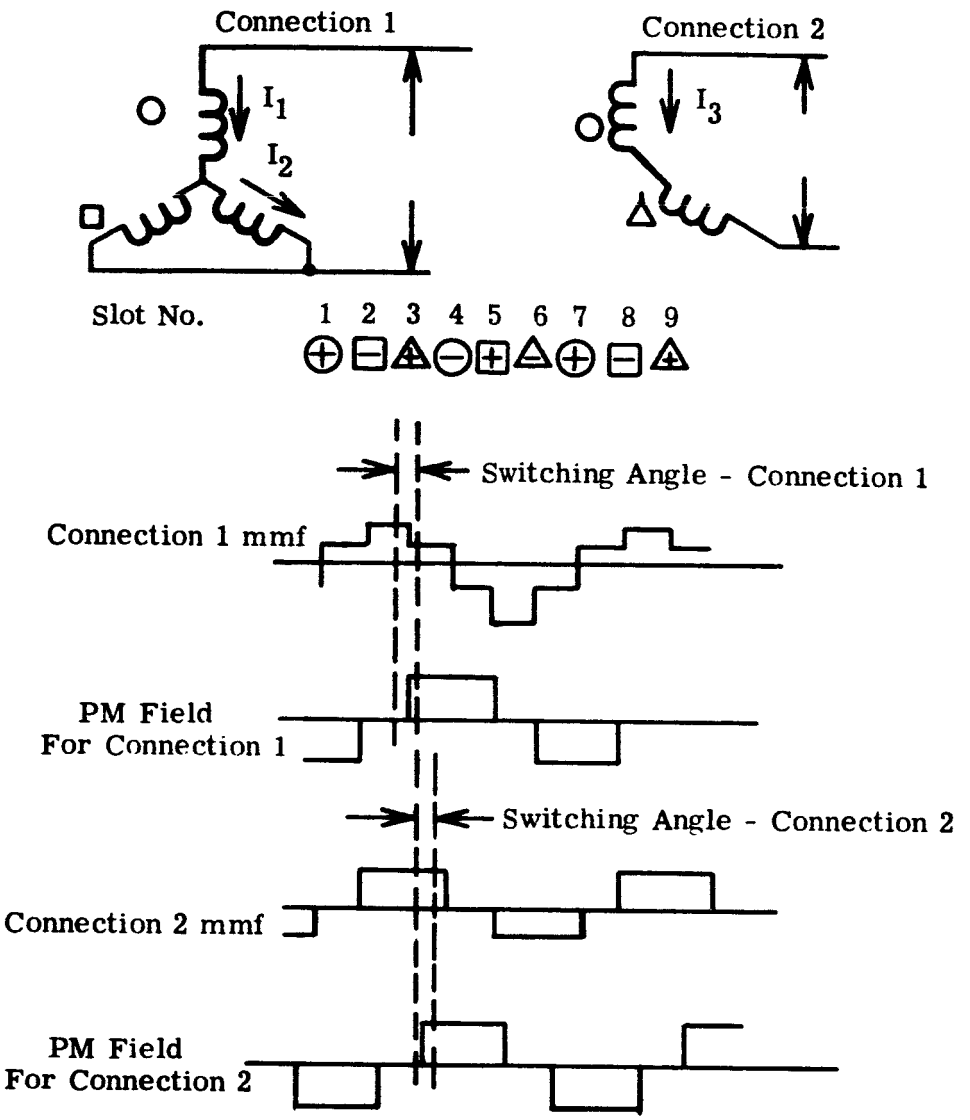

FIGURE 2. Connection and Magnet Lineup Diagram

Where
p = Number of poles
$\emptyset$ = Flux in lines per pole
Z = Total series conductors
I_a = Armature current
(pp) = Number of parallel paths

A more basic torque formula is

$$\text{Torque} = KBI_aZ$$

Where
K = Constant
B = Flux density perpendicular to conductors

Comparing the two equations, it may be understood that the first equation is based on having a square wave of flux density which links all the series conductors, Z. These conductors all carry I_a current. If the flux density is something other than a square wave, that is, a shorter wave with a higher flux density, it is taken care of in the formula by the fact that less conductors are linked. However, with the winding in question, in some instances, all of the conductors do not carry the same current nor are they all linked by the same flux density. It is therefore necessary to make some analysis to determine the effective conductors Z for the winding.

It was determined that a graphical procedure could be used in conjunction with the second equation assuming resistance limited currents (locked rotor).

Assume

1. A total flux per pole of 1 per unit.
2. This total flux gives an average density (square wave) of 1 per unit.
3. With the phases connected as shown in position 1 of Figure 1, I_1 = 1 per unit.
4. Rph - hot resistance per phase = 1 per unit.

Then for a quasi-square wave of flux density (120° conduction), which is what would be obtained, disregarding fringing flux, with a 0.667 pole enclosure, the peak density would be 1.5 per unit,

since the same flux must be crowded into an area which is 2/3 of the total. If I_1 is equal to 1 per unit, I_2 (see Figure 1) is equal to 0.5 per unit. The total per unit resistance of the connection 1 circuit is 1.5; the total for connection 2 is 2; therefore $I_3 = 1.5/2 = 0.75$ per unit.

Figure 1 also shows mmf plots for the two connections assuming a winding having one slot per phase per pole. The field corresponding to the magnet is shown located 90 electrical degrees from the armature field which is the theoretical position of maximum torque. A 0.667pole enclosure is assumed. The field magnet will vary its position in relation to the armature over a switching angle. This is 30 electrical degrees which is indicated by the dashed lines.

The per unit torque can then be found by applying the second equation on a per unit basis for each conductor and adding the results. For connection 1, assume that at the midpoint of the switching angle, the PM field half links conductors 3 and 5 and totally links conductor 4. Attention must be paid to the direction of the torque in the following analysis.

Per unit torque = BIZ

= (1.5)(1) + (2)(0.75)(0.5) = 2.25 for the three conductors. Since the situation around the stator is symmetrical, the total per unit torque = 2.25 Zph.

Where Zph = Series conductors per phase

In a similar manner for connection 2, conductors 4 and 5 only are linked giving

Per unit torque = (1.5)(0.75)(2)Zph = 2.25 Zph

Therefore, it would appear that the effective conductors to be used in Equation 1 should be 2.25 Zph with I_a determined using position 1. However, the assumption of one-half linkage of conductors 3 and 5 with connection 1 is false. It would appear that a more likely assumption would be that these conductors are not linked at all because of the slot opening. This would give a per unit torque for connection 1 of (1.5)(1)Zph = 1.5 Zph which not only would lower the average effective conductors, but would give an extremely high ripple torque. It is necessary to consider ways of lowering this ripple torque.

Obviously, lowering the slot opening would help. Therefore, the slot opening was held to a minimum practical which was considered to be 0.05. Increasing the pole enclosure was considered, but this would increase flux leakage in the magnet unless pole shoes were used which would entail a significant sacrifice in performance.

It was decided to investigate the effect of skew. By way of illustration, the procedure was performed on a winding having one slot per phase per pole for both 30 and 60° skew. Figure 3 shows a planar developed view of several slot openings of the stator with the skewed magnet rotor superimposed on top of them in various positions corresponding to the switching angle. The figure is drawn to angular scale.

NOTE: Angles are in electrical degrees
Dashed lines for 30° skew
Solid lines for 60° skew

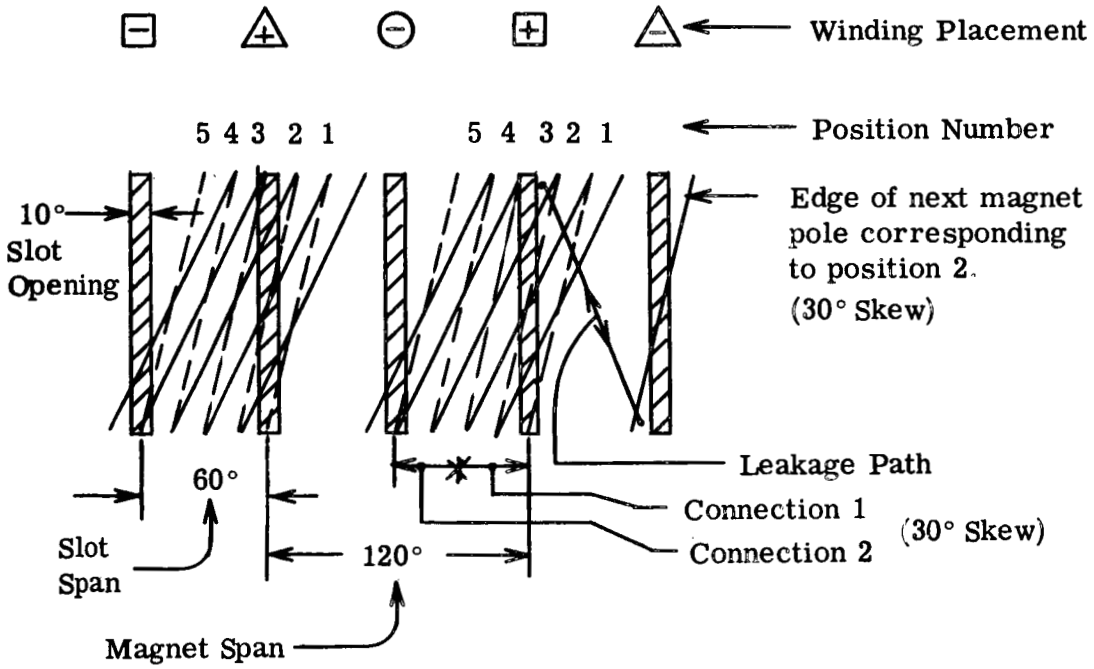

FIGURE 3. Layout for Illustration of Skew Effect

The peak quasi-square wave density was considered to link a conductor only to the extent that the PM linked the steel of the tooth on the outside (related to the magnet) of the conductor. The slot opening was assumed to be 10 degrees. Positions 1, 2 and 3 are related to connection 1. Positions 3, 4 and 5 are related to connection 2. (See Figure 1.)

Connection 1

Position 1

Conductor 4 is approximately 90% linked
Conductor 3 is 100% linked
Conductor 2 is not linked

Peak Density = 1.5 per unit
Current = 1 per unit in conductor 3, 0.5 in conductors 2 and 4
Per Unit Torque = (1.5)(1)Zph + (1.5)(0.5)(0.9)(Zph)

= 2.175 Zph

Position 2

Conductors 4 and 2 are approximately 40% linked
Conductor 3 is 100% linked

Torque = (1.5)(1)Zph + (1.5)(0.5)(0.4)(2)Zph = 2.1 Zph

Position 3

Conductor 4 is not linked
Conductor 3 is 100% linked
Conductor 2 is 90% linked

Torque = 2.175 Zph

Connection 2

Position 3

Conductor 4 is not linked
Conductor 3 is 100% linked
Conductor 2 is 90% linked

Current = 0.75 in conductors 3 and 2, 0 in conductor 4

Torque = (1.5)(0.75)(1.9) Zph = 2.14 Zph

Position 4

Conductors 2 and 3 are 100% linked

Torque = 2.25 Zph

Position 5

Same as position 3

Torque = 2.14 Zph

Average torque = 2.17 Zph

Ripple peak-to-peak = 2.25 - 2.1 = 0.150

$$\% \text{ Ripple} = \frac{(0.150)(100)}{2.17} = 6.92\%$$

A similar calculation for a 60° skew showed that the ripple would be much higher.

The edge of the next magnet pole corresponding to position 2 is also shown on Figure 3. A major flux leakage path in the tooth-face is indicated due to the skew. Consequently, if skew is used, a winding having 2 slots per phase per pole should be used to break up the leakage path shown.

Therefore, it was decided to try a 48 slot, 8 pole winding with the rotor skewed 30 electrical degrees. A preliminary design indicated that a stator inside diameter of 2 inches would be close. Therefore, a 48 slot stator punching (same as that shown in Figure 4) with a 2 inch inside diameter and a slot opening of 0.05 was laid out with the winding placed in the slots having the winding direction indicated by + or - signs. A movable rotor was made similar to that shown. By rotating the rotor to positions corresponding to the extremes and the middle of the switching angle for both connections, the effective conductors and the ripple were determined using the procedures previously described.

Also examined by the same procedure were a 48 slot, 8 pole winding short-chorded by one slot with 1 slot skew and a 36 slot (fractional-slot) 8 pole winding wound full pitch with a half slot skew.

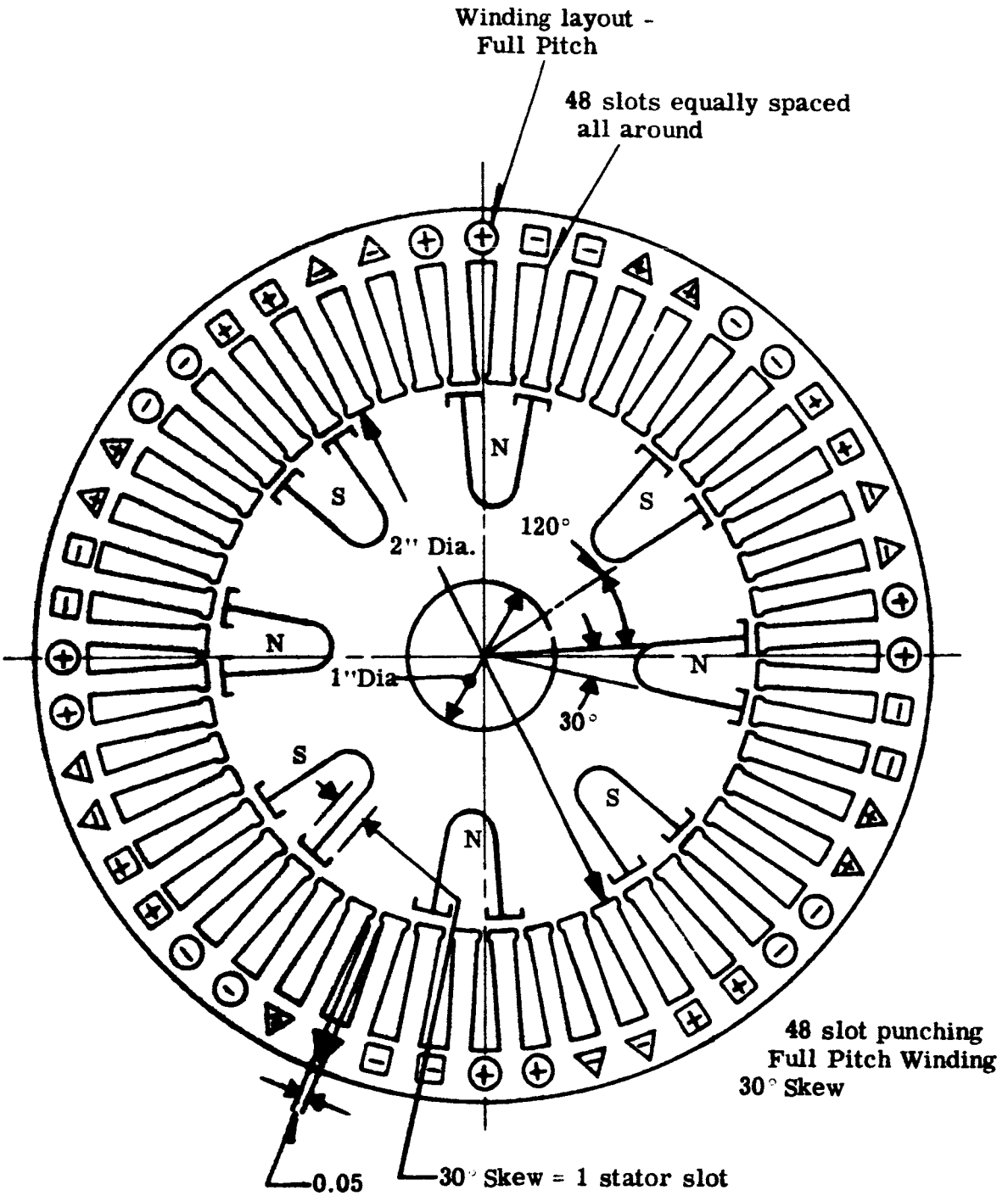

FIGURE 4. Layout for Ripple Determination

The results are tabulated below.

Type	Average Effective Conductors	Peak-to-peak Ripple Torque
48 slot - Full Pitch	2.05	12.8%
48 slot - Short Chord	1.956	19.3%
36 slot	1.90	16.1%

It was concluded from the above that a winding wound full pitch, having 2 slots per phase per pole, and having 30 electrical degrees skew would give the least ripple. Therefore, these parameters were used to design the PM motor.

It was noticed on the completed motor that severe reluctance cogging existed between the permanent magnet rotor and the motor stator. A crude measurement of the torque gave 15 oz-in. To investigate the effect of skew on the cogging torque, a stack of loose punchings was machined to have a slip fit in the frame so that the skew could be changed. Only slight reduction in the cogging effect could be obtained with practical amounts of skew.

Next a graphical layout was made with the stator slots and PM poles laid out in a straight line to approximately a 5 to 1 scale. A 48 slot and a 45 slot punching were laid out. The flux fringing area permeance and the air-gap permeance over the poles were graphically integrated as the stator and rotor moved relative to each other. The integration was performed for 5 positions in one slot pitch. The results showed that the permeance variation of the 45 slot punching was negligible compared to the permeance variation of the 48 slot stator.

A stack of loose 45 slot punchings was made and tested as before. The results gave approximately 5 oz-in. of cogging torque. Again, skewing any practical amount had only a small effect.

A can made of 0.008 inch thick unannealed Hiperco 27 magnetic steel was installed crudely in the stator (after machining the stator bore oversize) with a gap left at the seam. In spite of the cogging introduced by the seam gap, it was determined that the cogging torque was reduced to below 1 or 2 oz-in. It was felt that this was sufficient indication to go ahead with the redesigned 45 slot stators with a can in the bore.

The final can configuration is made of 0.006 inch thick hypernik steel butt-welded with an electron beam welder and having a shrink fit in the stator bore. The hypernik steel was chosen for its sharp magnetic saturation point and for ease in welding. To avoid removing

too much material from the stator, the rotor magnet O.D. was lowered by 0.006 inch.

The layout was also used to determine the effective conductors with 30 and 60 degree switching angles for delta and wye connections using both two and three-phase conduction. It was determined that the least electrical ripple (as distinguished from the cogging effect) was obtained with zero skew for the 45 slot punching. It was also determined that use of an 8/9 pitch would not lower the torque or increase ripple.

It was also determined that a 60 degree switching angle using a delta connected winding with three-phase conduction gave the least ripple. The ripple at zero speed for the 30 degrees switching angle for a wye connection was 11.8 percent; the ripple for the 60 degree switching angle, delta connected winding, with three-phase conduction was 9.8 percent. The ripple torque at higher operating speed for the former rose to approximately 27 percent at certain combinations of voltage and speed while the ripple torque of the latter decreased to below 5 percent.

Use of a 60 degree switching angle implies that two power switches must be operated simultaneously to take advantage of the lower ripple. This would entail some sort of positive device for insuring that the two power switches operate exactly alternately. Since work on the project has progressed too far for major modification, it was decided to leave this for future improvements. Winding the stator with a delta connection was considered in case it was desired later to make the change. However, a 30 degree switching angle with a delta connection gave approximately 19 percent ripple at zero speed. Consequently, the winding was left wye connected.

It is apparent from all the ripple calculations made on the various configurations that no one optimum value of skew will give the least ripple. The optimum value must be determined for each individual case. The amount of short chording must also be determined individually.

c. PM Motor Design

The first step in the design of the PM motor was the selection of active electrical materials. For minimum size and weight, it is necessary to use the best available materials for the intended task. It was necessary to select the following materials before proceeding with the design.

(1) Permanent Magnet. It is desirable to use a cast rotor both for simplicity and to avoid the added weight of fabricating a rotor. Alnico V was selected as the magnetic material having the highest energy content that could still be cast. Use of a higher energy material was considered later in the design. In order to take full advantage of Alnico V, it is necessary that the magnet be magnetized while in the stator. The demagnetization curve for Alnico V is shown in Figure 5.

(2) Electrical Steel. For minimum size and weight, it is necessary to work the electrical steel at a high magnetic density. The steel giving the highest permeability at the high sensities considered is Hiperco 27. Lamination thickness of 8 mils was chosen because of availability only. The magnetization curve for Hiperco 27 is shown in Figure 6.

(3) Magnet Wire. Heavy build ML enameled wire was chosen. This has low outgassing characteristics and has outstanding electrical and mechanical properties. ML is the trade name of a polyimide type insulating resin developed by DuPont.

(4) Slot Insulation. An insulation thickness of 8 mils was assumed in the design. This is composed of 2-3 mil thicknesses of Pyre ML adhesive tape plus a small allowance for punching stagger. Pyre ML is glass impregnated with ML resin.

The next step in the design is to state the starting electrical and mechanical limitations and assumptions. These are enumerated and justified below. The design calculations are shown for the original 48 slot design. The effect of changing to a 45 slot with a can in the rotor is described later in the text.

(1) Poles = 8 (A 10 pole design will be considered)

(2) Slots = 48

(3) Outside Diameter = 3.313 inches. This is the highest punching diameter allowed by the 3.5 inch diameter specification limitation and the frame thickness.

(4) Pitch = Full

(5) Pole Enclosure = 2/3

(6) I_a = 1 amp.

(7) V = applied voltage = 40

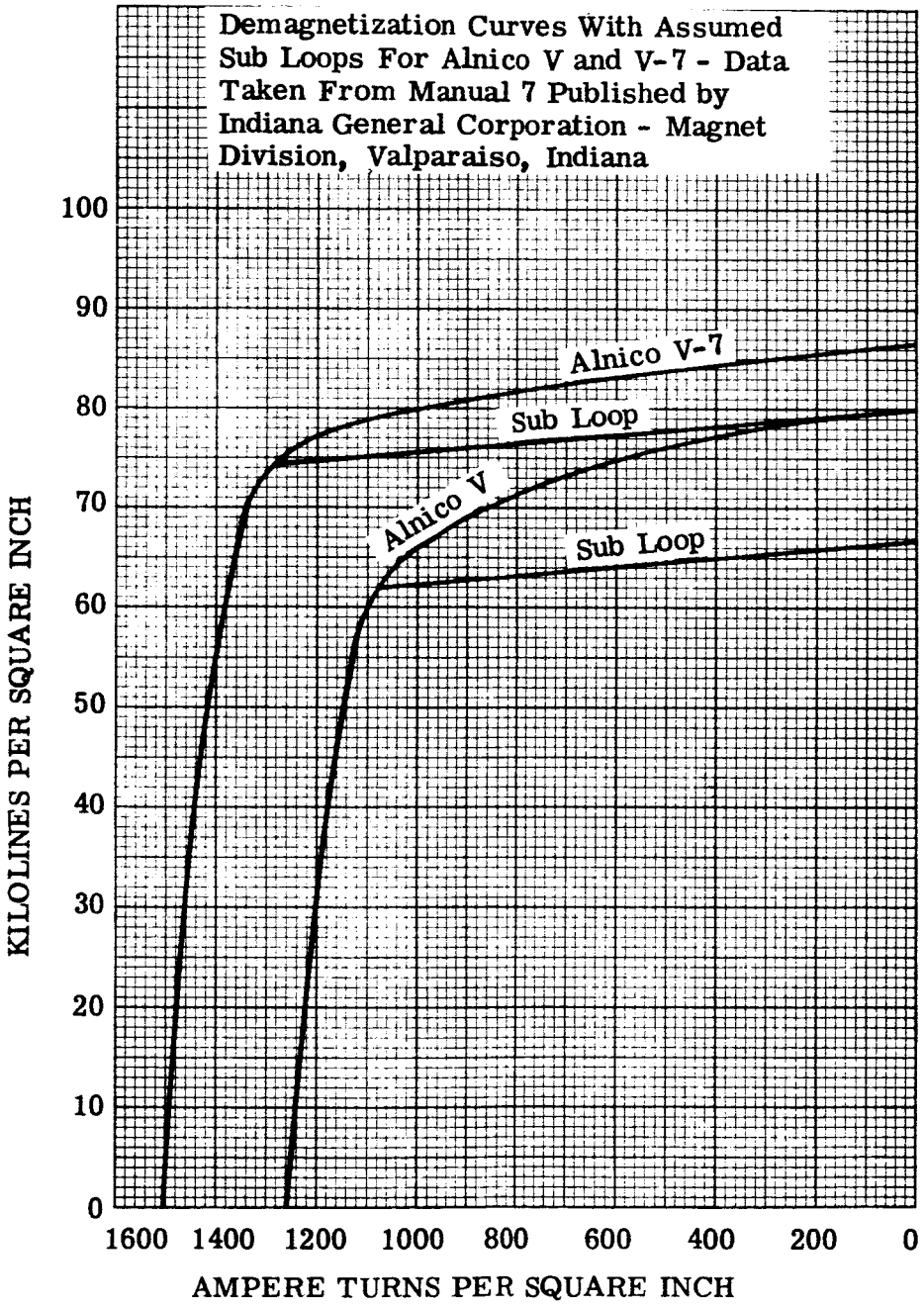

FIGURE 5. Permanent Magnet Demagnetization Curves

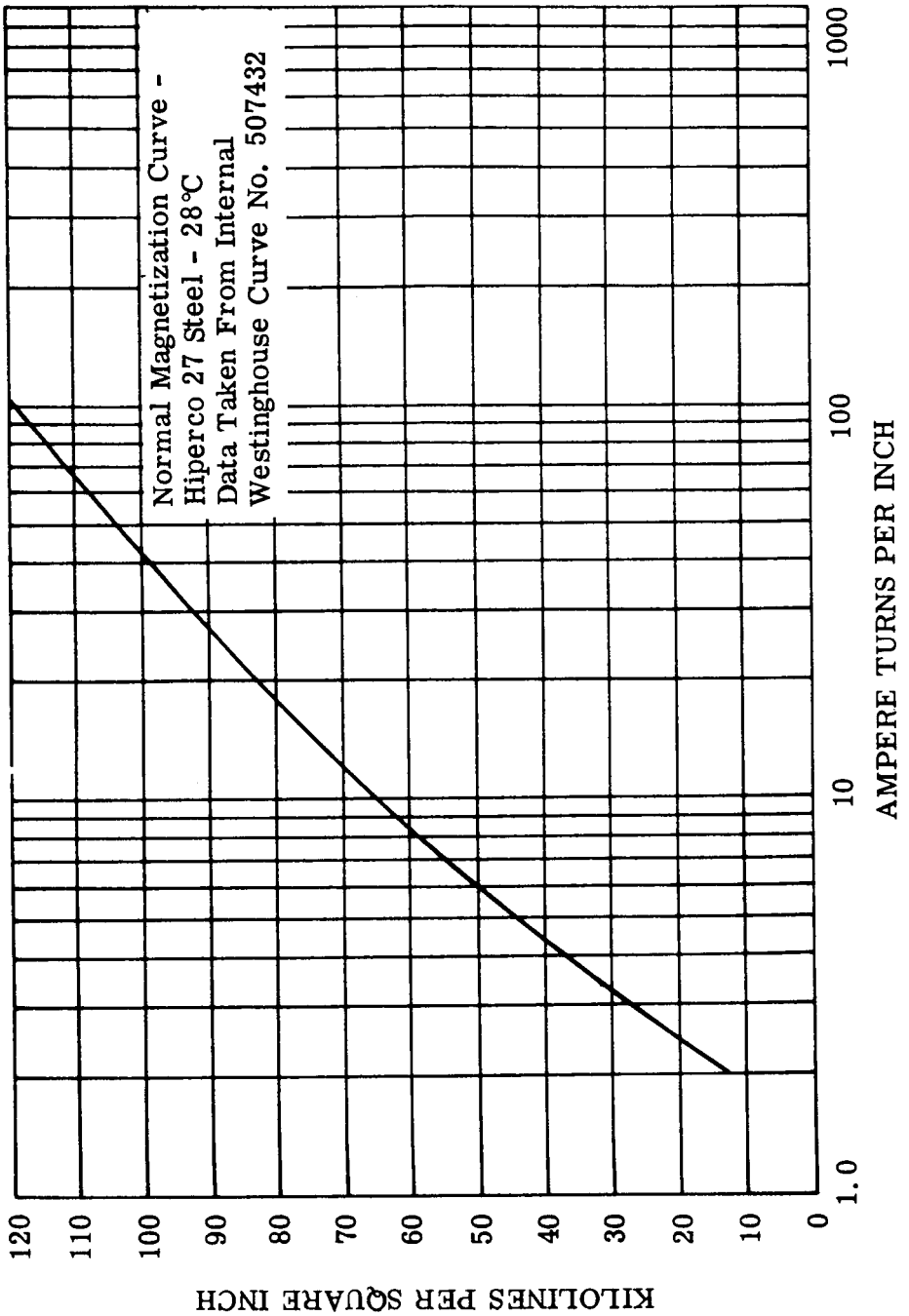

FIGURE 6. Hiperco 27 Magnetization Curve

(8) Drop in Switches = 0.5 volts. This figure was assumed before full knowledge of the control circuit was available. The actual drop will be approximately 1.5 volts. This would cause a theoretical drop in the current and torque over that calculated of 2.5 percent.

(9) Permanent magnet inside diameter = 1.00. This was obtained from a preliminary layout. It is determined by the necessary bearing bore.

(10) Slot opening = 0.05

(11) Tooth tip thickness = 0.025. This follows usual practice for aircraft motor punchings.

(12) Skew = 30 electrical degrees. The effect of skewing the PM rotor is to lower the length of leakage paths. The effect of skewing the stator is to lessen slot winding area. In an 8 pole design, 30 electrical degrees correspond to 7.5 mechanical degrees. Half of the skew was put in the stator and half in the PM rotor making the skew in each only 3.75 mechanical degrees. The deleterious effects of this slight skew were ignored in the calculation.

(13) Heat Factor = 1.2. This corresponds to an average stator wire temperature of 76°C. The cooling in a vacuum would be from radiation and conduction. The actual cooling conditions are not known. The assumed heat factor would probably not be large enough in a 70°C ambient. The heat factor was set at the above value with the thought of keeping the required performance nominal rather than minimum.

The first part of the actual design is the design of the magnetic circuit. The formulas used are derived below. The general procedure to be used will be to assume a maximum tooth flux density and to derive all the rest of the circuit dimensions.

Tooth area = (e)(s)(ATW)(w)(0.95)

Where

e = pole enclosure in per unit
s = slots per pole
ATW = tooth width in inches
w = stack length in inches
0.95 = stacking factor

Total flux = ϕ = (B_T)(Tooth Area)

Where

B_T = tooth density in lines per square inch

or

$$\phi = (e)(s)(ATW)(w)(B_T)(0.95) \text{ in lines}$$

Let D equal the diameter at the center of the air gap and assume it also applies to the OD of the magnet. This will be close enough for practical purposes since D will not be used to determine the air gap length.

$$\text{Air Gap Area} = \frac{(\pi)(D)(w)(e)(s)(1.08)}{S_p}$$

Where

S_p = Number of stator slots

1.08 = Factor to allow for fringing flux (This factor was added after several iterations)

Since the same total flux is present in the air gap as is present in the teeth

$$\text{Air gap density} = B_{AG} = \frac{\phi}{\text{Air Gap Area}}$$

$$= \frac{(B_T)(ATW)(S_p)(0.95)}{(\pi)(D)(1.08)}$$

The ampere turns required for the air gap

$$= \frac{(S_f)(B_{AG})(L)}{3.19}$$

Where

S_f = saturation factor = multiplier on air gap length to allow for saturation of the steel.

L = Effective air gap length including a multiplier to allow for the stator slot openings. This multiplier is commonly called Carter's Coefficient.

Ampere turns for air gap (substituting from previous equations)

$$= \frac{(S_f)(B_T)(ATW)(S_p)(L)(0.95)}{(3.19)(\pi)(D)\ 1.08}$$

$$\text{Area of Magnet} = \frac{(\pi)(D)(e)(s)(w)}{S_p}$$

This is the circumferential area of the magnet assuming D is the OD of the magnet. Actually, the chordal area should be used. Since these equations are to be used for design and not for performance, the error involved is small and can be neglected.

B_m = flux density in the magnet

$$= \frac{(L_f)(\phi)}{\text{Magnet Area}}$$

where:

L_f = leakage factor = multiplier on air gap flux to obtain the magnet flux. The magnet flux is equal to the air gap flux plus the leakage flux.

$$B_m = \frac{(L_f)(B_T)(ATW)(S_p)(0.95)}{(\pi)(D)}$$ substituting for ϕ and magnet area.

$$ATW = \frac{(\pi)(D)(B_m)}{(L_f)(B_T)(S_p)(0.95)}$$

Refer to Figure 7 for symbol definition for the following derivation of magnet length.

a = 1/2 the magnet width at the air gap.

$$= \frac{(\pi)(D)(e)(s)}{2\ S_p}$$

$$l = \frac{D}{2} - \frac{ID}{2} - \frac{a}{2} = \frac{D}{2} - \frac{ID}{2} - \frac{(\pi)(D)(e)(s)}{4\,S_p}$$

$$= \frac{2(S_p)(D) - 2(S_p)(ID) - (\pi)(D)(e)(s)}{4\,S_p}$$

$$l_1 = \frac{(ID + a)(\pi)}{2p} - \frac{a}{2}$$

$$l_1 = \frac{2(\pi)(ID)(S_p) + (\pi)^2(D)(e)(s) - (\pi)(p)(D)(e)(s)}{4(S_p)(p)}$$

Total Magnet Length = $l + l_1$

$$= \frac{2(S_p)(p) - 2(\pi)(e)(s)(p) + (\pi)^2(e)(s)]\,D - 2(S_p)(ID)(p) + 2(\pi)(ID)(S_p)}{4(S_p)(p)}$$

Ampere turns per inch in magnet

$$= \frac{\text{Ampere turns for air gap}}{\text{Magnet length}}$$

$$= \frac{4(S_f)(B_T)(ATW)(L)(p)(S_p)^2(0.95)}{(1.08)(3.19)(\pi)(D)\left[[2(S_p)(p) - 2(\pi)(e)(s)(p) + (\pi)^2(e)(s)]D - 2(S_p)(ID)(p) + 2(\pi)(ID)(S_p)\right]}$$

Substituting equation for ATW

$$AT/in = \frac{4(Sf)(L)(p)(S_p)(B_m)}{(1.08)(3.19)(L_f)\left[[2(S_p)(p) - 2(\pi)(e)(s)(p) + (\pi)^2(e)(s)]D - 2(S_p)(ID)(p) + 2(\pi)(ID)(S_p)\right]}$$

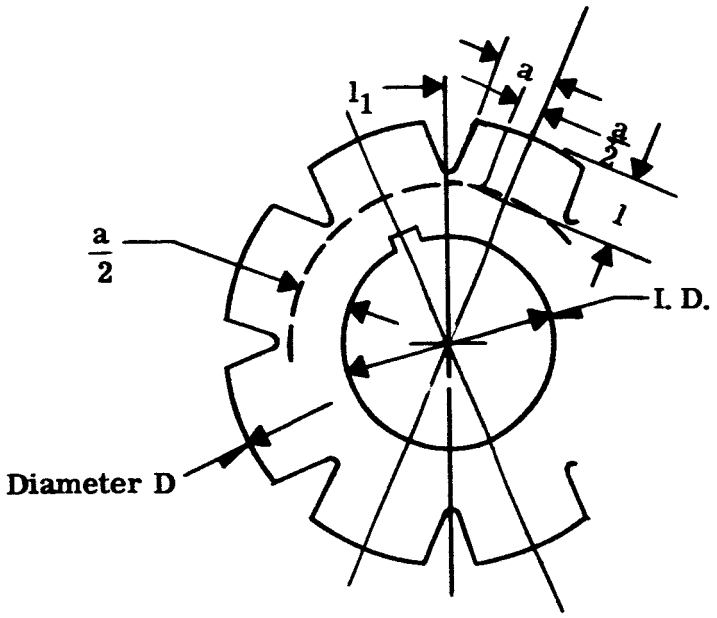

FIGURE 7. PM Rotor Definition of Symbols

It is necessary to match the characteristics of the permanent-magnet material with the design. With Alnico V magnet material, if the magnet is exposed to an air gap or demagnetizing mmf, the operating point on the demagnetization curve will move to the left along the curve. If the air gap or demagnetizing mmf is then removed, the magnet will not return to its original state, but will return along a sub loop. This sub loop, in the operating region, can be approximated by a straight line having the same slope as the main demagnetization curve where it intersects the B axis.

On Figure 5, the operating sub loop is assumed, so that most of the demagnetization mmf is available without too great a sacrifice in available flux density. The assumption of the sub loop is a matter of judgement. It is then desired to pick an operating point along the sub loop so that sufficient demagnetization mmf is left for armature reaction. Using the chosen sub loop and the chosen operating point, the magnetic circuit dimensions can be determined by solving the equation for ATW and ampere turns per inch.

The procedure to be followed is to assume a tooth density, a likely operating sub loop demagnetization curve, an operating point, a leakage factor, a saturation factor, and a stack length. Using these, the magnetic circuit is derived from the equations. The leakage factor and saturation factor are then calculated. The procedure is iterated at this point if these factors vary significantly from the assumed values. When these values finally are close enough, if the saturation factor is too high or too low, the tooth density is changed and the circuit is recalculated. When a satisfactory saturation factor is obtained, the electrical design is performed and torque is calculated. If torque is not right, stack length is changed and the calculation repeated. Armature demagnetizing mmf is then calculated and compared with the amount allowed for it on the original assumption at the operating point. If an insufficient or an excessive amount was allowed in the assumption, the operating point or the sub loop is changed. All calculations are then repeated.

Actually using this procedure usually requires some iteration. However, only the final calculation is given below.

Assumptions:

$S_f = 1.3$
$L_f = 1.25$
$B_T = 120,000$
$B_m = 65000$ (operating point)

AT/in = 430 (operating point)

L = 0.012

The assumed sub loop demagnetization curve is shown on Figure 4.

w = 0.53

Then

$$AT/in = \frac{(4)(1.3)(0.012)(8)(48)(65000)}{(1.08)(3.19)(1.25)\left[\left[(2)(48)(8)-2(\pi)(0.667)(6)(8)+(\pi)^2(0.667)(6)\right]D - (2)(48)(1.00)(8)+(2)(\pi)(1.00)(48)\right]}$$

$$= 430$$

Solving for D

$$606.4D - 467 = 840$$

$$D = 2.16$$

Assume actual AG length = 0.0093

Stator ID = 2.16 + 0.0093 = 2.17

Magnet OD = 2.16 - 0.0093 = 2.15

From equation 3

$$ATW = \frac{(\pi)(2.16)(65000)}{(1.25)(120,000)(48)(0.95)} = 0.064$$

DBS = depth below slot

It is desired to keep the density in the core (or yoke) the same as in the teeth since the steel is worked so hard. With a 0.667 pole

enclosure, the flux from 2 teeth flows into the core. Therefore, the core area should be twice one tooth area.

DBS = (2)(0. 064) = 0. 128

Width of magnet (chordal)

= (2)$\frac{(OD)}{2}$ sin (1/2 the angle subtended by the magnet face at the air gap)

= (2)(1. 075) sin 15° = 0. 557

Magnet area = 0. 557 x 0. 53 = 0. 295

a = 0. 279

The permanent-magnet rotor design is shown on Figure 8.

$$l = 1.075 - 0.5 - 0.139 = 0.436$$

$$l_1 = \frac{1.279\pi}{16} - 0.139 = 0.112$$

Total magnet length = 0. 548

Teeth area = (0. 064)(4)(0. 53)(0. 95) = 0. 129

$$\text{Teeth length} = \frac{3.313 - (2)(0.128) - (2.17 + 0.05)}{2} = 0.425$$

$$\text{Circumferential air gap length} = \frac{(\pi)(2.16)(4)}{48} + 0.012 = 0.578$$

The 0. 012 is an allowance for fringing flux

= one air gap length

Axial air gap length = 0. 53 + 0. 03 = 0. 56

The 0. 03 is an allowance for end fringing = tooth tip length

+ 1/2 (air gap length)

Air gap area = (0. 578)(0. 56) = 0. 324

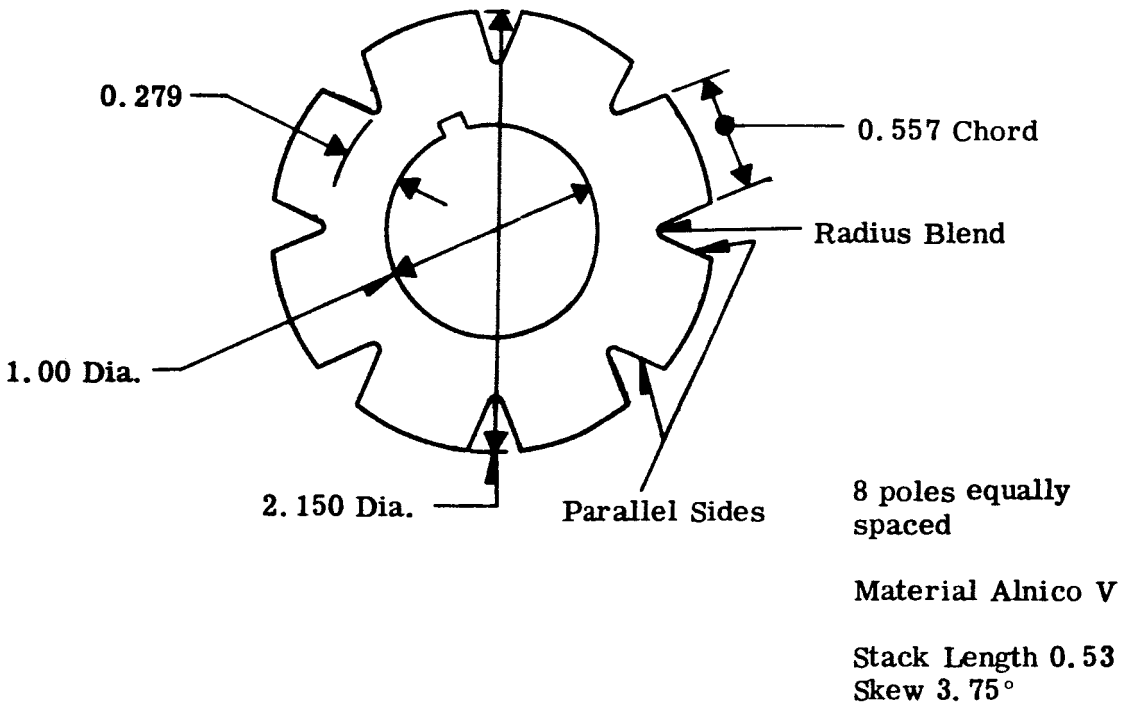

FIGURE 8. Permanent Magnet Rotor

$\phi = (0.129)(120,000) = 15500$

$B_{AG} = \frac{15500}{0.324} = 47,900$

Ampere Turns - $AG = \frac{(47,900)(0.012)}{3.19} = 180$

To calculate the ampere turns required for the stator steel, refer to Figure 5.

AT/in for teeth at 120 Kl/in^2 = 105

Ampere turns - teeth = (105)(0.425) = 45

The mmf required for the core does not change appreciably with position because of the skew. Therefore, for determining the mmf required for the core, the simplest position is used which is that with a centerline between teeth on the center of a magnet pole. Then in the core the flux is zero for 1/2 of a tooth pitch. Then the flux from one tooth flows for a tooth pitch after which it is joined by the flux from 0.962 of a tooth. This combination flows for a tooth pitch after which it is joined by the flux from 0.038 of a tooth. This whole combination flows for 1/2 of a tooth pitch. The fractions of a tooth stem from the skew. Therefore, for a tooth density of 120,000 lines per square inch, the core has a density of zero for 1/2 tooth pitch, 60,000 for one tooth pitch, 118,000 for one tooth pitch and 120,000 for 1/2 tooth pitch.

The ampere turns per inch for three densities are:

Density	AT/in.
120,000	105
118,000	95
60,000	8

Tooth pitch at the average core diameter

$= \frac{(3.313 - 0.128)\pi}{48} = 0.208$

Ampere turns - core = 0.208 (52.5 + 95.0 + 8) = 32

Total ampere turns = 180 + 45 + 32 = 257

$$S_f = \frac{257}{180} = 1.428$$

It is estimated that S_f should be between 1.3 and 1.6 so the above value is satisfactory.

The next step is the calculation of the leakage factor for which it is necessary to know the leakage permeance. The leakage permeance is obtained using formulas using the methods of Rotors[1]. See Figure 9 for an identification of the various leakage paths. See Appendix I for derivation of the leakage formulas used below.

$$R = 1.075$$

$$a = 0.279$$

$$\sin \frac{\theta}{2} = \sin 22.5^\circ = 0.383$$

$$c = \frac{0.279}{0.383} = 0.729$$

$$r_2 = 1.075 - 0.729 = 0.346$$

$$r_1 = 0.5 + 0.279 - 0.729 = 0.05$$

$$e = \frac{c}{2} = \frac{0.729}{2} = 0.365$$

$$r_4 = 1.075 - 0.365 = 0.710$$

$$r_3 = 0.5 + 0.279 - 0.365 = 0.414$$

$$C_f = \frac{0.296 + 0.279 + (0.112)(2)}{0.548} = 1.46$$

$$P_3 = \frac{(2)(3.19)(0.53)(8)}{(0.296)(\pi)} \left(0.296 + 0.05 \ln \frac{0.05}{0.346}\right)(1.46)$$

$$= 8.45$$

[1]The superscript number refers to reference numbers in the bibliography.

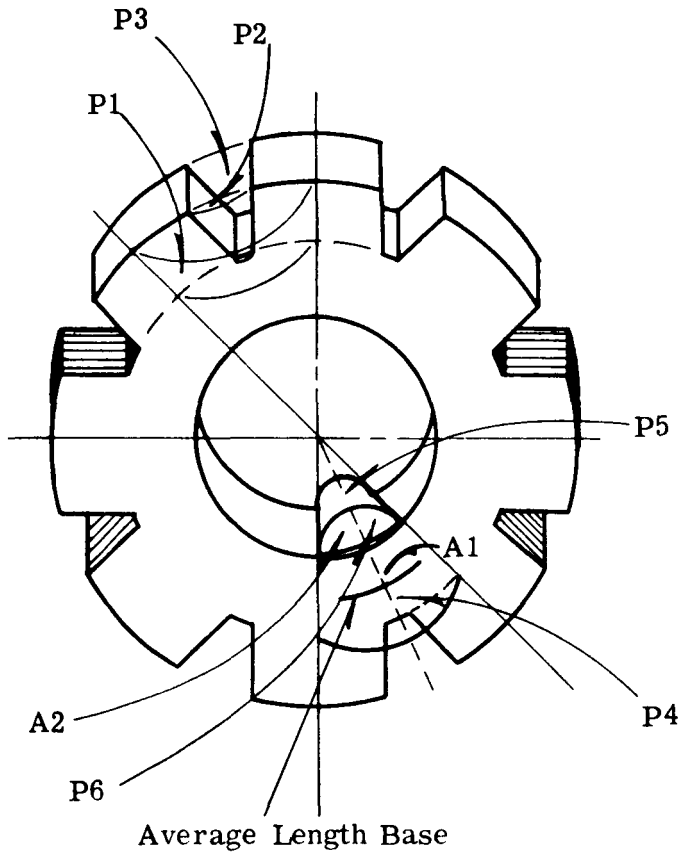

Path

P3 = Path between poles

P2 = Tapered semi-cylinder with pole edges forming locus of ends of the semicircles

P1 = Tapered half-annulus immediately over P2 and with a thickness equal to one-half of a pole width

P4 = Tapered semi-annulus with a center semi-cylinder of zero diameter starting just below P1 and P2 and extending to the ID

P5 = Approximate semi-annulus with a center semi-cylinder of zero diameter in the center of the magnet and running the length of stack

P6 = Approximate shell of a quadrant of a sphere between P4 and P5 having a center quadrant of a sphere of zero diameter

FIGURE 9. Definition of PM Rotor Leakage Paths

$$P_2 = (1.04)(3.19)(0.296)(1.46) = 1.43$$

$$P_1 = \frac{(8)(3.19)(0.279)}{(\pi)(0.296)(0.383)} \left[0.296 + 0.414 \ln \frac{0.414}{0.710}\right] (1.46)$$

$$= 2.1$$

$$P_4 = \frac{(4)(3.19)(0.279)(1.279)}{(8)(0.548)} = 1.04$$

$$P_5 = \frac{(2)(3.19)(0.53)(1)}{(8)(0.548)} = 0.771$$

$$P_6 = \frac{(3.19)(1)^2(\pi)^2}{(4)(8)^2(0.548)} = 0.224$$

$$P_3 + P_2 + P_1 + P_4 + P_5 + P_6 = 14.02$$

Total leakage permeance = $P_e = 14.02$

+ 10% for paths not considered

= 15.5

Permeance of air gap

$$= \frac{(3.19)(0.324)}{0.012} = 86.2$$

Actual AG permeance = $\frac{86.2}{1.428} = 60.4$

$$L_f = \frac{60.4 + 15.5}{60.4} = \frac{75.9}{60.4} = 1.255$$

Flux in magnet = (1.255)(15500) = 19,460

$$B_m = \frac{19,460}{0.295} = 65,900$$

Ampere turns per inch in magnet

$$= \frac{257}{0.548} = 469$$

This is close enough to the operating point.

One final step in the magnetic design is to verify that a 0.0093 air gap will give a 0.012 effective gap.

Tooth pitch at the air gap

$$= \frac{(2.17)(\pi)}{48} = 0.142 = T_p$$

$$\text{Carter's Coefficient} = \frac{T_p\left[(4.4)(\Delta) + (0.75)(e_s)\right]}{T_p\left[(4.4)(\Delta) + (0.75)(e_s)\right] - (e_s)^2}$$

Where

Δ = single air gap length = 0.0093

e_s = slot opening

$$\text{Carter's Coefficient} = \frac{0.142\left[(4.4)(0.0093) + (0.75)(0.05)\right]}{0.142\left[(4.4)(0.0093) + (0.75)(0.05)\right] - (0.05)^2}$$

$$= 1.295$$

$$(1.295)(0.0093) = 0.0122$$

The next step is the design of the winding. The punching has the dimensions shown in Figure 9.

From Figure 9:

ASW = 0.109 = average slot width
b_s = 0.419 = length of tooth

$$GSWA = (ASW)(b_s) - I_T\,(2b_s + 5ASW)$$

Where

GSWA = Slot winding area after insulation has been subtracted except for wire enamel

I_T = Insulation thickness

$$GSWA = (0.109)(0.419) - 0.008\left[(2)(0.419) + (5)(0.109)\right]$$

$$= 0.035$$

The above formula for GSWA is derived empirically from standard practice.

Coil Perimeter = C_p

$$= 2(w) + \frac{2(P_f)(\pi)(D_a)(ACT)}{S_p}$$

Where

P_f = empirical constant

D_a = average diameter of winding

ACT = coil throw in slots

$$D_a = \frac{\text{Pchg OD} - 2\ \text{DBS} + \text{Pchg ID} + 2\ (\text{tooth tip thickness})}{2}$$

$$= \frac{3.313 - 0.256 + 2.22}{2} = 2.64$$

$P_f = 1.65$ for an 8 pole winding

ACT = 6 slots for a full pitch winding

$$C_p = (2)(0.53) + \frac{2(1.67)(\pi)(2.64)(6)}{48} = 4.52$$

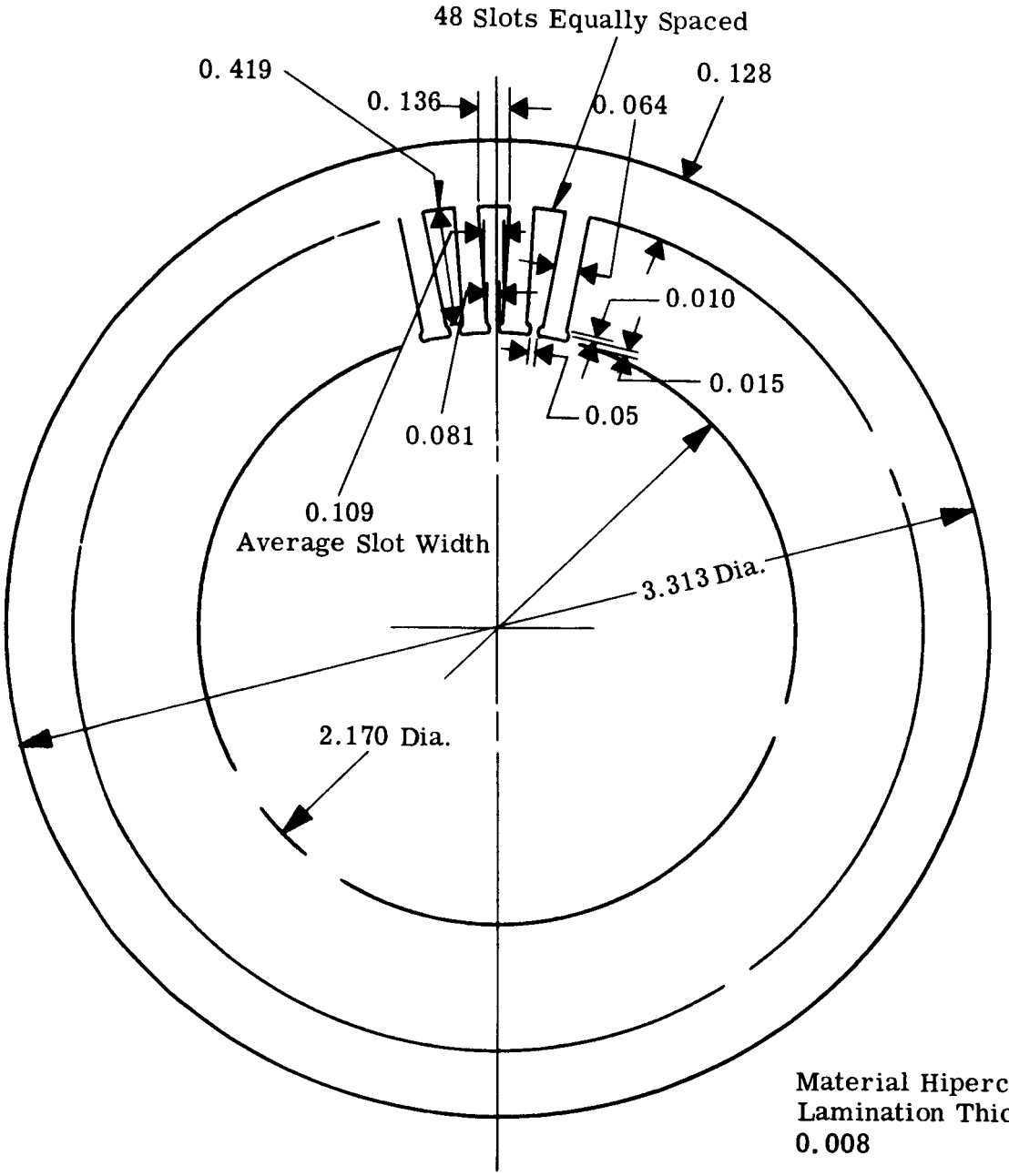

FIGURE 10. Armature Punching

For Connection 1.

$$\text{Rhot} = \frac{(1.2)(1.5)(\text{TPC})(C_p)(S_p)(\Omega)}{3}$$

Where

Rhot = hot resistance of winding

TPC = turns per coil

Ω = Resistance of one inch of wire

In the range of wire sizes that will result, the insulated wire diameter is approximately $(1.175)(D_b)$ where D_b is the bare diameter.

Assume a slot fullness of 0.687 per unit

$$\text{Conductors per slot} = \frac{(0.687)(\text{GSWA})}{(\text{Insulated Dia})^2}$$

$$= \frac{(0.687)(\text{GSWA})}{(1.38)(D_b)^2}$$

$$\text{TPC} = \frac{\text{Cond. per slot}}{2} = \frac{(0.687)(\text{GSWA})}{(2.76)(D_b)^2}$$

$$\Omega = \frac{(0.692)(10^{-6})(4)}{(D_b)^2(\pi)} = \frac{(0.881)(10^{-6})}{(D_b)^2}$$

for copper wire.

$$\text{Rhot} = \frac{(1.8)(0.687)(0.035)(48)(4.52)(0.881)(10^{-6})}{(2.76)(3)(D_b)^4} = 39.5$$

With 40 volts applied and 0.5 volts drop in the switches Rhot must equal 39.5 to obtain one ampere of current.

Solving above for D_b

$$D_b = 0.0126$$

Use No. 28 wire

Ohms per 1000 feet = 66.17 (from wire table)

TPC = 55

$$\text{Rhot} = \frac{(1.8)(4.52)(66.17)(55)(48)}{(3)(12)(1000)} = 39.5 \quad \text{Check}$$

$$\text{Zph} = \frac{(55)(48)(2)}{3} = 1760$$

$$Z = (2.05)(1760) = 3610$$

$$\phi = 15,500$$

$$\text{Torque} = \frac{(22.6)(8)(15,500)(3610)(1)(10^{-8})}{1}$$

= 101 oz. in.

The magnet must have a sufficient mmf reserve to withstand armature reaction. The worst armature reaction is at -10°C with 60 volts applied at locked rotor.

Effective Ampere Turns per Pole

$$= (\text{TPC})(2)(1.5)\left(\frac{1.2}{\text{Heat Factor at } -10°\text{C}}\right)\left(\frac{60}{40}\right)$$

The 1.5 is obtained from an mmf plot of the winding. The peak mmf on the same basis is 2 times the conductors per slot.

$$= (55)(2)(1.5)\left(\frac{1.2}{0.865}\right)\left(\frac{60}{40}\right) = 344$$

Changing this to ampere turns per inch in the magnet

$$= \frac{344}{0.548} = 628$$

Total Ampere Turns = 628 + 469

= 1097

This value exceeds the maximum allowed by the assumed operating sub loop. However, if this figure is approached the flux must fall and the ampere turns required for the magnetic circuit must also fall. At the mmf extremity of the curve, B_m = 62, 400. If this was assumed to be constant over the whole pole, the new air gap flux would be

$$\frac{62400}{65900} (15,000) = (0.947)(15,500) = 14,700$$

Ampere Turns Air Gap = (0. 947)(180) = 170

B_T = (0. 947)(120, 000) = 113, 600

AT/in from Figure 5

= 76

Ampere Turns Teeth = (0. 425)(76) = 32

The core ampere turns should remain approximately the same.

Therefore 10 + 13 = 23 ampere turns are saved which are reflected in the magnet as

$$\frac{23}{0.548} = 42 \text{ AT/in}$$

When the above reduction plus the increase in leakage flux resulting from the increased mmf (which would further lower air gap and tooth flux) are considered, the reserve mmf in the magnet is seen to be sufficient to handle armature reaction in the worst case. The actual specification for the magnet was that the demagnetization curve would fall above the point 62. 5 kilolines per square inch and 1050 ampere turns per inch. It is possible that, within the limits of manufacture, a magnet with such a minimum demagnetization curve cannot be procured. It is seen, however, that the slope of the assumed sub loop was conservative and that some further reduction in the demagnetization curve could be tolerated if necessary.

A 10 pole motor design was considered. The motor was designed using the same procedure up to the point where leakage permeance was calculated. The sum of P1, P2, and P3 was 23.5. This was considered excessive and the design was not carried further.

The use of a better permanent-magnet material was considered. On Figure 5, the curve for Alnico V-7 is shown with an assumed sub loop. It would appear that the new flux density would be approximately 77 kilolines per square inch, instead of 65 and that the ampere turns per inch at the operating point would be approximately 650 instead of 450.

The magnet length could be reduced to approximately

$$\left(\frac{77}{65}\right)\left(\frac{450}{650}\right)(0.548) = 0.450$$

The OD of the magnet then could be reduced approximately by

$$\frac{0.450}{0.548} = 0.821$$

Since with a constant pole enclosure the magnet area varies with diameter, the actual air gap flux would be

$$\left(\frac{77}{65}\right)(0.821) = \text{approximately the same}$$

The increase in slot length would be approximately

$0.548 - 0.450 = 0.098$

The dimension at the bottom of the slot is now 0.081 (See Figure 10). Therefore the increase in winding area would be less than

$(0.081)(0.098) = 0.008$

Present GSWA = 0.035

New GSWA will be less than 0.043

Per unit increase $= \frac{0.043}{0.035} = 1.23$

The advantage is reflected in torque as the square root of the increase (with a constant current). Therefore, the per unit increase in torque will be less than

$$\sqrt{1.23} = 1.11$$

This figure will be reduced to less than 1.1 because of increased leakage flux. The same increase could be attained with slightly more than a 10 percent increase in stack length which would amount to an increase of slightly more than 0.053 inches.

The Alnico V-7 material cannot be cast and hence the rotor would have to be fabricated from straight bar magnets. It is felt that the small weight saving due to the reduction in stack length when using the Alnico V-7 would be replaced by the material weight necessary for fabrication. Therefore, the use of stronger magnetic materials was given no further consideration. The use of a high mmf, low flux density material would lead to impractical design proportions. Therefore, this type of magnet material was eliminated.

After the initial 48 slot unit was built, the previously mentioned cogging problem necessitated changing to a 45 slot punching with zero skew. The new punching was made with the same slot die as was used for the 48 slot punching. This gave changes in the following parameters. The new values are listed below.

Parameter	48 Slot Value	45 Slot Value
ATW	0.064	0.075
Teeth Area	0.129	0.1415
Carter's Coefficient	1.295	1.254
Effective air gap length	0.0122	0.01254
Air-gap flux	15.5 kilolines	15.46 kilolines
Effective phases	2.05	2.05

The air-gap flux was determined by re-calculating the motor saturation curve. The effective phases were determined using the previously described layout and using the methods previously described. As can be seen from the above, the actual value of air-gap flux and effective phases changed very little.

From the experience gained from the first winding, it was apparent that the perimeter of the winding could be shortened more than just that due to the short chording. Consequently a perimeter of 4.0 inches was used on the new winding. Also from the previous winding, an emperical factor was used to make the calculated winding resistance agree more closely with the actual resistance. The drop in the switches was changed to 1.5 volts to agree with the expected value. The winding was recalculated as follows:

Turns per coil = TPC = 62
Flux per pole = Φ = 15.46
Perimeter = PER = 4.0
Ohms per 1000 feet of No. 28 wire = Ω = 66.17
Emperical factor = 1.05
Heat Factor = HF = 1.2
Number of slots = Sp = 45
Effective phases = 2.05 (from layout)
Desired total resistance with three legs connected = 38.5
(for I = total armature current = 1.0 amp at 40 volts with 1.5 volts drop in the switches).
Desired phase resistance = 38.5/1.5 = 25.7

$$\text{Hot resistance per phase} = \frac{(HF)(PER)(\Omega)(TPC)(Sp)(1.05)}{(\text{Phases})(12)(1000)}$$

$$= \frac{(1.2)(4)(66.17)(62)(45)(1.05)}{(3)(12)(1000)} = 25.8$$

$$\text{Conductors per phase} = \frac{(TPC)(Sp)(2)}{\text{Phases}} = \frac{(62)(45)(2)}{3} = 1860$$

Total effective conductors = Z = 2.05 x 1860 = 3810

$$\text{Torque} = \frac{(22.6)(P)(\Phi)(Z)(I)}{\text{Parallel paths}} \quad \text{oz-in.}$$

$$= \frac{(22.6)(8)(15.46)(38.10)(1)}{1} = 106.7 \text{ oz-in.}$$

The can in the stator bore will shunt some of the flux but it is difficult to exactly assess the effect. The approximate effect was calculated in the following manner. The total mmf for the teeth and yoke of the stator was calculated at 59.8 ampere turns for one-half pole pitch.

Length of can for one-half the distance between poles = 0.143
Amp turns/inch = 59.8/0.143 = 420
From a magnetization curve of hypernik, the flux density = 101.5 Kl/in^2
Area of can = (0.006(0.53) = 0.00316
Flux = (101.5)(0.00316) = 0.321 Kl.
Total flux = (2)(0.321) = 0.641 because of having 2 sides to a pole.
If torque varies directly as flux,

$$\text{New Torque} = \frac{15.46-0.641}{15.46} (106.7) = 102 \text{ oz-in.}$$

2. Electrical Design of Reluctance Switch

a. General

The voltage output of the reluctance switch will be sensed by a triggering circuit which will not allow current to flow until the voltage reaches a certain level. At that time the signal voltages are applied to the bases of the switching transistors. This triggering on amplitude is necessary to prevent the transistor switches from operating out of saturation. The triggering, therefore, required a high reluctance-switch secondary voltage to obtain this discrimination.

From the size and sensitivity of the electronic components, it was concluded that the secondary reluctance-switch voltage has to be approximately 9 volts on a square wave. The current draw, taking into account the filtering of the output, has to be approximately 30 milliamps per secondary at 9 volts.

The switching time of some of the electronic components limits the frequency of the oscillator drive for the reluctance switch to approximately 5000 cycles per second. This frequency also approaches the limit for available magnetic steels from a reasonable core loss standpoint.

The design of the oscillator for the reluctance switch is such that a 28 volt (0-to-peak) square wave with a fundamental frequency of 5000 cps is applied to the primary winding of the reluctance switch. The primary of the reluctance switch must be center-tapped to work with the oscillator.

The punchings, both rotor and stator, are shown on Figure 11. The primary winding is placed around the portions of the stator punching without teeth and is center-tapped. There are 6 required secondary windings. These are wound around each tooth. The windings around diametrically opposite teeth are connected in series to form one winding.

In operation, with the primary excited, the two halves of the primary winding are connected in opposition so that flux is driven through the teeth. Flux flows only through the teeth that are lined up with the rotor poles and a voltage is generated only in the secondary windings on those teeth.

The rotor is fastened to the shaft of the main motor and thus the position of the main motor shaft is sensed by the reluctance switch. The position is determined by the voltages generated in the secondary windings. It is desirable that the voltages in the secondary windings build up to approximately 65 percent of the final voltage before the triggering circuit allows use of the voltage. The symmetrical placement of the teeth would give a zero voltage at the desired switching time if the rotor poles were made two stator slot pitches wide. Tests made on a crude preliminary reluctance switch with rotor poles two stator slot pitches wide indicated that the pole width should be increased approximately 28.5 percent over two slot pitches for the voltage to obtain 65 percent of the final value at the desired switching time. This was done in this punching design.

The punching design shown was arrived at mainly from mechanical limitations. The steel thicknesses approach the minimum allowable section for punching. The rotor ID was determined by the necessary shaft diameter. The stator OD had to allow enough room for primary winding clearance. The ID of the stator was a matter of judgement. It is a compromise between the need for secondary winding space and the need for minimizing leakage permeance.

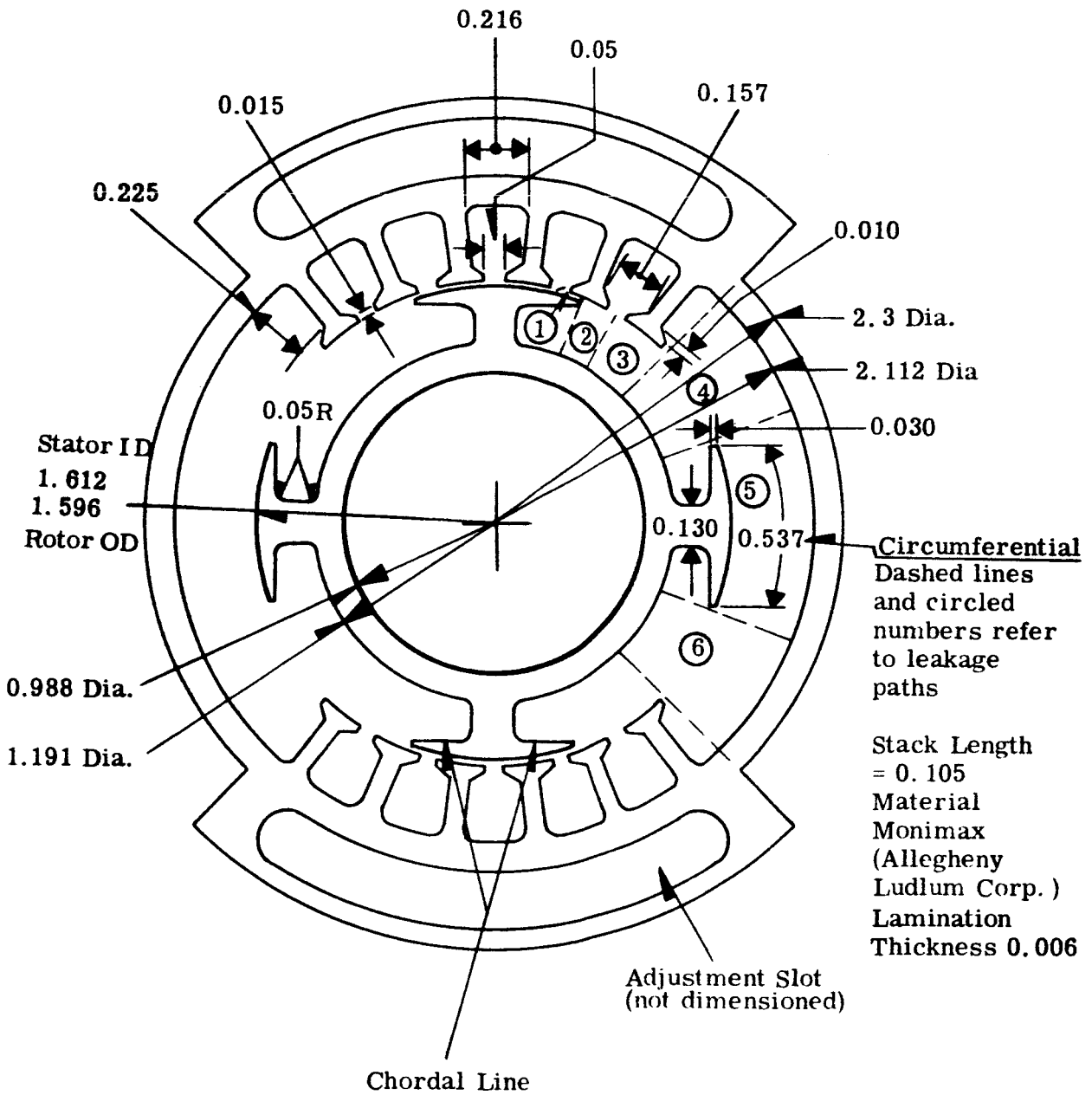

FIGURE 11. Reluctance Switch Punchings and Leakage Paths

The stack length was judged to be the minimum practical to avoid large errors due to misalignment.

The steel chosen for the reluctance switch is Monimax. Monimax is a trade name for a steel made by Allegheny Ludlum. It is especially made for high frequency applications having low core loss and low maximum flux density. The steel must be worked below 50 kilolines per square inch to avoid saturating the steel. A lamination thickness of 6 mils was chosen. It was felt that mechanical difficulties would be experienced with a thinner lamination with such a short stack length.

Heavy build ML enamelled wire was chosen for the primary winding and triple build for the secondary.

b. Electrical Design

The electrical circuit will be solved on the basis that 2 secondary windings are excited and drawing current. The midpoint of this situation will be with a rotor pole centered under two teeth as shown in Figure 11. Only the two secondary windings are excited, so that a flux flowing in any other tooth is regarded as leakage flux.

The first step in the design is the calculation of leakage permeance. As shown in Figure 11, the leakage paths are divided into 5 sections.

Path 1

$$\text{Tooth Pitch} = \frac{\pi(1.612)}{24} = 0.211$$

(refer to Figure 11 for dimensions)

Air gap = $0.008 = \Delta$

$$\text{Carter's Coefficient} = \frac{T_p\left[(4.4)(\Delta) + (0.75)(e_s)\right]}{T_p\left[(4.4)(\Delta) + (0.75)(e_s)\right] - (e_s)^2}$$

$$= \frac{0.211\left[(4.4)(0.008) + (0.75)(0.05)\right]}{0.211\left[(4.4)(0.008) + (0.75)(0.05)\right] - (0.05)^2}$$

$$= 1.194$$

Effective Air Gap = L = (1. 194)(0. 008)

= 0. 00955

Stack Length = 0. 105

Circumferential Length of Leakage Path 1

$$= \frac{(0.285)(\pi)(1.604)}{(24)} + 0.010 = 0.0698$$

(0. 285 is additional pole width over 2 slot pitches)
(1. 604 is the average air gap diameter)
(0. 010 is an allowance for fringing at the pole tips)

Area of Leakage Path 1 = (0. 0698)(0. 105) = 0. 00733

Allowance for fringing at the ends of the stack:

$$P = \frac{(3.19)(0.26)(0.0698)}{1.194} = 0.05$$

= Rotor's formula for a half cylinder divided by Carter's Coefficient to approximately allow for slot openings.

$$P = \frac{(3.19)(0.0698)}{1.194\,\pi} \ln\left(1 + \frac{0.040}{0.008}\right) = 0.11$$

= Rotor's formula for a half annulus. The 0. 040 is 2 times the average tooth tip thickness. Again the formula is divided by Carter's Coefficient as an approximate allowance for slots.

$$\text{Main } P_1 = \frac{(3.19)(0.00733)}{0.00955} = 2.44$$

Total P_1 = 2. 44 + 0. 05 + 0. 11 = 2. 60

Path 2

$$\text{Average Diameter} = \frac{1.612 + 1.191}{2} = 1.402$$

$$\text{Area} = \frac{(2 - 0.285)(1.402)(\pi)(0.105)}{24} = 0.033$$

$$\text{Length} = \frac{1.612 - 1.191}{2} = 0.211$$

$$P_2 = \frac{(3.19)(0.033)}{0.211} = 0.499$$

Path 3

Circumferential Length of Path

= 2 - 0.285 = 1.715 slot pitches

$$\text{Average Diameter} = \frac{2.112 + 1.191}{2} = 1.651$$

$$\text{Area} = \frac{(1.715)(1.651)(\pi)(0.105)}{24} = 0.0389$$

$$\text{Length} = \frac{2.112 - 1.191}{2} = 0.461$$

$$P = \frac{(3.19)(0.0389)}{0.461} = 0.269$$

P is not completely effective

P occupies 1.715 slot pitches

Total slot pitches = 6

P averages 0.857 slot pitches less than fully effective

$$P_3 = \left(\frac{6 - 0.857}{6.00}\right)(0.269) = 0.231$$

Path 4

P_4 occupies 2.57 tooth pitches

$$\text{Average Diameter} = \frac{2.112 + 1.596}{2} = 1.854$$

$$\text{Area} = \frac{(2.57)(1.854)(\pi)(0.105)}{24} = 0.0655$$

$$\text{Length} = \frac{2.112 - 1.596}{2} = 0.258$$

$$P = \frac{(3.19)(0.0655)}{0.258} = 0.81$$

P is only half effective

$P_4 = 0.41$

Path 5

$$P_5 = P_3 \left(\frac{0.857}{6}\right) = 0.033$$

Total of Paths

$= 2.60 + 0.499 + 0.231 + 0.41 + 0.033$

$P_{1p} = 3.77$ = total primary leakage permeance for half the magnetic circuit

Slot Leakage (See Figure 12)

$$\frac{a_1}{a_2} = \frac{0.164}{0.216} = 0.76$$

$\phi_s = 0.433$

$$K_s = (0.433)\ \frac{0.225}{0.216} + \frac{0.015}{0.050} + \frac{0.020}{0.214} = 0.844$$

$P = (3.19)(0.844)(0.105) = 0.283$

Average Slot Width = 0.190

Slot Length = 0.225

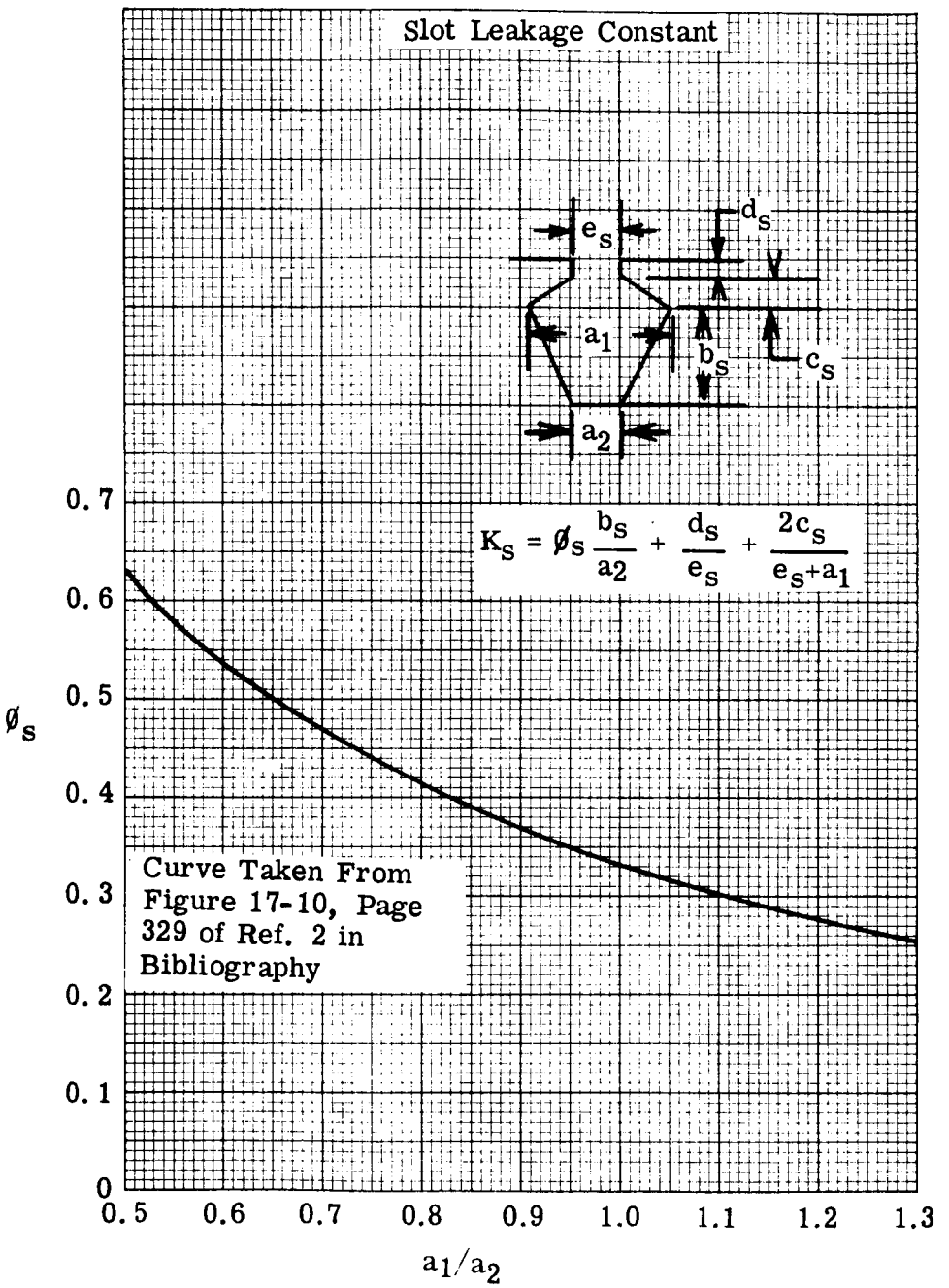

FIGURE 12. Slot Leakage Constant

$$\text{Average Permeance} = \frac{(3.19)(0.225)(0.105)}{0.190} = 0.396$$

For a semi-cylinder from one tooth to the next using Rotor's formula.

$$P = (3.19)(0.26)(0.225) = 0.374$$

For a semi-annulus from the edge to the center of one tooth to the edge to center of the next using Rotor's formula.

$$P = \frac{(3.19)(0.64)(0.225)(2)}{\frac{0.190}{0.03} + 1} = 0.125$$

Total average $P = 0.125 + 0.374 + 0.396 = 0.895$

$\frac{0.895}{0.396} = 2.26$ allowance for end fringing

Total P_{sl} = total slot leakage $= (2.26)(0.283) = 0.64$

Mutual Path

$$\text{Mutual Permeance} = \frac{3.19 \text{ Area}}{\text{Length}} = P_{pm}$$

Area = (2 slot pitches)(stack length) + fringing

$$\frac{(2)(1.604)(\pi)}{24}\left(\frac{2.60}{2.44}\right)(0.105) = 0.0468$$

The $\frac{2.60}{2.44}$ is the same allowance for fringing as was used for leakage path 1.

$$P_{pm} = \frac{(3.19)(0.0468)}{0.00955} = 15.65$$

A diagram of the equivalent circuit (with final circuit values) for the reluctance switch is shown in Figure 13. The dotted line can be eliminated in the circuit because of symmetry.

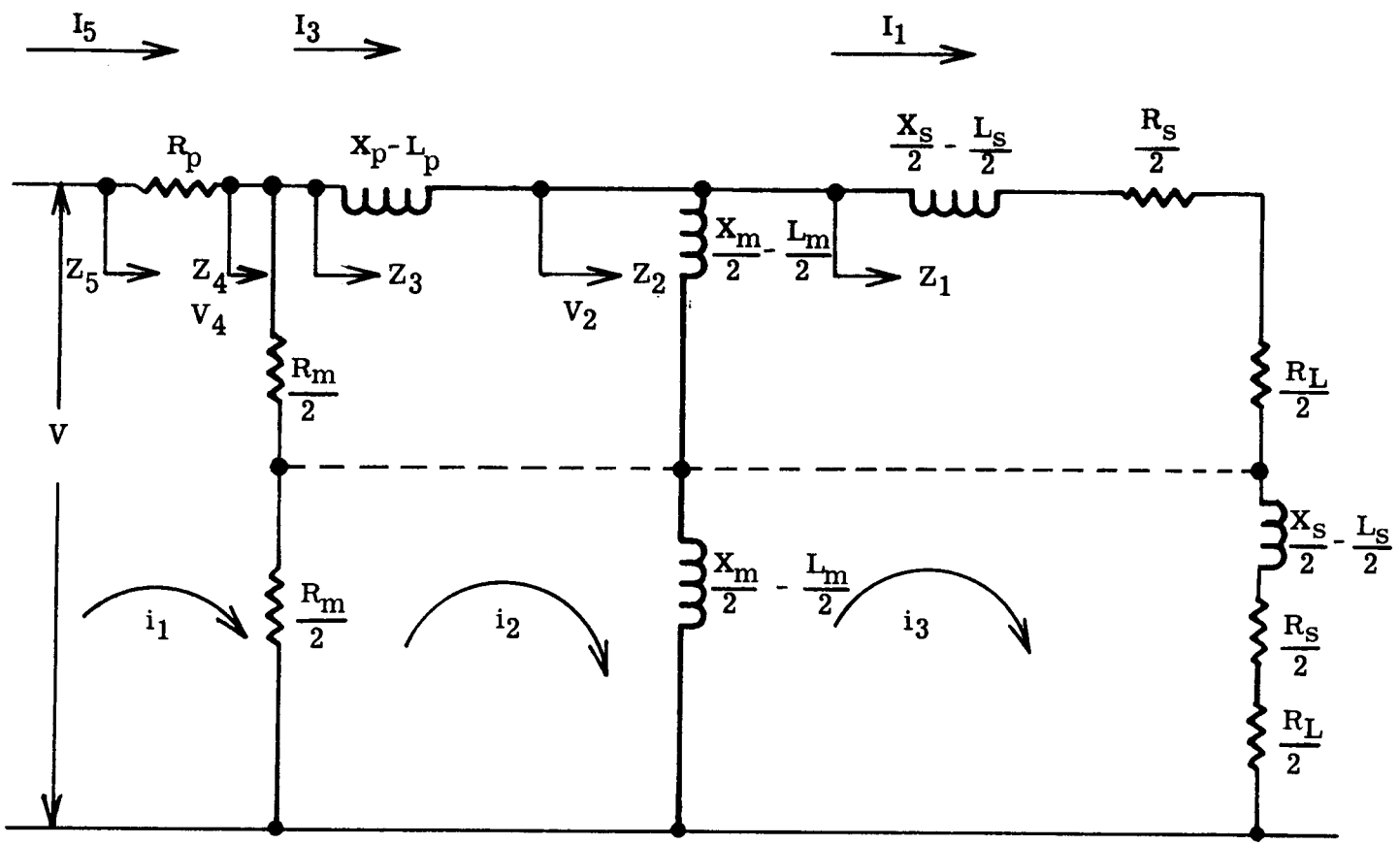

Final Values

$R_p = 2.0$	$L_p = 0.00763$	$L_m = 0.01588$	$L_s = 0.00775$
$R_m = 921$	$X_p = 239$	$X_m = 499$	$X_s = 243$
$P_p = 3.77$	$P_m = 7.83$	$P_s = 3.83$	$R_s = 19.4$
			$R_L = 600$

FIGURE 13. Equivalent Circuit For Reluctance Switch

An electrical circuit which is analogous to the magnetic circuit for the primary is shown in Figure 14. (Using the principal of superposition, the primary and secondary magnetic circuits can be handled separately.)

In the circuit

$P_{pm} = 15.65,\ 2P_{lp} = 7.54$

$P_{pm} = 2P_{lp} = 23.19$

Adding the two series permeances (which add like resistances in parallel) gives a total of 11.6.

P_p = Primary leakage permeance (series equivalent)

$$= \left(\frac{7.54}{23.19}\right)(11.6) = 3.77$$

P_m = Mutual permeance (series equivalent)

$= 11.6 - 3.77 = 7.83$

An electrical circuit which is analogous to the magnetic circuit for the secondary is shown in Figure 15a. Using the principle of superposition, this can be regarded as the sum of the two circuits shown in Figure 15b. If one circuit is solved for I_{lp} and I_m, the values can be multiplied by two. In the following, refer to Figure 15 for symbol definitions.

$$P_b = \frac{P_{pm}}{2} + 2P_{lp}$$

$$I_T = \frac{V\left(\frac{P_{pm}}{2}\right)\left(\frac{P_{pm}}{2} + 2P_{lp}\right)}{P_{pm} + 2P_{lp}}$$

$$V_b = \frac{I_T}{P_b} = \frac{V\left(\frac{P_{pm}}{2}\right)}{P_{pm} + 2P_{lp}}$$

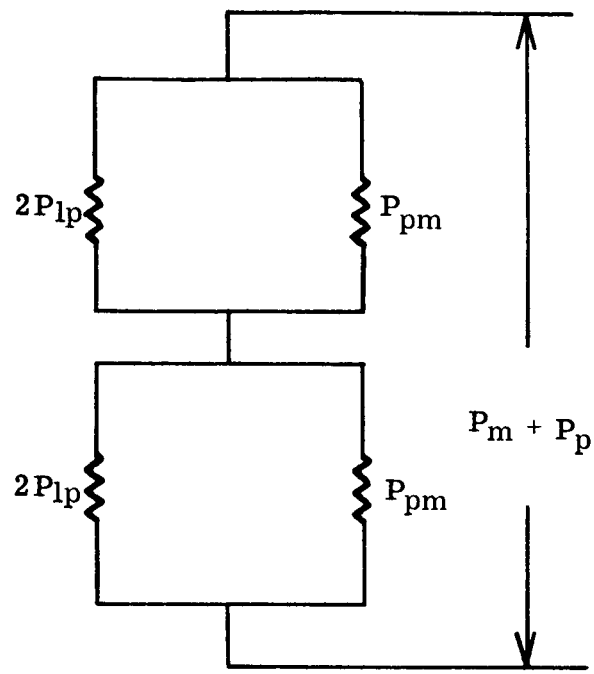

FIGURE 14. Primary Permeance Equivalent Circuit

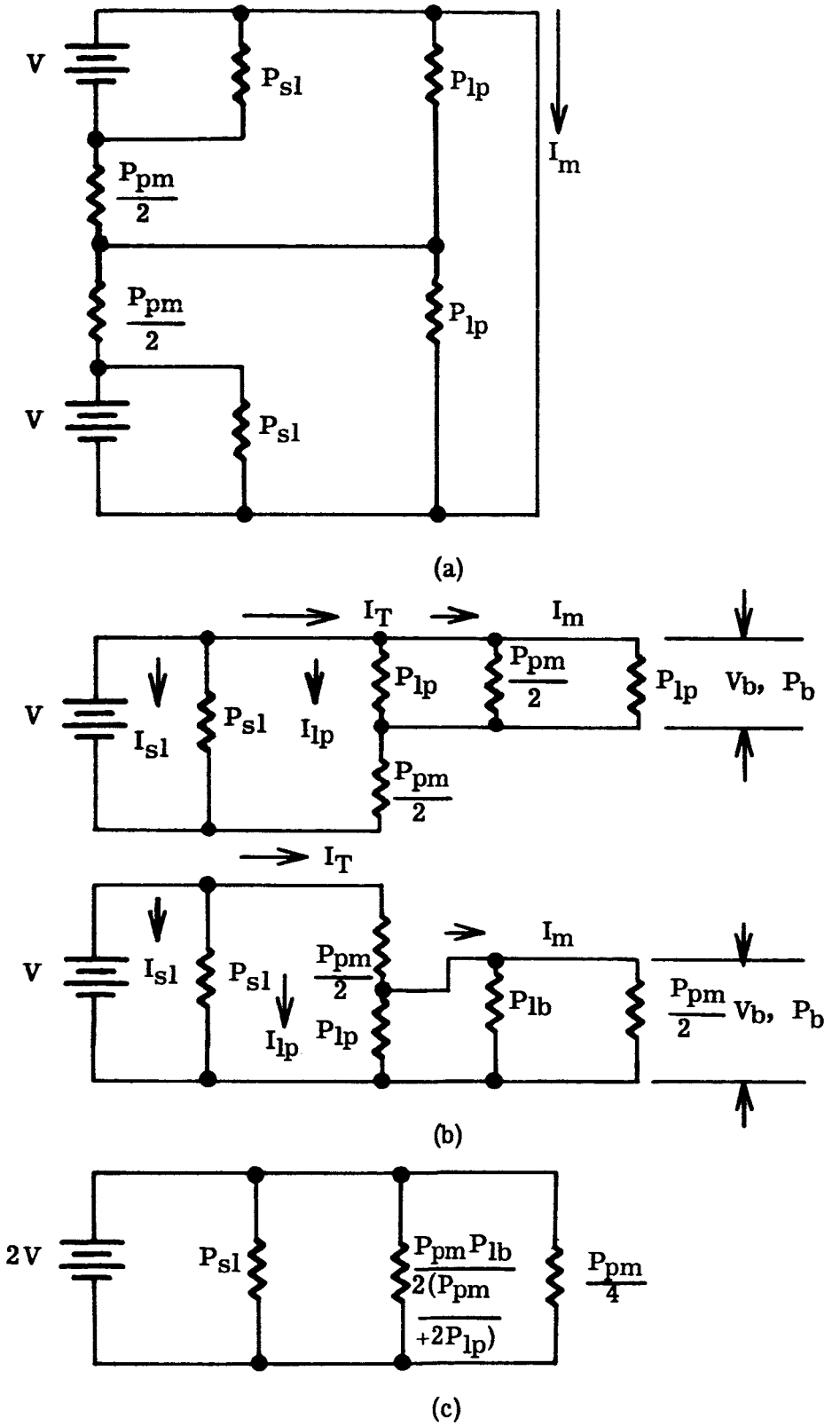

FIGURE 15. Secondary Permeance Equivalent Circuits

$$I_m = V_b \left(\frac{P_{pm}}{2} + P_{lp}\right)$$

$$= \frac{V\left(\frac{P_{pm}}{2}\right)\left(\frac{P_{pm}}{2} + P_{lp}\right)}{P_{pm} + 2P_{lb}} = \frac{V(P_{pm})}{4}$$

$$I_{lp} = (V_b)(P_{lp}) = \frac{(V)\left(\frac{P_{pm}}{2}\right)(P_{lp})}{P_{pm} + 2P_{lp}}$$

$$I_{lp} = \frac{(V)(P_{pm})(P_{lp})}{2(P_{pm} + 2P_{lp})}$$

$$I_{sl} = V(P_{sl})$$

In the analogy I_{sl} and I_{lp} correspond to leakage fluxes and I_m corresponds to flux that links the primary. These currents are half the total but the half circuits are driven by the mmf from only one tooth winding whereas in the total equivalent circuit, 2 opposite teeth windings form the secondary. Therefore, the circuit may be replaced by one as shown in Figure 15c. The total series permeance of the circuit is then

$$\frac{P_{pm}}{4} + \frac{P_{pm}\,P_{lp}}{2(P_{pm} + 2P_{lp})} + P_{sl}$$

The total series equivalent leakage permeance is

$$\frac{(P_{pm})(P_{lp})}{2(P_{pm} + 2P_{lp})} + P_{sl}$$

$$= \frac{(15.65)(3.77)}{2\,(23.19)} + 0.64 = 1.914$$

The mutual permeance $= \frac{15.65}{4} = 3.91$

These are for only one of the two secondary windings. Therefore,

$P_m = (2)(3.91) = 7.83$

$P_S = (2)(1.914) = 3.83$

Published data for 6 mil Monimax Steel shows that the core loss varies as the 1.71 power of the flux density at 5000 cycles per second. The core loss data for the steel gives 26 watts per pound for the core loss at 6 kilogauss or 38.7 kilolines per square inch. To take into account various punching stresses and high flux density areas, it is customary to multiply the value from the curve by a factor to make it agree empirically with what will occur in punchings like those used in motors. In this case the factor used was 1.92 giving a core loss of 50 watts per pound at a density of 38.7 kilolines per square inch.

ATW = 0.060
Stator teeth density = B_T
Rotor tooth width = 0.130

Each rotor tooth handles the flux from approximately

$(2)\left(\frac{7.83+2.6}{7.83}\right)$ stator teeth because of the 28.5 percent increase in rotor pole width over 2 slot pitches. Therefore

$$\text{Rotor Tooth Density} = \frac{(2)(0.060)(1.33)(BT)}{0.130}$$

$= 1.235\ B_T$

Rotor Core Thickness = 0.102

$$\text{Rotor Core Density} = \left(\frac{0.130}{0.102}\right)(0.5)(1.33)(BT)$$

$= 0.846\ B_T$

$$\text{Stator Core Thickness} = \frac{2.3 - 2.112}{2} = 0.094$$

The stator core and rotor core density would vary over the length because of leakage. However, for the purposes of this approximate analysis, the flux from 1.33 teeth are assumed to flow for the entire length of the core.

$$\text{Stator Core Density} = \frac{0.060}{0.094} \times 1.33\, B_T$$

$$= 0.85\, B_T$$

The weights of the various parts of the magnetic circuit as calculated from the dimensions of the punching and stack length assuming a density of 0.286 pounds per cubic inch and a stacking factor of 0.9 are as follows:

Stator Tooth Weight

$$= (0.225)(0.060)(0.105)(0.9)(0.286)(4) = 0.00146$$

Rotor Teeth Length = 0.325 approximately

Rotor Tooth Weight

$$= (0.325)(0.130)(0.105)(0.90)(0.286) = 0.00114$$

Rotor Core Weight

$$= \frac{\pi}{4}(1.191^2 - 0.988^2)(0.105)(0.9)(0.286) = 0.00944$$

Stator Core Weight

$$= \frac{\pi}{4}(2.3^2 - 2.112^2)(0.105)(0.9)(0.286) = 0.0176$$

Total core loss based on a fundamental sinusoid

$$= (50)\left(\frac{B_T}{38.7}\right)^{1.71}\Big[0.00146 + 0.00114\,(1.235)^{1.71} + 0.00944\,(0.846)^{1.71}$$

$$+ 0.0176\,(0.85)^{1.71}\Big]$$

$$= (50)(0.0017)(B_T^{1.71})\ (0.00146 + (0.00114)(1.435)$$

$$+ (0.00944)(0.751) + (0.0176)(0.757)$$

$$= 0.086\, B_T^{1.71}(0.00146 + 0.00164 + 0.00709 + 0.0133)$$

$$= 0.086\, B_T^{1.71}(0.02349) = 0.00202\ B_T^{1.71}$$

For a core loss of 0.642

B_T = 29 kilolines per square inch

This density is the peak flux density in the teeth. The peak flux in one tooth is

(29)(Tooth Area)

= (42)(0.060)(0.105)(0.9) = 0.1645 kilolines

The peak flux in the core is equal to the ratio of the total permeance to the mutual permeance times this value.

$$= \left(\frac{11.6}{7.83}\right)(0.238) = 0.243$$

Assuming the primary resistance is negligible in the circuit, the number of turns in the primary needed to drive this flux can be calculated using the basic transformer equation.

$$N_p = \frac{(22.5)(10^6)(\text{Effective Fundamental Voltage})}{(\text{Frequency})(\text{Peak Flux})}$$

$$= \frac{(22.5)(10^6)(24.3)}{(5000)(0.243)} = 450$$

Therefore, there will be 450 turns per side for the primary.

Depth of the primary slot = 0.225
The slot is 6 slot pitches wide

$$\text{Total Area} = \left(\frac{1}{4}\right)\left(\frac{\pi}{4}\right)\ (2.112^2 - 1.662^2) = 0.334$$

$$\text{Insulation Area} = \left[\frac{2.112\,\pi}{4} + (2)(0.225)\right] 0.01 = 0.021$$

0.01 is the thickness of the insulation

Net Area = 0.334 - 0.021 = 0.313

Use Number 25 wire for the primary

$$D^2 = \frac{0.313}{450} = 0.000695 \text{ available}$$

D^2 of #25 = 0.000424

$$\text{Slot Fullness} = \frac{0.000424}{0.000695} = 0.61$$

Assume that the width of one side of the primary coil cannot exceed the slot depth which is 0.225. Since the width of the core is 0.094 and the stack length is 0.105, the dimensions of the coil are known. Allowing 0.115 for clearance on two sides

$$\text{Length Mean Turn} = 2\left[0.225 + 0.105 + 0.225 + 0.094 + 0.115\right] = 1.538$$

Using a heat factor of 1.05

Rphot = hot primary resistance

$$= \frac{(1.05)(1.538)(450)(33)}{(12)(1000)} = 2.0 \text{ ohms}$$

For the secondary slot, the average slot width is 0.190; the slot depth is 0.225. Using an insulation thickness of 8 mils, the slot area

$$= (0.190)(0.225) - 0.008\left[(3)(0.225) + (2)(0.190)\right]$$

$$= 0.0344$$

Only half of this is available giving

Slot Area = 0.0172

The length mean turn is equal to

$$2\left[\frac{0.190}{2} + 0.060 + \frac{0.190}{2} + 0.125 + 0.105\right] = 0.964$$

where

0.060 = ATW

0.125 = 2 times the clearance per side

0.105 = stack length

$\frac{0.190}{2}$ = 1/2 of the average slot width

Ohms per inch for copper

$$= \frac{(0.881)(10^{-6})}{D_b^2}$$

where

D_b = bare diameter of wire

Assume N_2 turns per tooth and a 0.70 full slot.

$(\text{Insulated Diameter})^2 = 1.3D_b^2$ approximate.

$$\frac{(0.7)(0.0172)}{N_2} = 1.3D_b^2$$

$$D_b^2 = \frac{(0.7)(0.0172)}{1.3N_2}$$

$$\text{Rshot} = \frac{(1.05)(N_2)(0.881)(10^{-6})(0.964)(2)}{D_b^2}$$

for the winding on two teeth.

Substituting for D_b^2

$$R_s = 0.0001926N_2^2$$

$$\text{The turns ratio} = T = \frac{\text{Primary turns}}{\text{Secondary turns}}$$

$= \frac{450}{2N_2}$ (N_2 is the turns around one tooth)

Rshot referred to the primary

$$= \left(\frac{450^2}{4N_2^2}\right)(0.0001926)(N_2^2) = 9.74$$

The total secondary resistance is 2 times this

$$R_S = 19.4$$

$$R_m = \frac{24.3^2}{0.642} = 921$$

$$\text{Load Resistance} = \frac{9 \text{ volts}}{0.03 \text{ amps}} = 300 \text{ ohms}$$

For two circuits and referred to the primary

$$R_L = 600T^2$$

Therefore all the permeances and resistances for the circuit have been calculated. Inductances are related to the permeances by the turns squared

$$L_p = (450)^2(P_p)(10^{-8}) = (450)^2(3.77)(10^{-8}) = 0.00763$$

$$L_m = (450)^2(P_m)(10^{-8}) = (450)^2(7.83)(10^{-8}) = 0.01588$$

L_S referred to the primary

$$= \left(\frac{450}{N_2}\right)^2 (N_2)^2(P_s)(10^{-8}) = (450)^2(3.83)(10^{-8}) = 0.00775$$

$$X_p = 2(\pi)(5000)\ L_p = (31,400)(0.00763) = 239$$

$$X_m = (31,400)(0.01588) = 499$$

$$X_S = (31,400)(0.00775) = 243$$

All the constants of the equivalent circuit have thus been calculated. These constants are shown in Figure 13. The steady state solution of the circuit is given below for an assumed turns ratio of 1.

Several iterations on the turns ratio showed that the most optimum turns ratio is approximately 1. The solution is for a fundamental sine wave only.

$$Z_1 = 619 + j\,243 = 666 \angle 21.4$$

$$Z_2 = \frac{(666 \angle 21.4)(499 \angle 90)}{619 + j\,742} = 344 \angle 61.2$$

$$= 166 + j\,302$$

$$Z_3 = 166 + j\,302 + j\,239 = 166 + j\,541$$

$$= 566 \angle 72.97$$

$$Z_4 = \frac{(566 \angle 72.97)(921 \angle 0)}{921 + 166 + j\,541} = 430 \angle 46.5$$

$$= 296 + j\,312$$

$$Z_5 = 298 + j\,312 = 431 \angle 46.3$$

$$I_5 = \frac{24.3 \angle 0}{431 \angle 46.3} = 0.0564 \angle -46.3$$

$$\text{Peak } I_5 = \left(\sqrt{2}\right)(0.0564) = 0.080$$

$$I_5 R_p = 0.1128 \angle -46.3 = 0.078 - j\,0.0815$$

$$V_4 = 24.22 \angle 0$$

$$I_3 = \frac{24.22 \angle 0}{566 \angle 72.97} = 0.0428 \angle -72.97$$

$$I_3 X_p = (0.0428 \angle -72.97)(239 \angle 90) = 10.24 \angle 17.03$$

$$= 9.8 + j\,3.0$$

$$V_2 = 14.42 - j\,3.0 = 14.7 \angle -11.78$$

$$I_1 = \frac{14.7 \angle -11.78}{666 \angle 21.4} = 0.0221 \angle -33.18$$

= 0.0312 peak

The above steady state analysis shows that the design is close to that desired. To actually show what the secondary current is, it is necessary to make a transient analysis. Since only the secondary current is of interest, it should be sufficient to make the analysis only over the initial half-cycle. There will be an initial transient exciting current, but this should not affect the secondary appreciably.

In the following, the equations use common differential equation notation. The Laplace transform is used for solution.

(See Figure 13.)

Write loop equations using Kirchof's law.

$$V - i_1 R_p - (i_1 - i_2)R_m = 0 \tag{1}$$

$$(i_2 - i_1)R_m + \frac{L_p di_2}{dt} + \frac{L_m di_2}{dt} - \frac{L_m di_3}{dt} = 0 \tag{2}$$

$$L_m \frac{di_3}{dt} - L_m \frac{di_2}{dt} + L_s \frac{di_3}{dt} + (R_s + R_L)i_3 = 0 \tag{3}$$

Solving Equations (1) and (2) simultaneously

$$(L_p + L_m)\frac{di_2}{dt} - L_m \frac{di_3}{dt} + i_2\left(\frac{R_m R_p}{R_p + R_m}\right) - \frac{VR_m}{R_p + R_m} = 0 \tag{4}$$

Using Laplace transforms with initial conditions of everything zero at t = o.

$$(L_p + L_m)sF_2(s) - L_m sF_3(s) + F_2(s)\left(\frac{R_m R_p}{R_p + R_m}\right) - \frac{VR_m}{sR_p + R_m} = 0 \tag{4}$$

$$-L_m sF_2(s) + (L_m + L_s)sF_3(s) + (R_s + R_L)F_3(s) = 0 \tag{3}$$

Solving the two equations simultaneously for F3(s), the following is obtained:

$$F_3(s) = \left[\frac{L_m V R_m}{(L_p + L_m)(L_m + L_s)(R_p + R_m) - L_m^2(R_p + R_m)}\right]$$

$$\left[\frac{1}{s^2 + \frac{\left[(L_p + L_m)(R_p + R_m)(R_s + R_L) + (L_m + L_s)R_m R_p\right]s}{\left[(L_p + L_m)(L_m + L_s)(R_p + R_m) - L_m^2(R_p + R_m)\right]} + \frac{(R_s + R_L)R_m R_p}{(L_p + L_m)(L_m + L_s)(R_p + R_m) - L_m^2(R_p + R_m)}}\right]$$

$$P_3(s) = \left[\frac{L_m V R_m}{a_3}\right] \left[\frac{1}{s^2 + a_4 s + a_5}\right]$$

where

a_3, a_4, and a_5 have the meaning indicated by their substitution.

Solving and taking inverse transforms

$$i_3 = \frac{L_m V R_m}{a_3} \left[\frac{e^{-\left(\frac{a_4}{2} - \sqrt{\frac{a_4^2}{4} - a_5}\right)t} - e^{-\left(\frac{a_4}{2} + \sqrt{\frac{a_4^2}{4} - a_5}\right)t}}{2\sqrt{\frac{a_4^2}{4} - a_5}}\right]$$

Substituting in values

$a_3 = 0.281$
$a_4 = 47,600$
$a_5 = 4.06(10^6)$

$\frac{a_4}{2} = 23,800$

$$\sqrt{\frac{a_4^2}{4} - a_5} = 23,700$$

$$L_m V R_m = 410$$

At 5000 cps, one-half period equals 0 0001 seconds

$$i_3 = \frac{410}{(0.281)(23,700)2}\left[\frac{e^{+2.37} - e^{-2.37}}{e^{2.38}}\right] = 0.0302$$

Solution at other times shorter than 0 0001 seconds indicates that this current rises steeply to start Thus, it approaches a square wave. It is thus seen that the design is adequate for the output desired.

It is desired to obtain an estimate of the peak input current after the initial transient To do this, assume that the resistances of the circuit remain constant for the third harmonic.

The total impedance of the circuit to the third harmonic

$$= 692 \angle 31.2$$

Third harmonic voltage = 8.1

$$\text{Third harmonic current peak} = \frac{(\sqrt{2})(8.1)}{692}$$

$$= 0.0165$$

Assume the peak third and the peak fundamental add giving.

Peak input current = 0.080 + 0.0165 = 0.097

Therefore the calculations indicate that the reluctance switch as designed will deliver the 0.03 amps per secondary winding at 9 volts with a peak input of 0.097 amps The calculations are necessarily approximate However, considerable variation in the reluctance switch can be tolerated by the control circuit.

3. Mechanical Design of Rotating Package

A cross-sectional view of the design is shown in Figure 16. The external dimensions are shown in Figure 17. It is necessary for the functioning of the device that the rotating field of the PM motor be mounted to the same shaft as the rotors of the reluctance switches. It would ordinarily be necessary in the construction to keep track of the placement of the various phases in the PM armature, the location of the PM rotor in relation to the reluctance switch rotors, the relation of the reluctance switch stator to the PM armature, the relation of the reluctance switch secondaries to the control power bridge, and the relation of the power bridge to the various phases of the PM armature. However, since some adjustment of the reluctance switch is necessary, it was decided to leave enough adjustment so that the components would be assembled at random and the optimum adjustment determined later by test.

It was decided that adjustment of the reluctance switch stator would be more convenient than adjustment of the rotor. Therefore, provisions were made in the design so that both reluctance switches could be separately adjusted by approximately 45 mechanical degrees. It is necessary with this method to leave the determination of which reluctance switch is used for either rotation to the testing.

The stator of the PM motor is a conventional three-phase induction motor wound primary. It is held in place in the aluminum frame with a shrink fit to the frame. End bells are also made of aluminum with lightening holes. The end bells are piloted and held with safety wired screws to the frame.

The rotor of the PM motor is an 8 pole cast magnet with a keyway. The magnet has a slip fit with the shaft. A stainless steel ring with an extended tang fitting the permanent magnet keyway is pressed onto the knurled non-magnetic steel shaft. The tang extends into the keyway allowing a minimum of play. The cast magnet is machined to dimension, assembled to the rotor, and magnetized in place.

The reluctance switch rotor and stator punching laminations are bonded together with an epoxy resin. The reluctance switch stators have a slip fit to the reduced frame diameter. One stator fits against a shoulder on the frame. The second stator mounts against a spacer butting against the first stator. They are both held with two diametrically opposite screws. These screws mount into the frame shoulder and are locked with a stainless steel tab washer. Holes are drilled in the frame over the reluctance switch stators to allow the tester to rotate and lock the stators during the adjustment. Adjustment of the stator is allowed by long slots in the punchings.

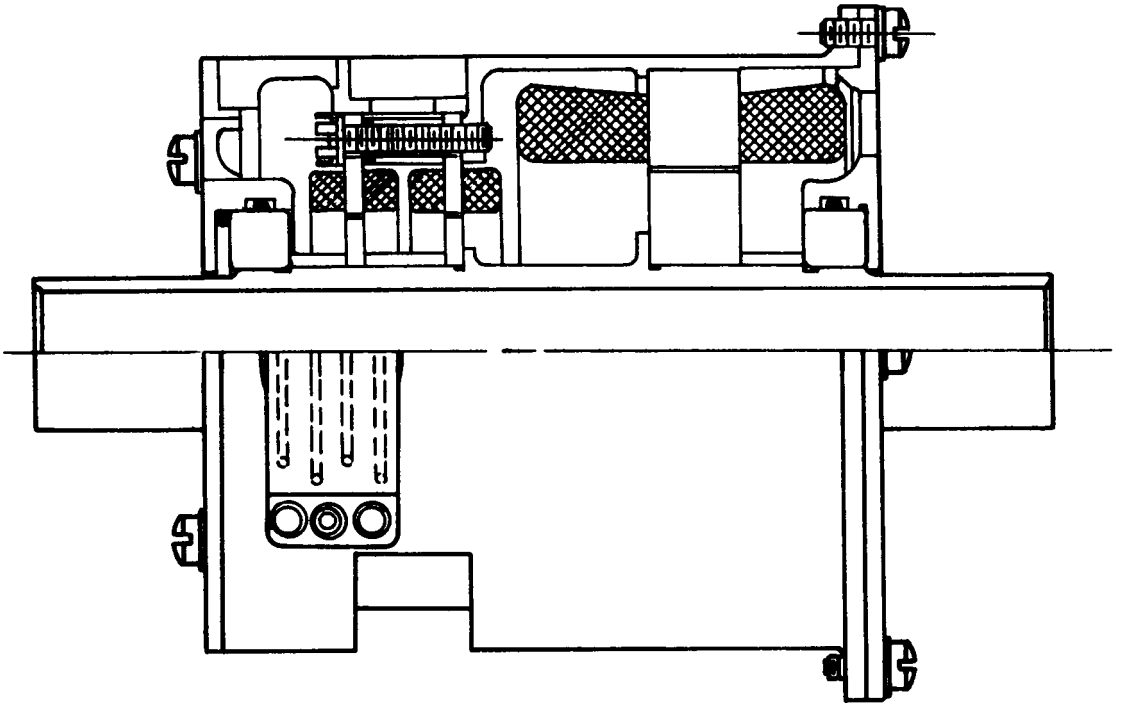

FIGURE 16. General Assembly of Rotating Package

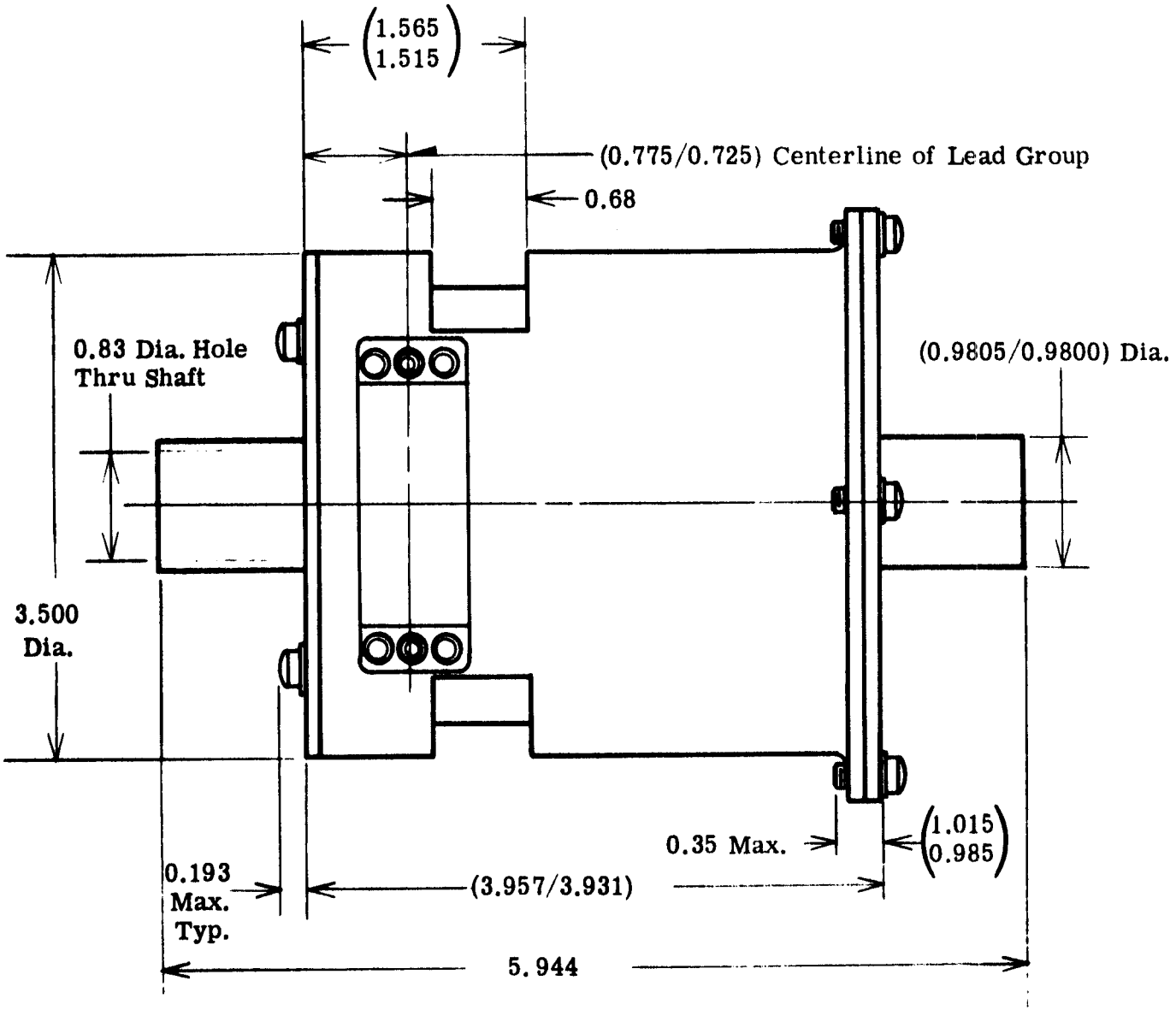

FIGURE 17. Outline of Rotating Package

The reluctance switch rotors are pressed on to a knurled shaft against a shoulder. The rotors are spaced by an aluminum spacer which is also pressed on the shaft. A second aluminum spacer is pressed onto the shaft outside and butting against the outside rotor to give a bearing shoulder. Shims are used in mounting the stators to insure alignment of rotors and stators.

All slot insulation is Pyre ML (glass impregnated with ML resin) and all wire enamel is ML. ML is a relatively new polyimide insulating resin developed by DuPont. The varnish is a chemically related aromatic polyether developed by Westinghouse called Doryl. All 33 teflon insulated leads are brought out through a Viton A grommet and through a teflon sleeve to the connector. The solder connections to the connector are covered with shrinkable irradiated polyethylene tubing. All hardware is stainless steel.

The bearings are modified MRC (Marlin Rockwell) catalogue number 1905-S extremely light series bearings. The modification consists of the removal of one shoulder of the outer race and the substitution of a new cage. The new cage is composed of a silver-mercury and teflon amalgram formed at high temperature and pressure.

Some short lab tests were run to establish the best combination. These are reported in Appendix V.

Since one shoulder is cut away, the bearings can sustain thrust in only one direction. The bearings are mounted so that they take thrust in opposite directions. Axial freedom of movement is obtained by placing a compressed O-ring in a groove in the aluminum housing between the housing and the bearing OD. Allowance for expansion, tolerance buildup, and some preload is made by installing an O-ring to be compressed between one bearing and the end bell in an axial direction. This arrangement avoids the possibility of cold welding of the bearing to the housing in the vacuum. The O-rings are made of Viton A synthetic rubber.

Balancing of the rotor is a requirement of the specification. The rotor is dynamically balanced to 0.01 ounce-inches squared by drilling holes in the shaft. These holes are drilled in two areas to obtain two balancing planes.

The aluminum was treated with a chemical film and all other components are inherently corrosion resistant, including the magnetic steels. Therefore, no provision was made for painting or otherwise protecting any surface.

During manufacture, heavy build ML enamel wire was substituted for the triple build for the reluctance switch secondary windings and a silicon rubber grommet was used instead of Viton A because of unavailability of material.

Using the dimensions of the parts and the specific weights of the various materials, the following calculation of the weights of the various components of the rotating assembly was made.

	Component	Weight
(2)	Reluctance Switch	0.354
	PM Motor Stator	0.873
	PM Motor Field Magnet	0.342
Total Active Electrical Weight		1.569 lbs.
	Shaft	0.338
(2)	Bearings	0.230
	End Bells	0.349
	Frame	0.408
	Connector	0.100
	Miscellaneous	0.100
Total Mechanical Weight		1.517
Total Calculated Weight	=	3.1 lbs.

4. Solid State Commutator Design

a. General

The following requirements of NASA Specification Number 63-135 were considered in the design of the commutator circuit.

(1) The torque motor commutation circuit, which includes rotor-position sensing drive and armature switching circuits, must use a minimum number of components and conservative derating practice.

(2) The commutator design must permit torque motor shaft position and speed control to be achieved by:

(a) Variation of the armature D. C. voltage excitation. The commutator must then function properly for armature terminal voltages ranging from 0 VDC to 40 VDC.

or

(b) Armature-voltage pulse modulation (pulse width, pulse frequency, etc.) in a pulsed drive system. The commutator must then be compatible with such a system,

providing an armature switching method that can be suitably controlled.

(3) The torque motor commutator circuit must be designed for minimum losses not to exceed 0.5 watts.

The assumption was made in the original proposal that this requirement applied at the 30 RPM no-load speed condition. It was also estimated that the losses would approach 2.5 watts maximum. Present design requirements indicate that the commutator losses will approach this value.

(4) The commutator must be able to withstand continuous stall current at 60 VDC excitation (approximately 2.0 amperes) without damage or deterioration of performance.

(5) Semiconductor components are to be silicon wherever possible.

(6) The commutator must be capable of operating in a vacuum of 1×10^{-9} mm Hg for a 1 year period.

(7) The commutator must operate properly over a temperature range of -10°C to 70°C.

(8) The commutator must operate properly after 50g, 2 msec shock and 5 minutes of random vibration (20-2000 cps, 15g rms) in each of three mutually perpendicular directions.

(9) The size and weight considerations for the commutator package were not defined by the NASA Specification. However, the maximum outline dimensions and estimated weight which were established by the contractor is as follows:

Height	-	2.25 inches
Width	-	4.75 inches
Length	-	5.60 inches

Estimated Weight = 1.75 pounds maximum

The commutator circuit, exclusive of the reluctance switch which is considered part of the motor, consists of three subcircuits. These are:

(a) three-phase bridge inverter
(b) squaring circuit
(c) reluctance switch drive oscillator

The design considerations of each circuit will be discussed separately.

b. Three Phase Bridge Inverter

A bridge inverter as shown in Figure 18 is used to switch the armature current in the torque motor. The inverter utilizes silicon power transistors as switching elements. Controlled rectifiers could be adapted to this circuit; however, they were not selected because of gating problems resulting from operation in a direct current circuit.

The power transistors selected for this application are the RCA type 2N3442. Several factors influenced the selection of this transistor. The maximum operating voltage applied to the input terminals of the bridge is 60 volts d-c. It can be seen from Figure 18 that when transistor Q4 is in a saturated state, the collector to emitter voltage of Q1 will be

$$V_{CE(Q1)} = V_{input} - V_{CE\ (SAT.\ Q4)}$$

Since the saturation voltage is very low as compared to the input voltage it can be assumed for design purposes that full input voltage will appear across Q1. Therefore, a transistor with a V_{CE} capability of at least 120 volts should be used. This allows a safety factor for transient voltages. The type 2N3442 has sustained V_{CE} rating of 140 volts maximum. Other factors influencing the selection of this transistor are d-c gain, saturation voltage and current carrying capability.

Upon analyzing the bridge inverter, it can be seen that every current path traverses two collector to emitter voltage drops. Therefore, the total instantaneous collector power dissipation is equal to two times the collector voltage drop multiplied by the total instantaneous power supply current to the inverter bridge. Similarly, the total average collector power dissipation is two times the collector drop multiplied by the average inverter current. The collector losses due to switching are considered negligible since the speed of the motor determines the switching frequency For this application, the maximum motor speed is 100 RPM which represents a switching frequency of only 400 cycles per minute or approximately 7 cycles per second. Since the inverter must be able to operate at continuous duty during locked rotor conditions, it is therefore imperative that the collector voltage drop be maintained at a minimum in order to maintain high efficiency.

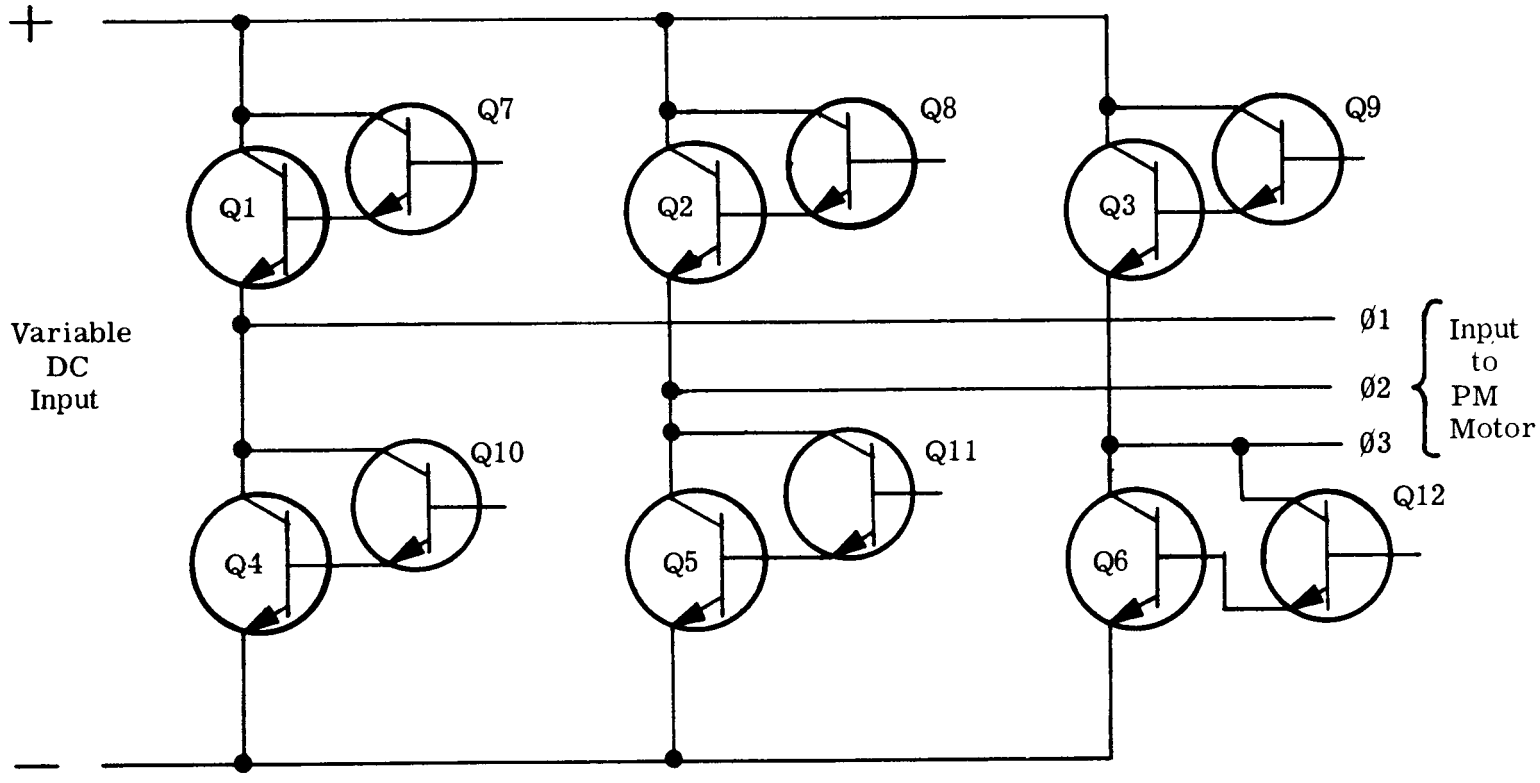

FIGURE 18. Three-Phase Inverter With Driving Transistors

The maximum collector current which will be sustained by any one of the bridge transistor is 2.08 amperes required by the motor design. This magnitude of current will occur at locked rotor conditions with 60 volts d-c applied at the input terminals of the bridge in a -10°C ambient.

With a collector current of 2.08 amperes, the minimum gain of the type 2N3442 is 20. (This value was taken from published data and occurs at a case temperature equal to 125°C.)

Under these conditions a base drive current of at least 0.1 ampere will be required. The source of drive power for the inverter switches is the reluctance switch. In order to keep the power requirements of the reluctance switch as low as possible, a single stage of amplification is used. The driver transistor is a RCA type 34381 connected to the power transistor in a direct-coupled (Darlington) configuration. It is recognized that when the direct-coupled amplifier configuration is used the collector-to-emitter voltage of the power transistor is dependent upon the collector-to-emitter saturation voltage of the driver plus the base-emitter drop of the power transistor. As a result, the collector-to-emitter voltage of the power transistor will be slightly higher than its saturation voltage because the power transistor will not be driven into complete saturation.

The addition of a series diode into the power transistor's collector circuit will cause saturation; however, it has not been included in this design since the power dissipation per power transistor will only approach 2 watts under the most extreme conditions. This dissipation is far below the capabilities of the power transistor selected.

c. Squaring Circuit

It was determined by testing a sample reluctance switch that the half-wave rectified and filtered base drive signals from the pick-up windings approach the wave shapes shown in Figure 19. This slowly varying output signal (in amplitude) provides the base drive for the inverter bridge power transistors. This type of signal is not compatible with the inherent high speed capability of semiconductor devices. As the base drive source varies from the "OFF" signal level to the "ON" signal level, the power dissipated in the switching transistor is somewhat as shown in Figure 20. The excessive power dissipation reduces the efficiency of the static commutator and is not tolerable in this application since the torque

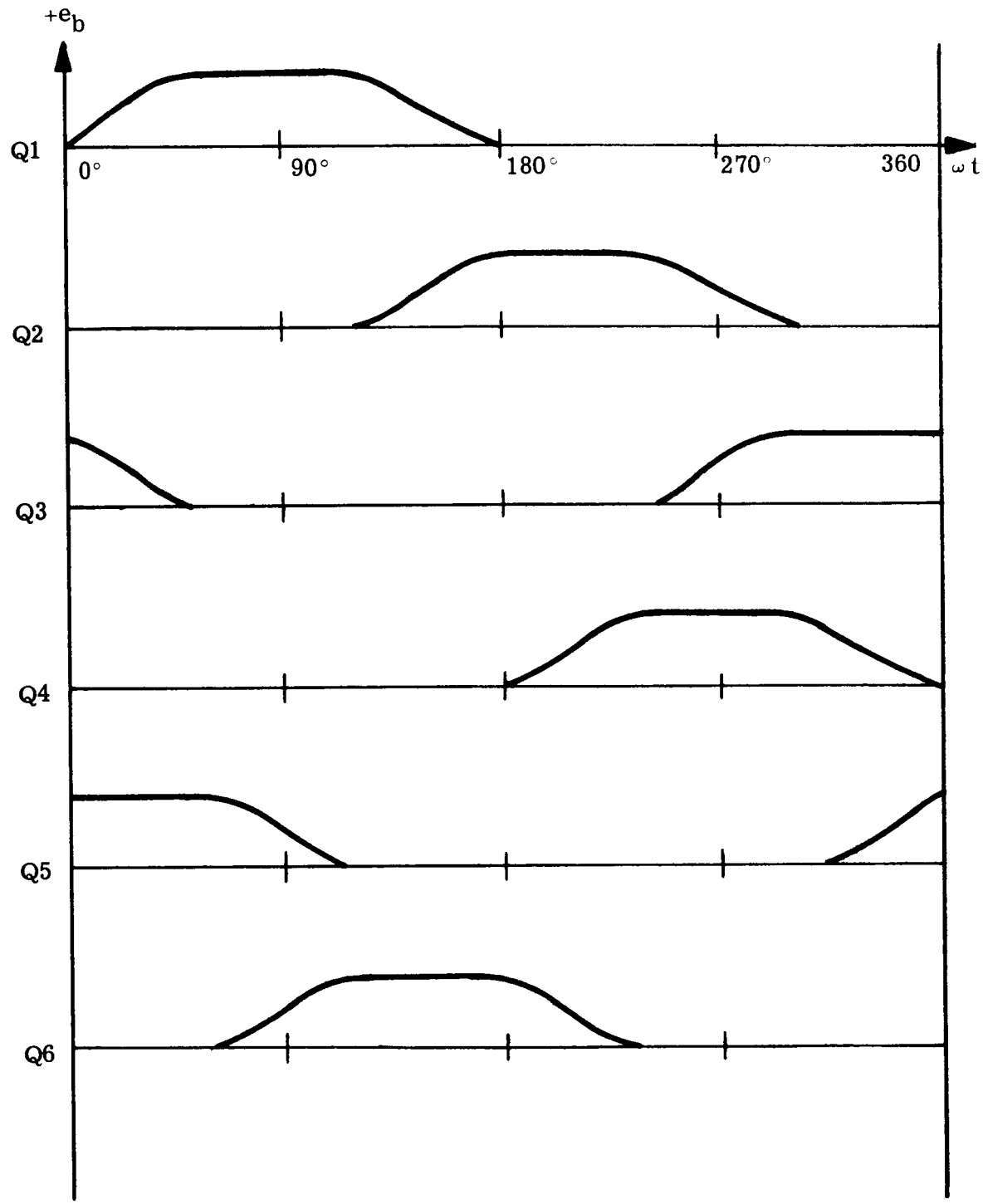

FIGURE 19. Base-Drive Waveforms

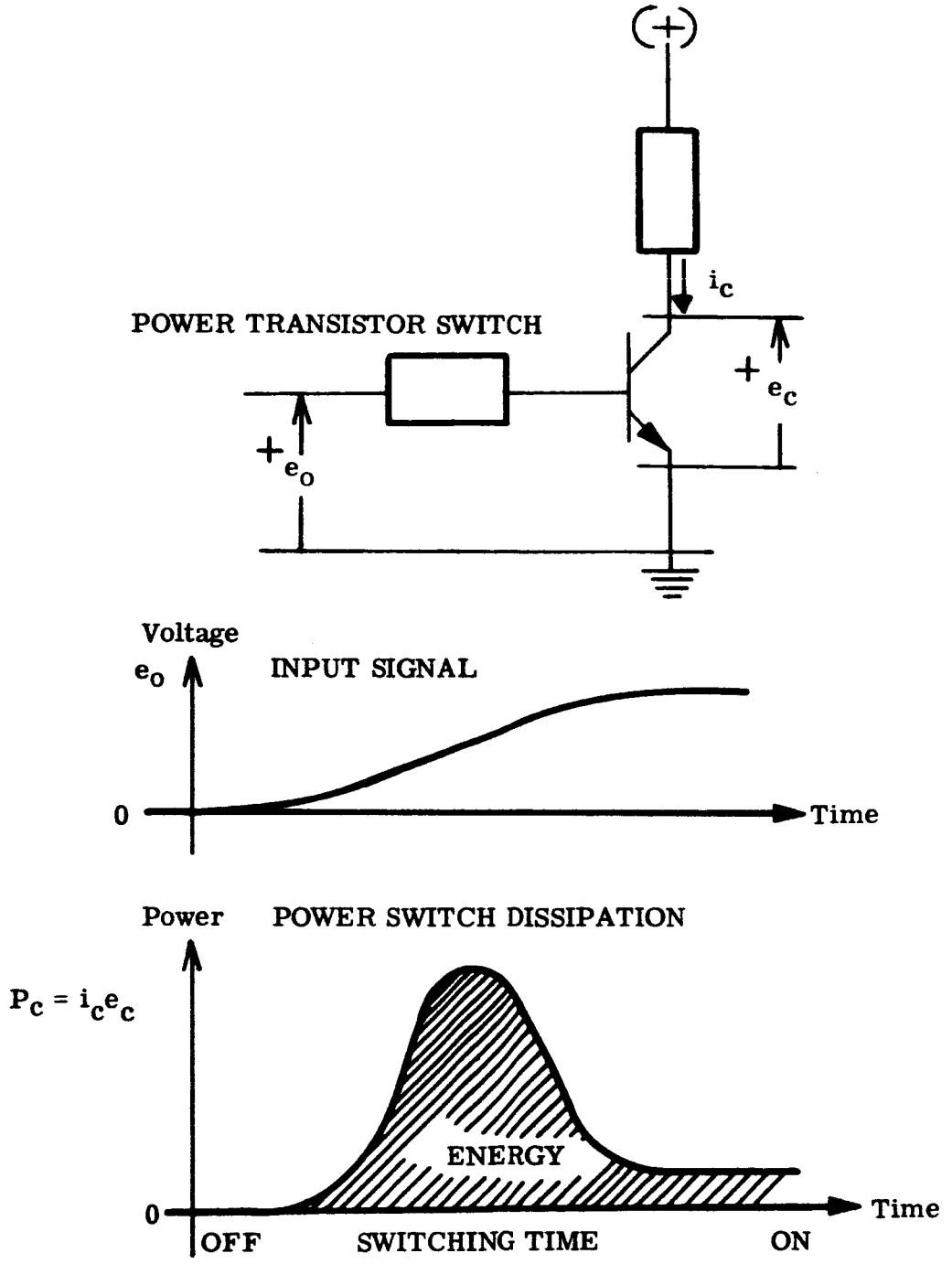

FIGURE 20. Switching Characteristics

motor must be operated in a locked rotor state. In order to take advantage of the high speed switching capabilities of semiconductors, it is necessary to convert the output signal from the reluctance switch to a digital "ON" or "OFF" voltage.

Various circuits employing the characteristics of semiconductors for converting an analog to a digital signal were considered for this application. One type of circuit which provides a square wave output independent of the shape of the input voltage is a Schmitt trigger. This type of circuit requires a d-c voltage supply which is independent of the source voltage. To adapt this type of circuit to the three-phase bridge inverter, isolated bias signals are required. This circuit was not further pursued because of its complexity. A tunnel diode driving a transistor provides the type of characteristic required to obtain a digital response; however, over the temperature range required for operation there is insufficient voltage supplied to assure turn on of the transistor. A silicon tunnel diode has a forward point voltage between 0.75 and 1.0 volts.

The squaring circuit used utilizes a silicon controlled rectifier. The low level silicon controlled rectifier has many advantages over other semiconductor devices for this application. This device is especially adaptable for digital response conversion since it has but two forward biased states, namely, conducting (on) and blocking (off). It is characteristic of this device, as opposed to a transistor, that the change of state from "OFF" to "ON" occurs over an interval of time which is independent of the magnitude of the input signal. A gate controlled switch could be used in place of the controlled rectifier. This would be necessary if the device was required to be turned "OFF" during the conduction period. Since the controlled rectifier is being applied in such a way that turn-off is not required, there is no apparent advantage in using a gate controlled switch.

The circuit used is shown in Figure 21. One of these circuits is required to drive each switch in the inverter bridge. The input to the squaring circuit is an amplitude modulated square wave which has a frequency of 5000 cycles per second and a peak voltage of 9 volts. A type 2N1595 silicon controlled rectifier (SCR_1) is used to determine the level of the source voltage. The controlled rectifier is gated from the voltage divider R_3 and R_4 and will be set to fire the controlled rectifier at approximately 6 volts. R_4 is a variable resistor and provides selectability of the response level. This in turn sets the width of the conduction angle for each power transistor, thus determining the waveform of the voltage applied to the motor stator windings. The controlled rectifier switches "ON" and "OFF" at the frequency of the source; there-

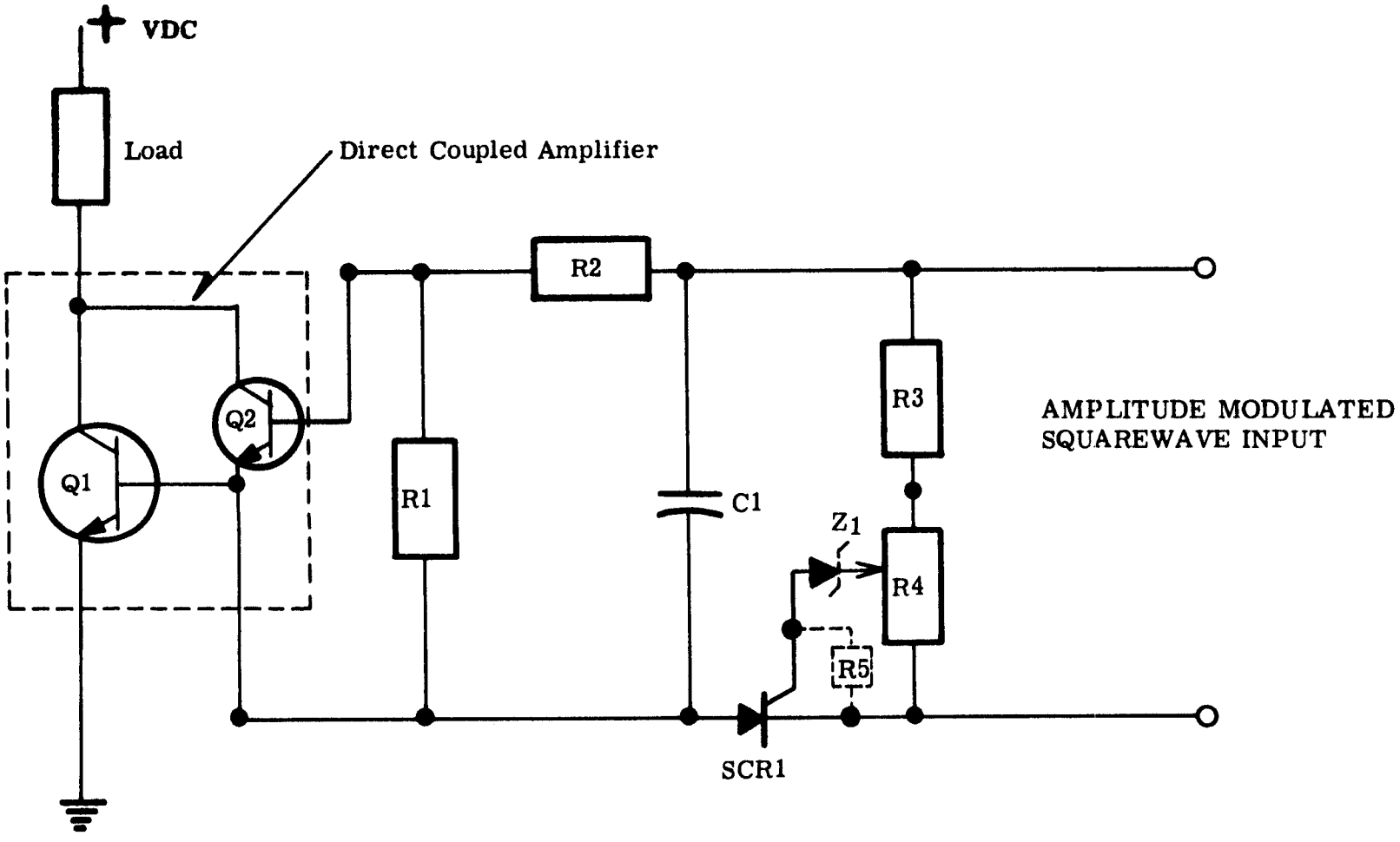

FIGURE 21. Squaring Circuit

fore, control is regained every negative half cycle. Resistor R_2 limits the base drive to transistor Q_2. This resistance is set at a level which assures saturation of Q_2 when the controlled rectifier fires. Resistor R_1 is a leakage bypass. It provides a path for leakage current to flow, and prevents partial turn on of Q_2 just prior to the firing of the controlled rectifier. Capacitor C_2 filters the half-wave rectified signal. The capacitor is charged during the positive half cycle. During the negative half cycle, when SCR_1 is in a non-conducting state, the capacitor will discharge through R_2 and Q_2, keeping Q_2 in a saturated state. Figure 22 is representative of the action made possible by this circuit and has been verified by test.

Tests made on the completed unit with the control unit heated to a high temperature (71°C) showed that the firing level of the SCR's changed excessively. Consequently a Zener diode was added to the circuit so that the SCR fired on the Zener breakdown voltage instead of its own. A resistor was added between the gate and cathode of the SCR to prevent false triggering resulting from pick-up. The added components are shown in dashed lines in Figures 21 and 22.

d. Reluctance Switch Drive Oscillator

A square wave oscillator is used to provide the drive power for the reluctance switch. Two identical oscillators are used in this application, one to provide power to one reluctance switch for clockwise rotation and the other to provide power to the second reluctance switch for counterclockwise rotation. Only one oscillator would be required if a multiple contact switch or relay for reversal is substituted. In line with the philosophy of using static components in the commutator circuit, two oscillators were selected.

Several arrangements of the square wave oscillator are possible - Royer, Jensen or resistive coupled. The resistive coupled oscillator as shown in Figure 23 will be used. This configuration assures self-starting without the addition of starting circuits; therefore, a minimum number of components are required. The design uses a saturable core transformer paralleled with the reluctance switch primary windings. Using this approach,the saturable core transformer is not required to carry the load power, thereby reducing its power losses and size. Electrical isolation is provided by the reluctance switch.

In addition to the saturable core transformer, the basic oscillator consists of two similar transistors and two base drive resistors. The oscillator is driven from a constant 28 volt d-c source. The peak collector current as determined from the requirements of the reluctance switch is approximately 100 milliamperes. Based on

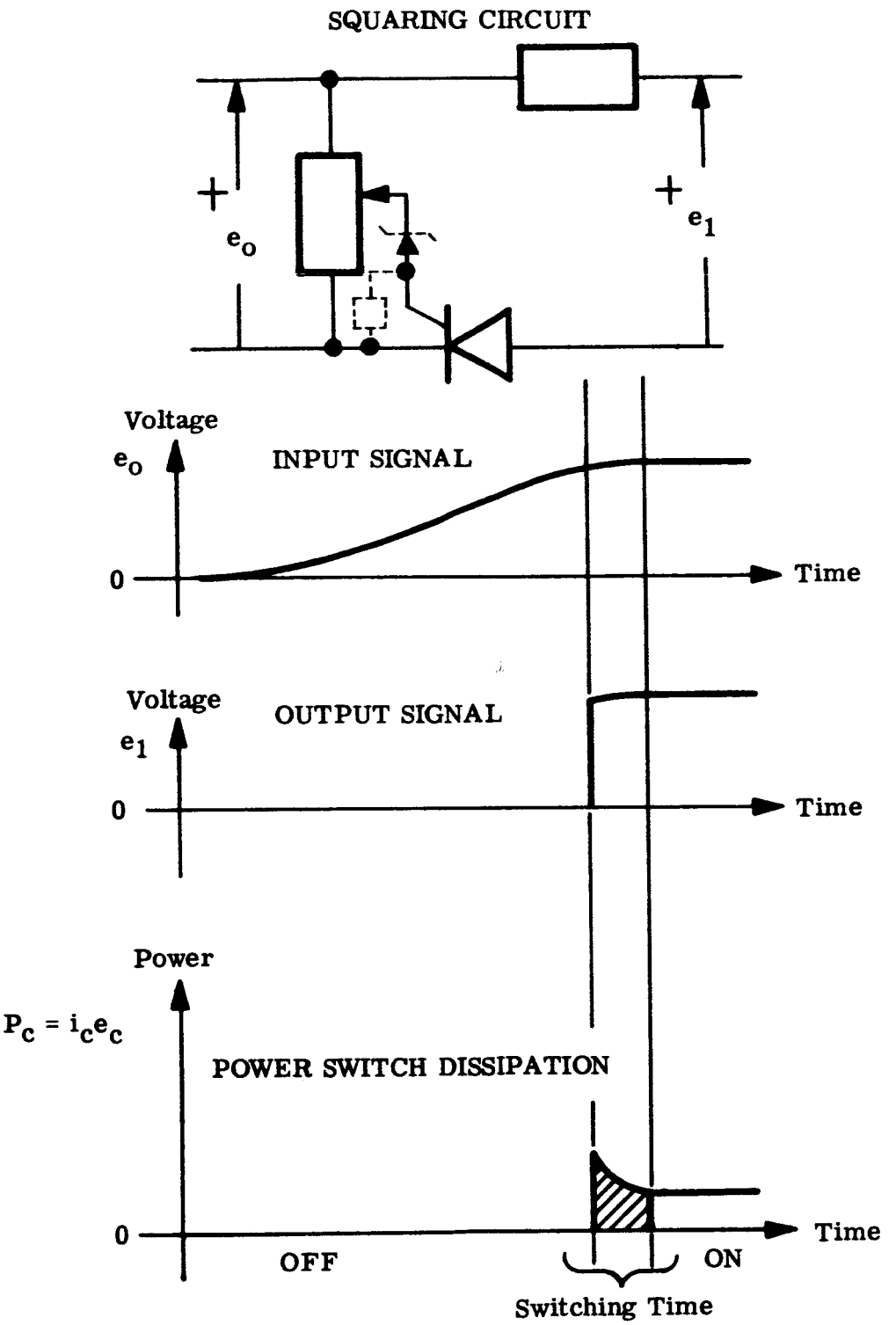

FIGURE 22. Digital Switching Characteristics

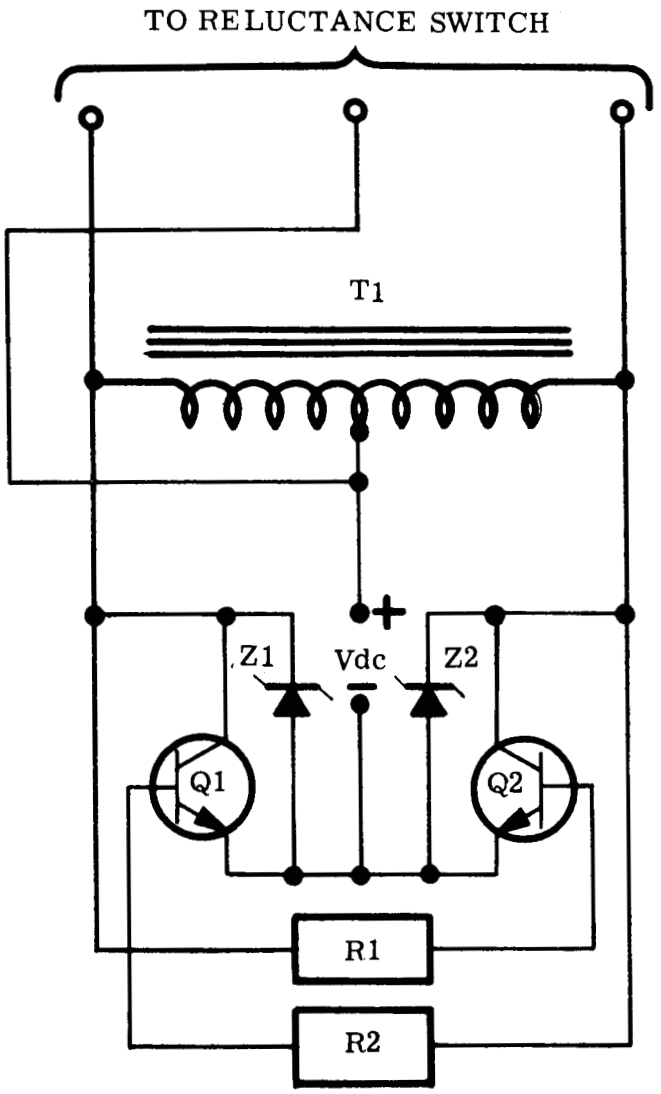

FIGURE 23. Resistive Coupled Oscillator

these requirements, RCA type 34381 transistors were used.

The determining factors in establishing the maximum drive frequency are core loss in the reluctance switch and turn-on time of the controlled rectifier in the squaring circuit.

For example, the turn-on time of the controlled rectifier as used in the squaring circuit was measured to be 8×10^{-6} seconds. Setting the time for one-half cycle equal to 10 times the turn-on time of the controlled rectifier, the maximum frequency can be determined. Using the equation

$$T_o = \frac{1}{f}$$

the resulting frequency is:

$$(10)(8 \times 10^{-6}) = \frac{1}{2f}$$

$$16 \times 10^{-5} = \frac{1}{f}$$

$$f = 6250 \text{ cps}$$

The drive frequency was set at 5000 cycles per second which allows a margin of safety.

Standard design techniques were used in determining the requirements of the saturable core transformer. Square-loop core material was used. The transformer is a toroidal type with two windings of 227 turns each. Double coated ML enamel wire Number 33 is used. The size of the transformer is approximately 0.44 x 0.75 inches.

Preliminary tests on a complete unit indicated that switching spikes of approximately 50 volts were present. De-spiking was accomplished by using Zener diodes in place of diodes for commutation.

5. Mechanical Design for the Control Package

The control is designed to operate in a vacuum of 1×10^{-9} mm of mercury. The thermal design is such that the unit will operate satisfactorily in this type of environment when cooled by radiation or conduction to a heat sink. During operation at sea level conditions, the unit is designed to cool by natural convection.

All components are mounted on aluminum brackets. The completed assemblies are coated with epoxy varnish to help retain the components and assure a constant heat path to the bracket. Heat generated by the components is conducted through the bracket to the base and outside surface. The type of mounting surface is unknown; however, if the mounting surface will conduct the heat away and if it is at a low enough temperature, most of the generated heat will be carried away by conduction. If this is not the case, most of the heat will be conducted to the outer skin of the package from which it will be radiated.

To facilitate the heat transfer to the base or the outer skin, all joints where a vacuum gap may occur under vacuum conditions, are filled with epoxy material to assure a constant heat path.

The control, while operating at locked rotor and high input voltage, will generate approximately 6 watts of heat. The surface area of the package is approximately 50 square inches; therefore, the surface must dissipate approximately 0.12 watts per square inch. Figure 24 shows an outline of the control package. The outline dimensions are in accordance with the dimensions originally established. The weight was estimated at 1.37 pounds.

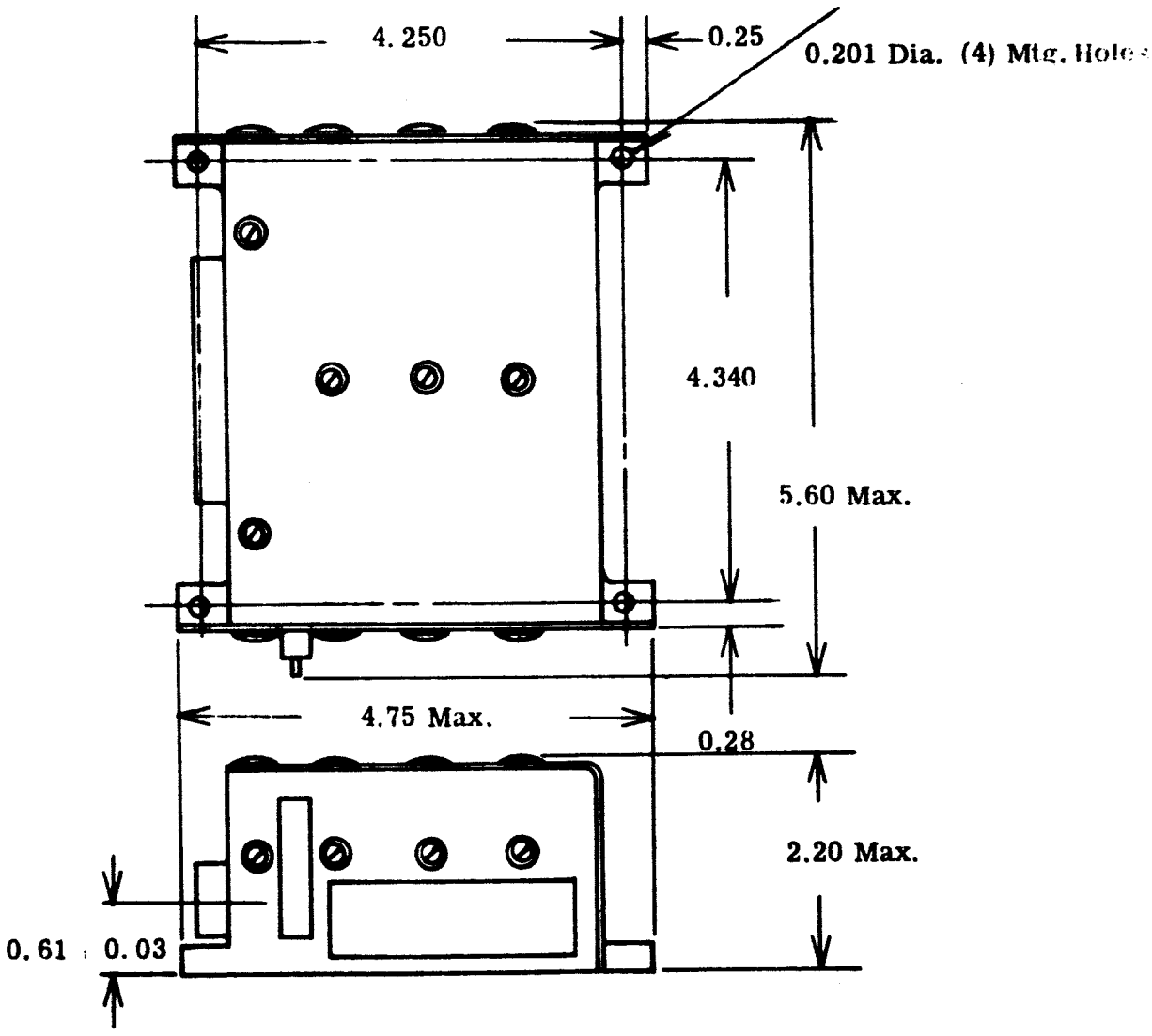

FIGURE 24. Outline of Control Package

C. Summary and Discussion of Test Results

Test results are given entirely in Appendix IV. The test methods and explanations are complete in that section. A summary and a comparison of specification, calculated, and test values are given in Table I. Each point in the table is discussed below.

1. Diameter

The maximum specification diameter was chosen in the design as offering the most efficient utilization of space.

2. Weight (Motor Only)

The specification weight of 2 pounds was intended to be the motor only. The addition of the two reluctance switches to the motor package increases the weight considerably. The test weight was larger than the calculated weight for the following reasons:

a. Insufficient allowance in the calculations for lead weight on the reluctance switch.

b. Insufficient allowance for varnish absorption in the electrical parts.

c. An error in the shaft weight calculations.

3. Torque

The torque motor exceeds the specification in this regard. Since the cooling characteristics of the motor in the application are unknown, the torque and current were measured when the motor temperature rise was approximately equal to the temperature rise used in the calculation. There is excellent agreement between calculated and test results.

4. Motor Current

The motor meets the specification in this regard also. Again test results agree almost exactly with calculated values.

5. Approximate No-Load Speed.

The voltage given is the voltage at the armature terminals per the specification. The actual line voltage was 5.0 volts with the difference being the drop in the switches. The voltage is approximate since it was obtained from an oscilloscope.

TABLE I. Comparison of Calculated,Test, and Specification Parameters

Parameter	Spec. Value Spec. No. 63-135	Calculated Value	Test Value
Diameter (Max.)	3.5 inches	3.5	3.5
Weight (Motor only)	2 lbs (without commutator)	3.1 lbs (Including reluctance switch)	3.4 lbs
Torque	100 oz-in. at 40 VDC	102 oz-in.	101.1 oz-in. average
Motor Current	1.0 amp at 40 VDC	1.0 amp at 76.5°C	0.99 amp at ≈ 79°C
Approximate No-load Speed	30 rpm at 3 VDC at armature	Not Calculated	28 rpm at 3.4 volts
No-load Losses at 30 RPM	0.5 watts	Not Calculated	0.19 watts at 28 rpm
Peak-to-Peak Ripple Torque	10 percent or 0.5 oz-in.	11.8 percent	14.8 to 23.3 percent or less than 2 oz-in.
Static Friction Torque	0.5 oz-in.	Not Calculated	2.5 oz-in (Includes cogging)
Commutator Losses	0.5 watt	2.5 watts	2.2 watts
Reluctance Switch Secondary Resistance Primary Resistance Output Voltage Output Current		 9.28 ohms 1.9 ohms 9.0 average 30 ma peak	 9.18 to 10.63 1.272 to 1.298 9.0 approx. 23.8 ma avg.
Motor Winding Resistance		21.4 ohms	21.2 to 21.5
Weight (Control)		1.37 lbs	1.4 lbs

6. No-Load Losses at 30 RPM

The motor is well under the specification.

7. Peak-to-Peak Ripple Torque

The specification and calculated values were considerably exceeded. This is primarily due to the inability to obtain exact adjustment of the firing angles on the triggers and hence the switching angles. As shown in Appendix IV, although the firing angle should have been 37.5 mechanical degrees and the switching angle 7.5 mechanical degrees, the actual values ranged from 34 to 40 and 3 to 11 respectively. The highest spread was obtained on Motor No. 2 which gave the highest ripple.

Because of manufacturing variations, there are differences in the output voltages of the reluctance-switch sensing windings. There are four firing periods for each switch in one revolution. Thus the output voltage is subject to variation because the particular sensing winding voltage is influenced by four different positions of the rotor with consequent variation in the magnetic circuit.

Even with this variation, it was usually possible to adjust the trimmer pot so that the length of the conduction periods for any one sensing winding and switch in one revolution were fairly equal and close to 37.5 mechanical degrees; however, the same trimmer pot is used to adjust the firing angles for the same switch when it is under the influence of the other reluctance switch for the opposite rotation. There was much more variation between reluctance switches than between positions on one reluctance switch. Consequently, it was necessary to make the adjustment a compromise between the clockwise (CW) and counterclockwise (CCW) adjustments with the resulting wide variation previously cited.

The effect of the variation in switching angle is to increase ripple and to lower average torque. This occurs because the PM field is farther than 15 electrical degrees away from its maximum torque position in relation to the armature field when the related switching period begins or ends.

The 14.8 to 23.3 percent ripple was obtained at 40 volts input at locked rotor. A 2.4 oz-in. ripple was obtained at 3 volts input. However, this appears to be considerably in error. The error is believed to be due to friction between the torque arm and scale and friction in the motor itself. Static friction torque (breakaway torque) was measured as 2.5 oz-in. This figure is divided between static friction torque and magnetic cogging. It is not known how much is due to which parameter. It is believed, however, from extension of the running torque values at 3 volts (which would not be subjected to the same errors) that the average value of locked torque is less than 2.0 oz-in. Therefore, the total ripple due to switching

angle variation and magnetic cogging is at most less than 2.0 oz-in. at 3 volts.

The above points show the need for having separate adjustments for each reluctance switch. The situation would be greatly improved by the elimination of one reluctance switch by some means or by sharpening of the voltage pulse by elimination of the tooth tips in the reluctance switch stator. If either or both of these were done, it is expected that the ripple would approach the calculated value of 11.8 percent. Use of a delta connected winding with 60 degree switching angles would also improve the ripple slightly.

8. Static Friction Torque

The specification value is exceeded by only a small amount since the total breakaway torque was measured as 2.5 oz-in. of which part is due to magnetic cogging.

9. Commutator Losses

The tested value is below the calculated value even though both exceed the specification value. Any improvement in this value would probably entail optimization of the reluctance switch and trigger design.

10. Rest of Table

The test values for the rest of the items in the table show good agreement with calculated values with the exception of the reluctance switch primary winding resistance. The lower value occurs because the actual winding had a lower average perimeter than that used for calculation.

Scope pictures of various voltages in the circuit were taken and are presented in Figures 27 through 34 in Appendix IV. These are discussed in the following text.

Figure 27. - This picture shows the approximate quasi-square wave line-to-line voltage applied to the armature terminals as the motor rotates.

Figure 28. - This picture shows the on-off periods of the Darlington amplifier as the motor rotates. The "on" period (high wave) should be 37.5 mechanical degrees while the "off" period should be 52.5 mechanical degrees or 150 and 210 electrical degrees respectively. The bottom or CCW picture shows approximate agreement with these values while the top or CW picture deviates. This is due to the previously mentioned inability to adjust the conduction periods exactly.

Figures 29 and 30. - These pictures show no-load and loaded line currents. The difference between current values for 2-leg and 3-leg conduction is apparent. Also the discrepancy between switching angles between CW and CCW rotation is evident.

Figure 31. - This picture shows the output at one oscillator. Values of the picture indicate a frequency of approximately 4750 cycles per second. Switching spikes present using the original circuit were clipped with Zener diodes.

Figure 32. - This picture shows the output voltage of a reluctance switch sensing winding. The bottom pulse is the one being used in the coupled state. The capacitor filters the switching spike from this pulse. The switching spike is obvious in the uncoupled state. This spike did not appear harmful to the operation of the motor.

Figure 33. - This picture shows the current in the driving circuit of a Darlington amplifier in the "on" state. The ripple, because of the half wave rectification, is obvious.

Figure 34. - This picture shows the trigger voltage at the input to the trigger for the coupled and uncoupled state. The top coupled picture is of interest. As time proceeds from right to left, the initial rise in voltage and drop due to charging the capacitor is evident. As time progresses, the capacitor charges and the voltage rises. Then the reverse pulse occurs and the capacitor discharges until another positive pulse occurs.

Speed-torque curves were run on one motor at several voltages in one direction of rotation. Another speed torque curve was run for comparative purposes on the second motor at 40 volts. These curves plus the currents are shown on Figure 25. Some points appear to be considerably in error. These are plotted and connected to the curve to which they apply. The reduction in torque at locked rotor is due partially to heating of the motor at the higher voltages and partially to errors inherent in the locked torque readings. The locked torque value for 3 volts input appeared to be considerably in error. Because of this and because the values are so small the 3 volt curve was not plotted. Only the 60 and 40 volt current curves for Motor No. 1 are plotted. The other current curves would be virtually indistinguishable from the 40 volt curve on the scale used.

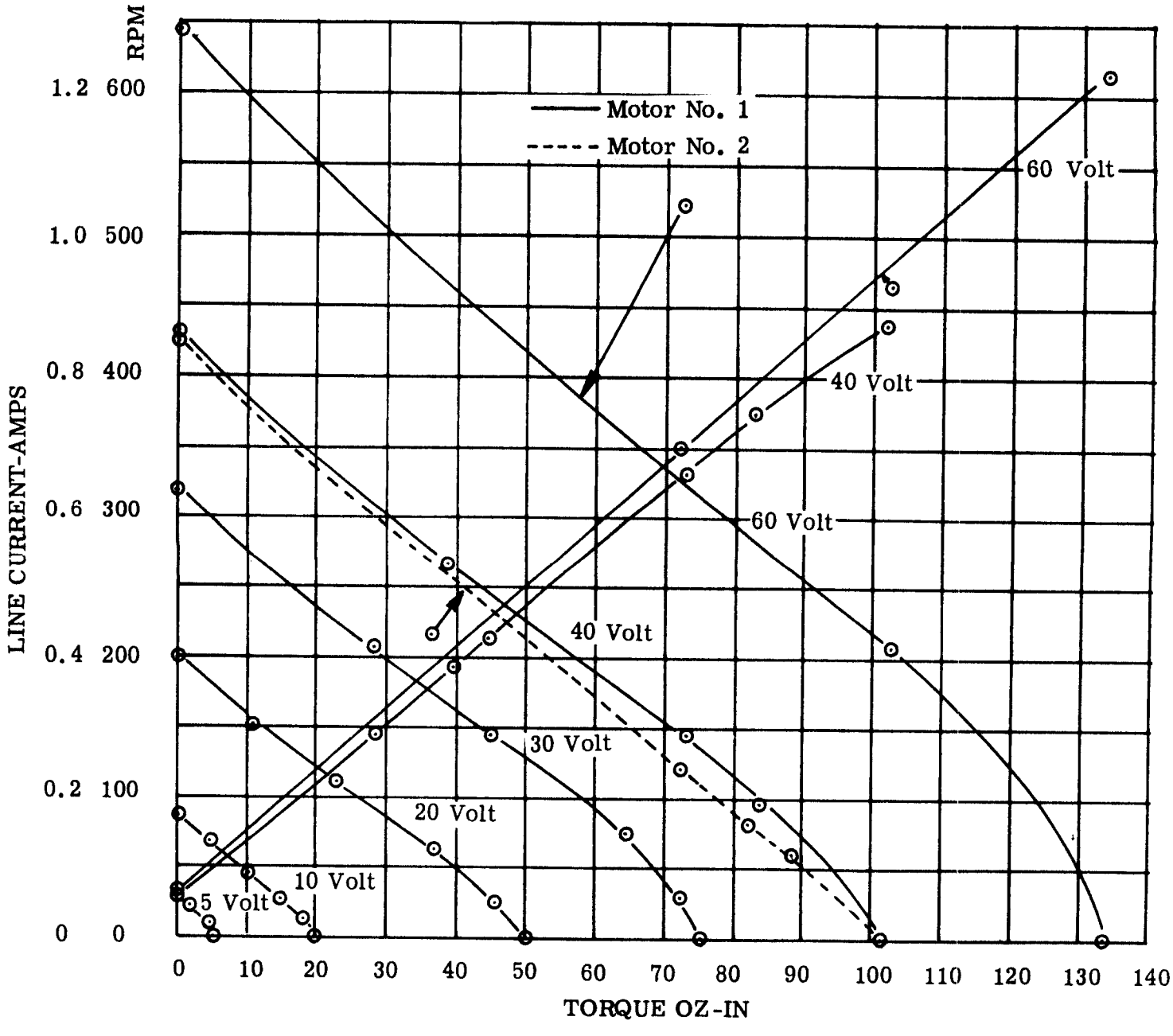

FIGURE 25. Speed and Current Vs. Torque

III. NEW TECHNOLOGY

To comply with the "New Technology" reporting requirements as defined by paragraph 3.2.3 of TID-S-100, exhibits A and D are included. These exhibits are identified to the following.

Exhibit A - Disclosure No. 63,411, Disclosure Book No. 7737, Page 17.

Exhibit D - Disclosure No. 64,500, Disclosure Book No. 7738, Page 18.

The disclosures are being processed by the Westinghouse Patent Department in accordance with Westinghouse policies and procedures. These were formerly reported in the first quarter report.

EXHIBIT A

Title:

A multiple pole rotor position sensing device for controlling a three-phase transistor bridge commutator.

Description:

This position sensing method uses a constant number of sensors, dependent upon the number of phases of the circuit being driven. The number of switching steps is changed by varying the number of separate entities into which the driving function is divided or the number of separate paths for the driving function on a rotor. (i. e. poles, light sources, etc.)

Uses:

Senses rotor position and provides drive signals to switch armature currents in brushless d-c motors and is being utilized in performance of this contract.

EXHIBIT D

Title:

Digital response level detector.

Description:

The use of a controlled rectifier gated from a voltage divider to obtain a quickly varying (digital) response from a slowly varying (analog) driving function.

Uses:

a. Circuit protection

b. Signal shaping circuit

c. Amplitude detecting circuit

IV. CONCLUSIONS AND RECOMMENDATIONS

A. Conclusions

1. The permanent magnet motor is close to the lightest and smallest that could be built with the design limitations. The motor weight was 3.4 pounds versus a calculated 3.1 pounds. Weight reduction could be obtained by utilization of the following four items.

   a. Elimination of one of the reluctance switches required for reverse rotation by some means (using relays or static switches).

   b. Use of smaller leads on the reluctance switch.

   c. Use of a smaller shaft. The present shaft exceeds the specification size because of a misinterpretation of the shaft diameter specification.

   d. Compaction of motor winding end turns. This would require tool development, but would save a small amount of weight due to length reduction in the frame.

2. The ripple torque due to switching angle variation is high. The amount of ripple due to this component could not be predicted in the original design. Consequently the specification values were accepted only as design objectives. The ripple could be lowered by incorporation of any of the following changes.

   a. Elimination of one reluctance switch by some means. The primary cause of switching angle variation is the differences in output voltage between reluctance switches.

   b. Elimination of tooth tips on the reluctance switch stator teeth and possibly sharpening the end of the teeth to obtain a sharper output voltage wave. This will also make the reluctance switch easier to wind and insulate.

   c. Use an adjustment potentiometer for both reluctance switches if one reluctance switch is not eliminated.

   d. Use of 60 degree switching angles with a delta-connected armature winding.

3. The magnetic cogging torque was reduced by the use of a 45-slot punching with a magnetic can in the bore of the stator. Even though the resulting value did not appear to meet the objective it is felt that it is approximately the minimum obtainable without entailing sacrifice in motor size and weight. The approximate value obtained was less than 2 oz-in. The specification value was accepted in the original proposal as a design objective.

4. Static friction torque specification design objectives were also exceeded. It is felt, however, that with the solid lubricant bearings in the size used, the value obtained was not excessive.

5. The weight of the control box agreed almost exactly with calculations at 1.4 pounds.

6. Torque and current specification values were met or exceeded with the design. There was excellent agreement between calculated and test values.

7. The specification requirement of a no-load speed of approximately 30 rpm with 3 volts at the armature terminals is considered to have been met. Test values were 28 rpm at 3.4 volts.

8. The no-load running motor losses at 30 rpm were 0.19 watts which is lower than the specification requirement of 0.5 watts.

9. The watts loss in the commutator circuit was 2.2 watts which is less than the proposed value of 2.5 watts but more than the specification objective of 0.5 watts. Some improvement in this value could be obtained by optimization of the reluctance switch and trigger circuit design.

B. Recommendations

1. The improvements mentioned above should be pursued and incorporated into the design.

2. Methods should be investigated for the incorporation of a pulse-width modulation speed control. Since the basic solid-state switching circuit is already present, introduction of the speed control should not prove expensive in complexity or size.

3. The present method of adjusting the reluctance switch is impractical. The position of the reluctance switch should be frozen with only a small adjustment allowed. The design should be changed to make adjustment easier.

4. The flanges on the top of the control package should be removed. This will ease the installation of the circuit boards.

V. BIBLIOGRAPHY

1. Roters, Herbert C., Electromagnetic Devices, John Wiley and Sons, Inc., 1941

2. Veinott, Cyril G., Theory and Design of Small Induction Motors, McGraw-Hill Book Co., Inc., 1959

3. Manual 7. Design and Application of Permanent Magnets, Published by Indiana General Corporation, Magnet Division, Valparaiso, Indiana

VI. NOMENCLATURE

Symbols and Abbreviations

NOTE: All length and area dimensions are in inches and square inches.

A - Area of flux path.

A_1 - Specific Area - See Figure 8.

A_2 - Specific Area - See Figure 8.

ACT - Coil throw in slots.

AG - Air gap.

ASW - Average slot width.

ATW - Tooth width.

AT/in - Ampere turns per inch.

a - Magnet dimension - See Figure 7.

a_1 - Slot dimension - See Figure 12.

a_2 - Slot dimension - See Figure 12.

a_3 - Symbol used for literal substitution for complex function.

a_4 - Symbol used for literal substitution for complex function.

a_5 - Symbol used for literal substitution for complex function.

B - Flux density (general).

B_{AG} - Flux density in the air gap in lines per square inch.

B_m - Flux density in the magnet in lines per square inch.

B_T - Flux density in the teeth in lines per square inch.

b_s - Tooth length.

VI. NOMENCLATURE
(Continued)

C - Designation for a capacitor.

C_f - Multiplier - See Appendix.

C_p - Coil perimeter.

CR - Designation for silicon diode.

c - Dimension of magnet - See Figure 26.

c_s - Slot dimension - See Figure 12.

D - Diameter at the center of the air gap.

D^2 - Maximum insulated diameter of wire squared.

D_a - Average diameter of winding.

DBS - Depth below slot.

D_b - Bare wire diameter.

d - Dimension of magnet - See Figure 26.

d_s - Slot dimension - See Figure 12.

e - Dimension of magnet - See Figure 26. Also pole enclosure in per unit.

e_o - Instantaneous input voltage.

e_1 - Instantaneous output voltage from squaring circuit.

e_b - Instantaneous base to emitter voltage.

e_c - Instantaneous collector to emitter voltage.

e_s - Slot opening.

$F_1(s)$ - Laplace transform.

VI. NOMENCLATURE
(Continued)

$F_2(s)$ - Laplace transform.

$F_3(s)$ - Laplace transform.

f - Frequency.

GSWA - Slot area excluding slot insulation.

H - Ampere turns per pole at any point.

H_1 - Total ampere turns per pole supplied by the magnet.

I, I_1, I_2, I_3, I_5 - Steady state current in amperes - Refer to text for specific application.

I_a - Total effective armature current in amperes.

ID - Dimension of magnet - See Figures 26 and 7.

I_{lp} - Analogous flux current - See Figure 15.

I_m - Analogous flux current - See Figure 15.

I_{sl} - Analogous flux current - See Figure 15.

I_T - Analogous flux current - See Figure 15. Also insulation thickness.

i_1, i_2, i_3 - Instantaneous currents - See Figure 13.

i_c - Instantaneous collector current.

VI. NOMENCLATURE
(Continued)

j - Symbol for $\sqrt{-1}$.

K - Constant in torque formula.

K_S - Slot leakage constant.

L - Effective air gap length.

L_f - Leakage factor - Multiplier on the air-gap flux to obtain the magnet flux.

L_m - Mutual inductance.

L_p - Primary inductance.

L_S - Secondary inductance.

l - Magnet dimension - See Figure 7. Also length of flux path.

l_1 - Magnet dimension - See Figure 7.

M - Designation for motor.

mmf - Magneto motive force.

N_2 - Turns per secondary tooth.

N_p - Turns in primary.

OD - Outside diameter.

P, P_1, P_2, P_3, P_4, P_5, P_6 - Permeances - See text for specific application.

VI. NOMENCLATURE
(Continued)

P_b - Permeance - See Figure 15.

P_f - Empirical constant in coil perimeter equation.

P_l - Total leakage permeance.

P_{ep} - Total primary leakage permeance for the reluctance switch for half the magnetic circuit.

PM - Permanent magnet.

P_m - Mutual permeance (series equivalent).

P_p - Primary leakage permeance (series equivalent).

P_{pm} - Mutual permeance.

P_s - Secondary leakage permeance (series equivalent).

P_{sl} - Total slot leakage permeance.

p - Number of poles.

p_c - Instantaneous power dissipation.

pp - Number of parallel paths.

Q - Designation for transistor.

R - Dimension of magnet - See Figure 26. Also designation for resistor.

Rhot - Total hot motor resistance.

R_L - Load resistance referred to the primary.

R_m - Core loss resistance.

R_p - Primary resistance.

Rph - Phase resistance.

Rphot - Hot primary resistance.

R_s - Secondary resistance referred to the primary.

Rshot - Hot secondary resistance.

r, r_1, r_2, r_3, r_4 - Dimensions of magnet - See Figure 26.

SCR - Designation for silicon controlled rectifier.

S_f - Saturation factor - Multiplier on air-gap length to account for the mmf required by the steel.

S_p - Number of armature slots.

s - Slots per pole - Also Laplace complex variable.

T - Turns ratio - primary to secondary. Also designation for transformer.

T_o - Period of oscillator output wave.

T_p - Tooth pitch.

TPC - Turns per coil.

t - Time.

V, V_2, V_4 - Voltages - See Figure 13 and text for particular designation.

V_b - Voltage - See Figure 15.

VI. NOMENCLATURE
(Continued)

V_{CE} - Collector to emitter voltage.

$V_{CE(SAT)}$ - Saturation collector to emitter voltage.

w - Stack length.

X_m - Mutual reactance.

X_p - Primary reactance.

X_S - Secondary reactance referred to the primary.

Z - Total effective armature series conductors.

Z_1, Z_2, Z_3, Z_4, Z_5 - Impedances - See Figure 13.

Zph - Total series conductors per phase.

Δ - Single air gap length.

θ - Angular dimension of magnet - See Figure 26.

μ - Absolute permeability of air = 3. 19.

ϕ - Flux in lines per pole. Also, designation for a particular phase.

ϕ_l - Leakage flux.

Ω - Resistance of one inch of wire.

VII. APPENDIX I

Derivation of Leakage Permeance Formula
Refer to Figure 9 and Figure 26.
Derivation of Permeance Formula For P_3

$$\theta = \frac{2\pi}{p} \quad , \quad p = \text{Number of Poles}$$

$$H \text{ at } r = \frac{H_1(r-r_1)}{r_2-r_1}$$

where:

H = mmf per pole at any point.

H_1 = total mmf per pole supplied by magnet.

The derivation is based on the mmf being zero at r_1 and rising to H_1 at r_2. This is a close assumption since the gap at r_1 is actually close to zero.

$$\text{Permeance} = \frac{\mu A}{l} \quad \text{generally}$$

where:

μ = permeance of material which in the case of air = 3.19

A = area of path

l = length of path

Therefore at r

$$dP = \frac{\mu \, wdr}{r \frac{\theta}{2}}$$

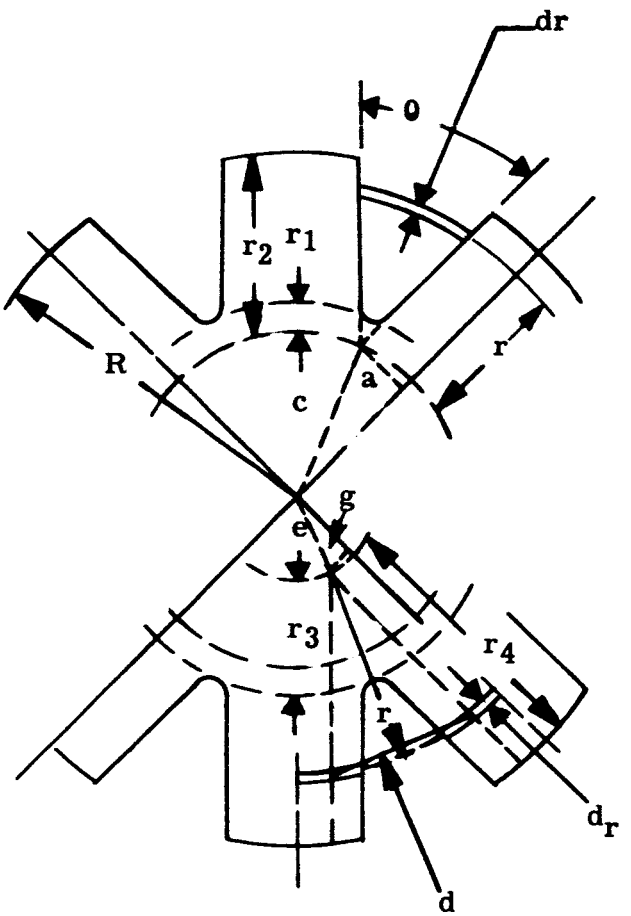

FIGURE 26. Symbols For Permeance Derivations

where:

w = length of stack

$r\frac{\theta}{2}$ = length of 1/2 of the arc (The permeance to be derived is half way across the gap because the mmf for the rest of the path is assumed to be supplied by the other pole.

$$\phi_1 = H_1 P_3$$

where:

ϕ_1 = the total leakage flux in permeance path P_3

P_3 = total leakage permeance P_3

$$d\phi_1 = \frac{2H_1(r-r_1)}{r_2-r_1} \quad \frac{\mu w dr}{r\frac{\theta}{2}}$$

The 2 multiplier comes from there being two sides to the magnet.

$$\phi_1 = \frac{2H_1 \mu w}{(r_2-r_1)\frac{\theta}{2}} \int_{r_1}^{r_2} (dr - \frac{r_1 dr}{r})$$

$$= \frac{2H_1 \mu w}{(r_2-r_1)\frac{\theta}{2}} \left[r_2 - r_1 + r_1 \ln \frac{r_1}{r_2} \right]$$

$$P_3 = \frac{\phi_1}{H_1}$$

$$P_3 = \frac{2 \mu w}{(r_2-r_1)\frac{\theta}{2}} \left[r_2 - r_1 + r_1 \ln \frac{r_1}{r_2} \right] C_f$$

a = 1/2 magnet chordal pole width

$$c = \frac{a}{\sin\frac{\theta}{2}}$$

$$r_2 = R - c$$

$$r_1 = \frac{ID}{2} + a - c$$

Because the average mmf does not occur at the middle of the pole length, it is necessary to multiply by a correction factor C_f. The same will be true of P_2 and P_1. The following value of C_f will tend to give high leakage.

$$C_f = \frac{r_4 - r_3 + a + 2l_1}{\text{Length of Magnet}}$$

Derivation of Permeance Formula for P_2

Use Roter's formula for a half cylinder (See Reference 1). The taper does not matter in this derivation.

Roter's formula for half cylinder is in the notation of this report.

$$P = 0.26 \ \mu \ (r_2 - r_1) C_f$$

The actual paths of interest since an mmf-per-pole basis is used are 4 quarter cylinders having a total of 1/2 the length and 4 times the area giving a multiplier of 8 on the above formula. However, only the average mmf is effective which is 1/2 the total approximately. Therefore, the total multiplier is 4 or

$$P_2 = 1.04 \ \mu \ (r_2 - r_1)$$

Derivation of Permeance Formula for P_1

$$d = 2r \sin \frac{\theta}{2} \quad \text{(chordal length)}$$

Average length of path d forms the base of the semicircle which describes the average path.

$$= \frac{\pi d}{4} = \frac{\pi r}{2} \sin \frac{\theta}{2} \quad \text{for half length}$$

Area of path = 4a dr (4 sides to one pole)

$$dP = \frac{8\mu\, a\, dr}{\pi r \sin\frac{\theta}{2}}$$

$$d\phi_1 = H\,dP$$

$$H = \frac{(r-r_3)H_1}{r_4-r_3}$$

$$d\phi_1 = \frac{8(r-r_3)H_1\mu\, a\, dr}{(r_4-r_3)\pi r \sin\frac{\theta}{2}}$$

$$\phi_1 = \frac{8\mu\, a\, H_1}{\pi(r_4-r_3)\sin\frac{\theta}{2}} \int_{r_3}^{r_4}\left(dr - \frac{r_3 dr}{r}\right)$$

$$P_1 = \frac{8\mu a}{\pi(r_4-r_3)\sin\frac{\theta}{2}}\left[r_4 - r_3 + r_3 \ln\frac{r_3}{r_4}\right] C_f$$

$$e = \frac{a}{2\sin\frac{\theta}{2}}$$

$$r_4 = R - \frac{a}{2\sin\frac{\theta}{2}}$$

$$r_3 = \frac{ID}{2} + a - \frac{a}{2\sin\frac{\theta}{2}}$$

Derivation of Permeance Formula for P_4

$$A_1 = \left[\left(\frac{ID}{2} + a\right)^2 - \left(\frac{ID}{2}\right)^2\right] \frac{2\pi}{p} = \text{Area of 4 sections per pole}$$

$$\text{Average length base} = \frac{(ID+a)\pi}{2p}$$

$$\text{Average length} = \frac{(ID+a)(\pi)^2}{8p} \text{ for half length}$$

$$P_4 = \frac{16\mu \left[\left(\frac{ID}{2}+a\right)^2 - \frac{ID}{2}^2\right]}{\pi\,(ID+a)}$$

$$= \frac{16\mu\ [ID+a]\ a}{\pi\ (ID+a)} = \frac{16\mu\ a}{\pi}$$

$$\text{Effective } P_4 = P_4\left(\frac{\text{Average mmf}}{\text{Total mmf}}\right) = P_4\left(\frac{\text{1/2 average length base}}{\text{Magnet Length}}\right)$$

$$= \frac{16\mu\ a}{\pi}\ \frac{(ID+a)\pi}{4p\ \text{Magnet Length}}$$

$$= \frac{4\mu\ a(ID+a)}{p\ (\text{Magnet Length})}$$

Derivation of Permeance Formula for P_5

Assume that path is a complete half annulus with a center cylinder of zero diameter.

$$A_2 = \frac{(ID)\ \pi\cdot W}{p} = \text{Area of 2 paths}$$

$$\text{Average Length Base} = \frac{(ID)\pi}{2p}$$

$$\text{Average Length} = \frac{(ID)\ \pi^2}{8p} \text{ for half length}$$

$$P_5 = \frac{\mu\,(ID)\ \pi W\ \ 8P}{P(ID)\ \pi^2}$$

$$= \frac{8\mu\ w}{\pi}$$

$$\text{Effective } P_5 = P_5 \left(\frac{\text{Average mmf}}{\text{Total mmf}}\right)$$

$$= \frac{8 \mu w}{\pi} \frac{(ID)\pi}{4p(\text{Magnet Length})}$$

$$= \frac{2 \mu w ID}{p(\text{Magnet Length})}$$

Derivation of Permeance Formula for P_6

P_6 is a spherical quadrant shell with the center sphere having zero diameter.

Average thickness of shell

$$= \frac{(ID)\pi}{2p}$$

$$P = \frac{\mu (ID)\pi}{8p} \quad \text{From Rotors}$$

But area is 4 times (4 paths from one pole) and length is half (per pole basis). Therefore there is a multiplier of 8.

$$P_6 = \frac{\mu (ID)\pi}{p}$$

$$\text{Effective } P_6 = P_6 \left(\frac{\text{Average mmf}}{\text{Total mmf}}\right)$$

$$= \frac{\mu (ID)\pi}{p} \frac{(ID)\pi}{4p(\text{Magnet Length})}$$

$$= \frac{\mu (ID)^2 \pi^2}{4p^2(\text{Magnet Length})}$$

VIII. APPENDIX II

General Engineering Test Procedure

Note: Figure 1 is used for reference in Appendices II and III for terminal and component designation.

The following is the general engineering test procedure followed to determine the operation of the control circuit and verify the component values selected for the design. This test procedure was performed on the first available unit. Design changes determined to be necessary were made at this point in the program and were incorporated in all units.

The investigations were made with the motor and control connected together. Voltage was applied to the reluctance switch drive oscillators only and was not applied to the main motor windings.

A. Resistance

Make resistance check in accordance with paragraph B of General Test Procedure (Appendix III).

B. Oscillator Frequency and Base Drive

1. Connect the motor and the control together. Apply 28 volts d-c (±0.1 volts) to input terminals D and E (+ to D). Using an oscilloscope, view the waveform across saturation transformer T_1. The magnitude of 1/2 cycle should be approximately 56 volts and the frequency should be approximately 5000 cps. Using a current probe, measure the oscillator peak collector current. Calculate the required base drive and compare to the actual.

2. Repeat paragraph 1 for the second oscillator. Apply 28 volts d-c across pins F and E (+ to F) and view waveform across transformer T_2.

C. Trigger-Trimmer Adjustment

Adjust the trigger-trimmer resistors in accordance with the procedure of Part D, paragraphs 1 through 5, of the General Test Procedure, Appendix III.

D. Darlington Base Drive

Determine the base current supplied to each transistor Q_7 through Q_{12}. This is done by exciting one of the oscillators with 28 volts d-c and measuring the

base current, using a current probe, when the associated controlled rectifier just turns ON. Compare this value with that required to switch maximum current in the power transistors (approximately 2.1 amps). Also view the base emitter voltages of Q_7 through Q_{12} while rotating the motor shaft to determine sharpness of turn-on and turn-off.

Note: If any component changes are made, recheck the trigger-trimmer adjustment to determine if any shift has taken place.

E. Discussion

The above tests were made substantially as written. In addition, the firing of the SCR's in the trigger circuit was evaluated at high temperature (71°C). The tests showed the following:

1. There was a high switching spike in the oscillator of approximately 50 volts. This was clipped by changing the commutating diodes to Zener diodes.

2. The voltage firing level of the SCR's decreased appreciably at the higher temperatures. A Zener diode was added in the gate circuit of the SCR's so that the SCR fired on the breakdown voltage of the Zener rather than on its own. This stabilized the firing levels of the trigger.

3. All other parameters in the circuit were satisfactory.

IX. APPENDIX III

General Laboratory Test Procedure

A. Dielectric Tests

Test in accordance with drawings.

B. Resistance

Disconnect motor from control. Measure ohmic resistance of motor stator winding Pin AA to W, AA toY, and W to Y. Measure reluctance switch primaries Pin BB to FF, FF to DD, BB to DD, V to T, T to X, and V to X. Measure all twelve secondaries, Pin N to F, M to E, L to D, K to C, J to B, H to A, XX to RR, WW to PP, VV to NN, UU to MM, TT to LL, and SS to KK.

C. Run-In

Drive motor at approximately 1700 rpm for 4 hours. Do not apply voltage to motor.

D. Trigger-Trimmer Adjustment (Engineer to be present)

1. Connect the motor to the control.

2. It is necessary to measure the angle through which the shaft is turned to the nearest 1/4 degree. Therefore, it is necessary to lay out a circular angular scale with a pointer on the shaft.

3. The cover of the control will be removed and points brought out as directed by the engineer. Apply 28 volts d-c (±0.1 volts) to terminals D and E (+ to D).

4. Apply the output of each of the six trigger circuits in turn on a scope. Adjust the trimmer until the trigger has output for 37.5 degrees (± 0.25 degrees) of shaft rotation in any one "on" period. (The trigger will have output 4 times in one shaft revolution. If the 4 conducting periods are different in angular length, the average should be adjusted to 37.5 degrees.) The input voltage must be maintained constant during this adjustment.

5. Record the angular lengths of conduction with voltage applied to terminals E and F (+ to F). Do not change trimmer adjustment unless advised to do so by the engineer.

E. Reluctance Stator Coarse Adjustment (Engineer to be present)

1. Set both reluctance switch stators in the approximate center of their adjustment.

2. Apply 28 volts to terminals D and E. Slowly apply d-c voltage (up to 10 volts) to terminals A and B (+ to A) until motor starts to rotate. Check (as directed by engineer) which reluctance switch is excited and make a note associating the direction of rotation with that reluctance switch.

3. Lock the rotor of the motor to a suitable torque measuring device. (Maximum torque will be approximately 210 oz-in.). Hold the stator in a V-block such that it is possible to obtain 90 degrees of stator rotation by loosening the restraints. With 28 volts d-c (±0.1 volts) applied to terminals D and E and 30 volts applied to terminals A and B (current will be approximately 0.7 amp at terminals A and B), loosen the holding screw on the reluctance switch stator and adjust the excited reluctance switch until torque is a maximum in the proper direction. The torque should be constant at this maximum over an angular excursion of the reluctance switch stator of 7.5 degrees. Set the reluctance stator approximately in the center of this span.

4. Free the stator and turn in a direction to obtain maximum torque. Simultaneously adjust the reluctance stator to keep the same angular relationship with the rotor. (Turn stator 2 degrees, turn reluctance switch stator back 2 degrees, for example.) Continue until the torque is the maximum obtainable.

5. Tighten reluctance switch in place. Increase voltage at A and B to 40 volts. Move stator through measured angular increments of 5 degrees for 90 degrees recording minimum and maximum torque readings. Average the torque readings and compute the difference between the maximum and minimum torque readings.

F. Stabilization (Engineer to be present)

With the same voltages as used in the previous step and the rotor locked, adjust the motor stator until all 3 phases are excited. (Check this on a scope as directed by the engineer.) Continue turning the stator until the unit just switches out of the 3-phase conduction mode to a 2-phase conduction mode. Turn the motor stator back until the 3-phase conduction just starts again. Determine the direction of the voltage and currents in the motor stator phases at this point. Lock the rotor and stator in place. Remove all voltages and disconnect the control. Apply a variable d-c voltage to the motor stator in such a manner as to duplicate the current flow and voltage directions applied to the motor stator with the control connected. Raise the voltage until 2.1 amps are attained in

the circuit. (Do not exceed this value by any amount for any length of time.) This will require approximately 90 volts. Do this quickly to avoid overheating the stator. Once the current is obtained, immediately remove the voltage.

G. Other Reluctance Stator Adjustment

Repeat Part E, paragraphs 3 (except use 40 volts at terminals A and B), 4, and 5 for the other reluctance switch. Connect the 28-volt control voltage to terminals E and F. Repeat paragraph F.

H. Reluctance Stator Fine Adjustment

1. Repeat Part E, paragraph 5, for the reluctance switch associated with control voltage terminals F and E with the reluctance switch stator position adjusted in increments of 2 degrees until the average torque is a maximum and the ripple torque is a minimum. Turn stator 2 degrees in one direction and measure values. If the values improve, move another 2 degrees; if not, go back 4 degrees and repeat measurement. Continue adjusting in the direction of improvement until the best position is found.

2. Repeat above for the other reluctance stator (attach control voltage to terminals D and E) except repeat the zero adjustment measurements.

3. When the final adjustment is reached, repeat the torque reading at each angular position with the control voltage set at 26, 27, 28 and 29 volts.

I. Voltage Tests

1. Take speed-torque curves including no load, locked torque and 3 intermediate points with 3, 5, 10, 20, 30, 40 and 60 volts applied to terminals A and B. Take locked torque at 60 volts quickly to avoid overheating the motor. Do not allow speed to exceed 1700 rpm.

2. Place two thermocouples on the end extension of the motor winding. Read the thermocouples for stabilized temperature at 60 and 40 volts for locked torque. Also take shut-down rise by resistance. Do not exceed 200°C winding temperature.

3. As readings are taken in number 1, measure volts and amps in the control voltage circuit. Also measure the volts and amps in the d-c motor circuit and the voltage at the motor terminals. (This voltage must be measured with an oscilloscope since it varies.) Take oscilloscope pictures of main d-c motor current, voltage at the motor terminals, and current in the control circuit.

X. APPENDIX IV

Test Results

A. Dielectric Tests

Dielectric and surge tests were taken on the completed parts prior to assembly.

B. Resistance

Resistances were measured at room ambients with a Wheatstone bridge. The resistances measured include the leads from the connector to the actual parts. Resistances are given in ohms.

Motor No. 1 - Ambient Temperature = 22.5°C

Reluctance Switch

Secondaries - 9.18 to 10.44
Primary No. 1 to center tap - 1.272 - 1.279
Primary No. 1 overall - 2.391
Primary No. 2 to center tap - 1.297 - 1.298
Primary No. 2 overall - 2.492

Motor Winding

Line-to-line - 42.54 - 42.55 - 42.43

Motor No. 2- Ambient Temperature = 24°C

Reluctance Switch

Secondaries - 9.42 to 10.63
Primary No. 1 to center tap - 1.326 - 1.332
Primary No. 1 overall - 2.500
Primary No. 2 to center tap - 1.303 - 1.303
Primary No. 2 overall - 2.448

Motor Winding

Line-to-line - 42.94 - 42.92 - 42.94

C. Run-In

The motors were driven at approximately 1700 rpm for 4 hours to insure that a lubricating film was present.

D. Trigger-Trimmer Adjustment

A circular angular scale with divisions from 0 to 360 mechanical degrees was attached to the shaft of the motor. A pointer was attached to the frame of the motor so that angular excursion could be measured. A voltage of 28 volts was

applied to the control circuit. The output of each trigger was connected in turn to a scope so that the conduction period could be measured. The length of each conduction period was to be adjusted as close as possible to 37.5 mechanical degrees by measuring conduction angle while rotating the shaft and adjusting the trimmer potentiometer.

There are 4 conduction periods per revolution; consequently, it was necessary to rotate the motor one complete revolution to measure all 4 conduction periods. The same trimmer potentiometer controls all 4 conduction periods plus the 4 conduction periods for the opposite rotation which uses the other reluctance switch. Because of differences in output voltage between the secondary of the reluctance switch and between reluctance switches, it was not possible to adjust all the conduction periods to exactly 37.5 degrees. The following range was recorded after the final adjustment.

Motor No. 1 - 35 to 39.5 degrees

Motor No. 2 - 34 to 40 degrees

To check the actual switching angles of the motor, a small voltage was applied to the motor. The reluctance switches were adjusted so that the motor ran. The motor was then rotated by hand and the switching angles measured during one revolution. With the alternate 3-leg, 2-leg modes of operation, the switching points could be determined by changes in line current. The theoretical switching angle should be 7.5 mechanical degrees. This was done only on Motor No. 1 at three different values of control voltage for both directions of rotation. The following results were obtained.

Control Voltage	27	28	29
Switching Angle Range	CW 5.0 - 11.0 CCW 3.0 - 11.0	4.0 - 9.5 4.5 - 11.0	4.0 - 9.0 3.5 - 11.0

E., G., and H. Reluctance Switch Adjustment

The method described in the test procedure for these three paragraphs proved to be impractical. The actual method used was the following.

The angular scale was left attached to the shaft. A 6-inch torque arm was attached to the shaft so that the other end rested on a scale. The control was excited at 28 volts and 30 volts was applied to the motor. The motor stator was mounted in a V-block such that it could be loosened and turned through 90 mechanical degrees by hand. The motor was rotated slowly by hand through 90 degrees while the minimum and maximum torque was read on the scale. Each reluctance switch was then adjusted in fine increments until minimum ripple was obtained.

F. Stabilization

Stabilization of the magnets was accomplished exactly as described in the test procedure.

H. Final Readings After Reluctance Switch Adjustment and Stabilization

Locked torque readings were taken using the same set-up by leaving the torque arm on the scale and rotating the stator by hand. Readings were taken every 2 degrees through 90 degrees including the minimum and maximum torque. The average torque was obtained by averaging all the readings. Peak-to-peak ripple torque was the difference between the highest and lowest readings.

The first readings were taken with a motor voltage of 40 volts with the control voltage varied. The temperature recorded was the temperature indicated by a thermocouple mounted to the end extension of the motor at the start of the run.

Motor No. 1

Rotation	Motor Line Volts	Motor Line Amps Hi	Motor Line Amps Lo	Temp. °C	Control Volts	Control Amps Hi	Average Torque (oz-in)	Ripple Torque (oz-in)
CW	40.0	0.99	0.74	66.5	30.0		101.6	13.2
CW	40.0	0.99	0.74	65.0	29.0		102.4	17.4
CW	40.0	0.99	0.74	67.5	28.0		100.3	19.2
CW	40.0	0.99	0.74	65.0	27.0		101.7	18.6
CW	40.0	0.99	0.74	65.0	26.0	Motor went completely off.		
CCW	40.0	0.99	0.74	66.5	29.0		102.2	14.0
CCW	40.0	0.99	0.74	66.0	28.0	0.079	100.5	14.4
CCW	40.0	0.99	0.74	66.5	27.0		101.0	15.0
CCW	40.0	0.99	0.74	66.5	25.5	Motor went completely off.		

Motor No. 2

CW	40.0	1.0	0.75	66.5	28.0	0.071	98.2	22.8
CCW	40.0	1.03	0.76	67.5	28.0	0.078	101.8	15.0

Motor terminal volts was recorded at 38.5 volts indicating a 1.5 volt drop in the switches.

I. Voltage Tests

Locked torque readings at various voltages were taken similar to the previous paragraph for the speed torque curves. Data was taken only on Motor No. 1 in a CCW direction. Control voltage was held constant at 28.0 volts.

Motor Line Volts	Motor Terminal Volts	Motor Line Amps Hi	Lo	Temp. °C Start	Finish	Control MA Hi	Lo	Average Torque	Peak Ripple
3.0	1.6	0.05	0.04	22.5	22.5	78.0	78.0	*4.22	*2.4
5.0	3.6	0.11	0.088	23.5	23.5	77.0	77.0	5.11	2.4
10.0	8.4	0.255	0.198	23.5	23.5	77.0	77.0	19.52	4.2
20.0	18.6	0.56	0.42	34.0	35.0	79.0	78.0	49.9	8.4
30.0	28.4	0.79	0.60	49.0	-	78.0	76.0	74.6	14.4
60.0	58.0	1.40	1.08	82.0	94.0	77.0	75.0	133.0	19.2

Speed torque curves at the various voltages were taken on Motor No. 1 in a CCW direction. A torque arm was loosely attached to the shaft. Torque was adjusted by tightening the torque arm. The friction torque thus obtained was measured on a scale. Control voltage was held constant at 28.0 volts. Control current stayed constant at 78.0 MA. The recorded temperature was the thermocouple reading at the end of the run.

Line Voltage	Line Amps	Torque oz-in	RPM	Temp. °C
3.0	0.035	0.0	4.36	24.0
3.0	0.035	0.3	3.81	24.0
3.0	0.035	0.6	2.93	24.0
5.0	0.038	0.0	28.0	24.0
5.0	0.039	0.3	26.0	24.0
5.0	0.054	1.8	19.0	24.0
5.0	0.072	4.2	10.5	24.0
10.0	0.043	0.0	85.0	24.0
10.0	0.080	4.5	66.0	24.0
10.0	0.125	9.6	44.0	24.0
10.0	0.172	15.3	24.8	25.0
10.0	0.197	18.6	11.3	25.0

*Note: Starred values appear to be considerably in error.

Line Voltage	Line Amps	Torque oz-in	RPM	Temp. °C
20.0	0.048	0.0	199.0	25.0
20.0	0.134	10.5	150.0	26.0
20.0	0.234	22.2	109.0	27.0
20.0	0.355	36.6	60.0	27.0
20.0	0.430	45.9	24.0	27.0
30.0	0.050	0.0	317.0	27.5
30.0	0.284	27.6	205.0	28.5
30.0	0.425	44.4	144.0	29.5
30.0	0.60	64.5	73.0	33.5
30.0	0.65	72.0	28.0	35.0
40.0	0.055	0.0	428.0	39.0
40.0	0.380	39.0	265.0	40.0
40.0	0.66	72.6	143.0	43.0
40.0	0.75	82.5	98.0	45.0
60.0	0.065	0.0	642.0	54.0
60.0	0.70	72.0	*520.0	56.0
60.0	0.93	102.0	207.0	57.5

The following was taken on Motor No. 2 in a CW direction. Control current was constant at 0.071 amps.

40.0	0.041	0.0	423.0	47.0
40.0	0.341	36.0	*214.0	47.0
40.0	0.65	72.0	120.0	48.0
40.0	0.78	88.0	60.0	49.5

The following no-load reading was taken on Motor No. 2 in a CCW direction. Control current was 0.077 amps.

40.0	0.053	0.0	436.0	46.0

Additional Tests

1. Stabilized winding temperatures were read both by the shut-down resistance method and by two thermocouples attached to the motor end extensions. Tests were taken with locked rotor at 40 and 60 volts on Motor No. 1. The motor was mounted in a micarta V-block in free air for the tests. Room ambient was approximately 25°C.

*Note: Starred values appear to be considerably in error.

Line Voltage	Temp. by Resistance	Thermocouple No. 1	Thermocouple No. 2
40.0	90.5	77.5	75.0
	Final line current = 0.95 amps		
60.0	143.0	122.0	118.5
	Final line current = 1.24 amps		

2. Static friction or breakaway torque was measured with a spring scale at 2.5 oz-in.

3. Motor weight = 3.4 lbs.
Control weight = 1.4 lbs.

4. With Motor No. 2 operating at no load (unless otherwise specified) with a line voltage of 40 volts and a control voltage of 28 volts, pictures were taken of various voltages and currents in the circuit. These are shown in the following illustrations.

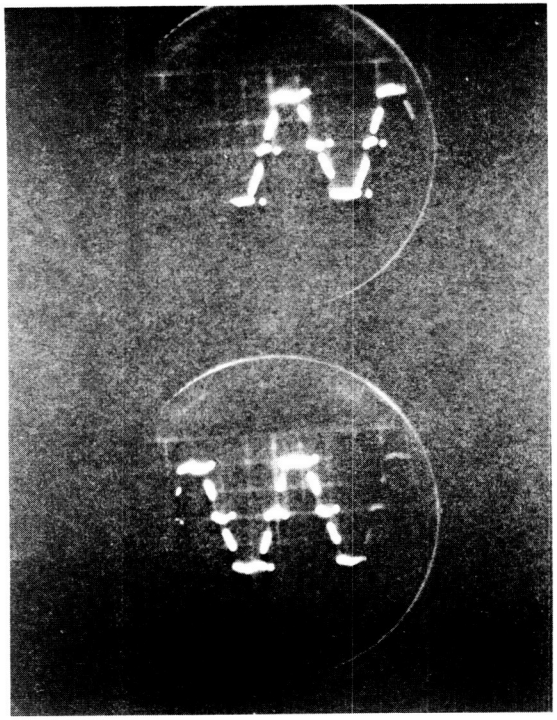

FIGURE 27. Line-to-Line Voltage at Motor Terminals
20 V/cm
Top - CW
Bottom - CCW

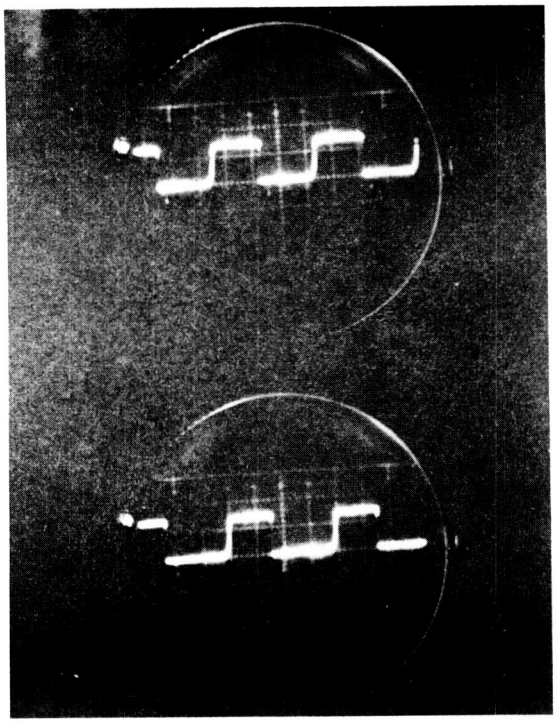

FIGURE 28. Base-Emitter Voltage on Darlington Transistor
0.5 V/cm
Top - CW
Bottom - CCW

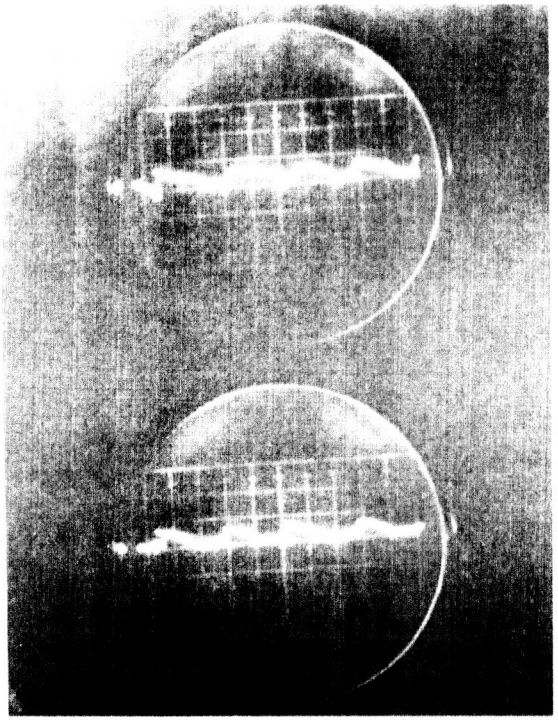

FIGURE 29. Line Current at No-Load
Top - CCW - 0.05 average amps
Bottom - CW - 0.04 average amps

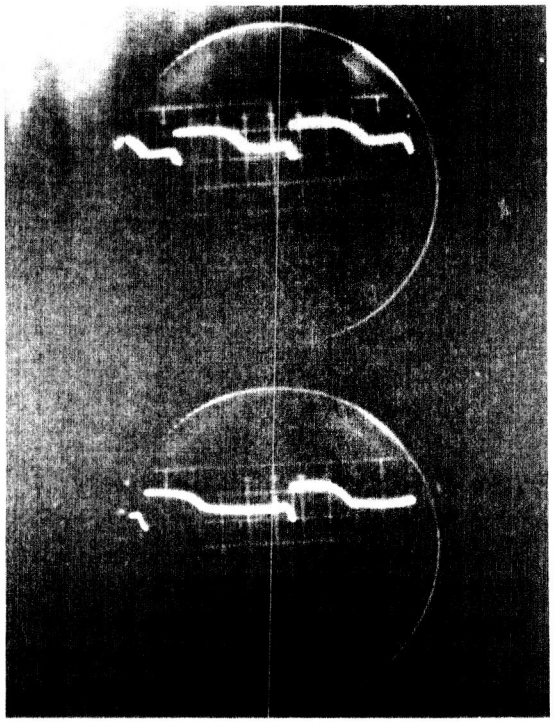

FIGURE 30. Line Current at Load
Top - CCW - 0.5 average amps
Bottom - CW - 0.5 average amps

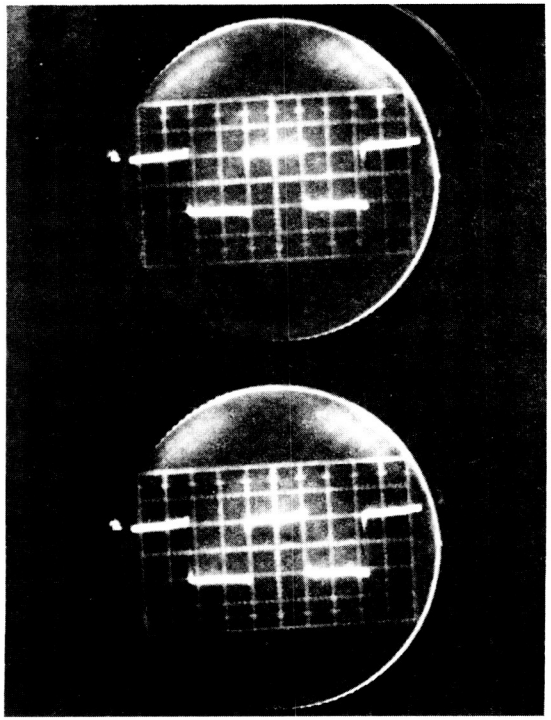

FIGURE 31. Oscillator Voltage
50.0 V/cm
50.0 micro sec/cm
Top-Bottom same

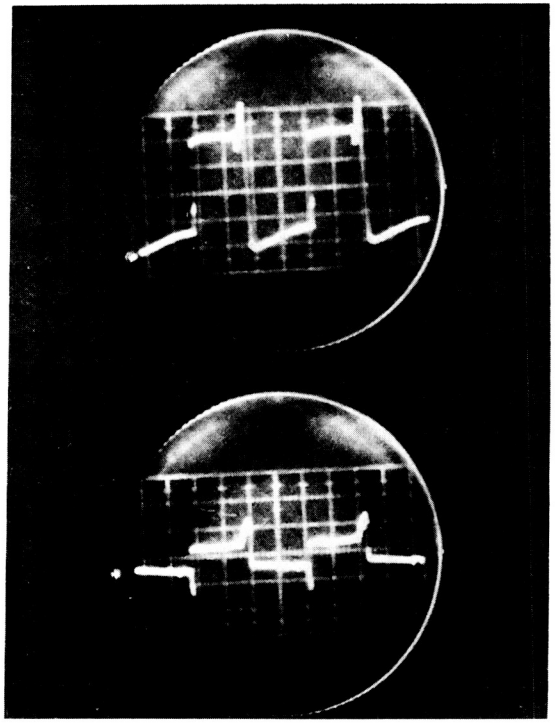

FIGURE 32. Reluctance Switch Secondary Output Voltage
5.0 V/cm
Top - Coupled
Bottom - Uncoupled

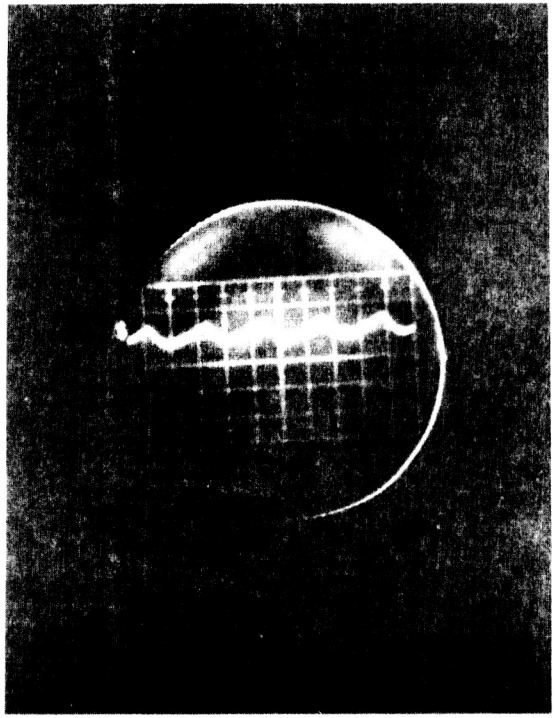

FIGURE 33. Voltage Across 464 Ohm Series Resistor in Control Filter Circuit (Measures drive current) 5.0 V/cm

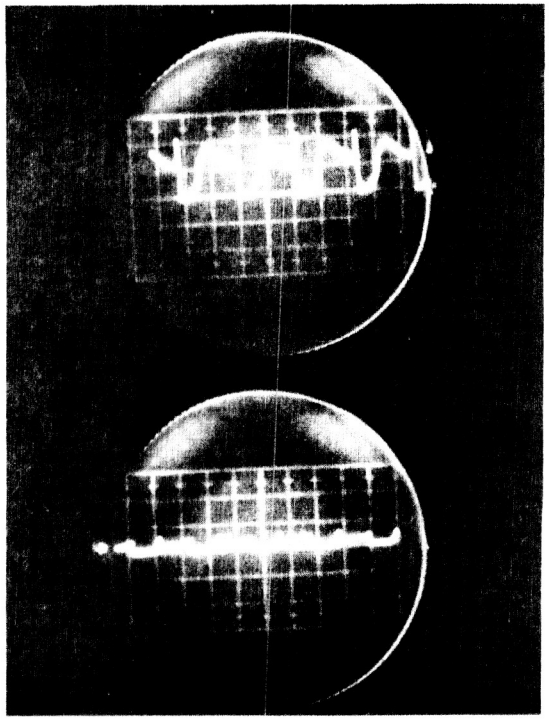

FIGURE 34. Trigger Voltage at Input to Trigger
5.0 V/cm
Top - Coupled
Bottom - Uncoupled

XI. APPENDIX V

Westinghouse Research Laboratories

Report on Solid-Lubricant Bearings

Note: This report is a typed copy of the original written by Westinghouse Research Laboratories.

Research Memo 64-8B5-347-M1 December 3, 1964

SELF-LUBRICATED TORQUE MOTOR BEARINGS FOR ULTRA-HIGH VACUUMS

D. J. Boes & G. R. Kelecava
Chemical Technology
Insulation & Chemical Technology R&D

INTRODUCTION

Sixteen ball bearings were equipped with high strength, self-lubricating retainers for use in an ultra-high vacuum of 10^{-9} torr under interworks requisition #39G1-338904. The work was sub-contracted by Lima AED under NASA contract NAS5-3934 from Goddard Space Flight Center. Prior to the fabrication and installation of the retainers, a short laboratory program was conducted to establish:

1. The optimum self-lubricating composite formulation from a mechanical strength consideration, and

2. the outgassing characteristics at 70°C and 10^{-9} torr of the candidate materials.

The dry lubricated bearings are to be used in a torque motor capable of prolonged operation in an ultra-high vacuum environment. They are required to meet the following specifications:

1. 0 to 100 RPM - inner race rotation with majority of life near zero RPM.

2. Rotor weight - 1 lb.

3. Shock - 50 G's of 2 millisecond duration in each of three mutually perpendicular directions.

4. Vibration - 5 minutes of random vibration from 20 to 2000 CPS at 15 G's RMS in each of three mutually perpendicular directions.

   Peak Force = 21.2 lbs. total on two bearings.

5. Vacuum of 10^{-9} mm Hg for a period of one year.

6. Ambient Temperature: -10 to +70°C.

7. Bearings to have minimum static friction torque.

SUMMARY

The sixteen bearings were equipped with a high strength self-lubricating composite retainer composed of a sintered silver-mercury amalgam matrix containing homogeneously distributed pockets of Teflon (PTFE). Screening tests indicated that for maximum mechanical strength both the Teflon and silver powder - before amalgamation - should consist of equal parts of sub-micron and coarse particles (PTFE-100 mesh; Ag-325 mesh). The blanks from which the retainer were machined were formed under a combination of heat and pressure into 1 1/2" long rings 1 1/2" O. D. x 3/4" I. D. The retainers were not shrouded and weighed approximately 20 grams each.

EXPERIMENTAL

Bearing Design

The MRC-1905 bearings selected for this application are an extremely thin series of an ABEC-1 non-precision grade. It was decided to employ as a retainer material a composite of maximum mechanical strength in view of (1) the high shock loading and vibration which the bearing must withstand, (2) the small cross-section of the ball retainer resulting from the narrow bearing design, and (3) the inability to encase the retainer in a reinforcing metal shroud.

Retainer Composition

As mentioned previously, it was necessary to determine the optimum retainer composition prior to fabrication. This was achieved by evaluating the friction, wear and mechanical properties of a number of candidate compositions of the silver-mercury type. A prior in-house program had already demonstrated that this composite exhibited the highest mechanical strength of the available Westinghouse self-lubricating materials. It was necessary, however, to establish what adjustments were necessary in the (1) particle size of composite components, (2) Teflon content, and (3) solid lubricant content that would provide a material best qualified to meet the unique requirements of the proposed application. A series of experiments were conducted to define the effect of the parameters on composite performance. Teflon and solid lubricant content was varied from 0-25% (vol) and 0-5% respectively. In addition, two particle size distributions were investigated for both Teflon and silver. All test specimens

were 1/2" dia x 1" long and fabricated at 260°C under a load of 60,000 psi. Holding time at temperature and pressure was 3 minutes. Optimum conditions of fabrication had been established during the previous program.

Outgassing Tests

In order to establish that the 70°C/10^{-9} torr environment to which the bearings will be subjected would not cause appreciable material losses through evaporation, outgassing tests were run on four composite formulations. The samples were held at 70°C and 10^{-6} torr for one week, after which the pressure was reduced to 10^{-9} torr by means of a cryopump and maintained for 72 hours. Following this period, the specimens were removed from the vacuum chamber and weight loss measurements made.

RESULTS

Table 1 lists the various material combinations studied in the optimization program and the effect of particle size and lubricant concentration on friction, wear and tensile strength characteristics.

The following pertinent points were brought out by these experiments.

Mechanical Properties

1. Tensile strengths vary inversely with the quantity of Teflon incorporated in the composite.

2. For a given composition, the substitution of as little as 5% solid lubricant (WSe_2) as a replacement for a corresponding amount of PTFE causes a substantial reduction in tensile strength.

3. Composites incorporating 325 mesh silver are at least 50% lower in tensile than a corresponding composition using a 50-50 combination of 325 mesh and sub-micron silver.

4. Maximum tensile strengths are obtained when the particle size distribution for both silver and PTFE is evenly split between submicron and 325 or 100 mesh respectively.

Lubricating Properties

1. The use of small quantities of solid lubricant (WSe_2-5%) resulted in a substantial reduction in friction coefficients.

2. Increasing PTFE contents did not improve appreciably composite friction coefficients at either 530 or 940 psi loads.

3. Low tensile properties do not result in a corresponding increase in composite wear rate.

Based on this information, a composite containing 15% (vol) PTFE in a silver-mercury amalgam matrix (No. 12-Table 1) was selected as that offering the best combination of properties for the proposed application. The authors do not believe the excessive wear rates experienced by this composite at 940 psi will cause any difficulty in view of the low bearing loads ($\sim$1 lb.) and speeds (0 to 100 RPM) involved. In this particular case, the more important consideration is the ability of the self-lubricating composite to carry moderate loads and withstand severe shock loadings. The physical properties of this material are given in Table 2.

The results of the outgassing experiments are given in Table 3. None of the four samples evaluated showed any significant weight loss from the exposure. The ability of these materials to successfully withstand ultra-high vacuum-moderate temperature environments has also been demonstrated during 100 hour functional tests at 10^{-8} torr on roller bearings utilizing these composites as retainers. The bearings carried a 3000 lb. load at 100 RPM and a temperature of 50°C. Bearing wear was negligible during the 100 hour run.

MRC-1905 Retainer Design & Fabrication

Figure 1 presents a detailed drawing of the bearing retainer and the bearing dimensions pertinent to its design. It is an inner race riding cage containing eleven ball pockets, and is designed to provide a 0.005 inch diametral clearance between its inner diameter and the O.D. of the inner race. Figure 2 is a photograph of the machined retainer and an assembled 1905 ball bearing utilizing the retainer as the self-lubricating member.

Ins. & Chem. Tech. R&D - Chemical Technology - D. J. Boes
- G. R. Kelecava

TABLE 1. Friction-Wear-Mechanical Strength of Silver/Mercury Composites
(80 Ag-20 Hg)

Sample No.	Composition-Vol % Alloy	PTFE	WS_2	Particle Size-Mesh	Tensile Strength (psi)	530 psi Fric. Coef.	530 psi Wear gm/hr	940 psi Fric. Coef.	940 psi Wear
1	100	--	--	Ag- 1/2-1/2*	35,450	--	--	0.52	0.008
2	85	15	--	Ag- 1/2-1/2 PTFE 100	5,650	0.15	0.005	0.18	0.003
3	80	20	--	Ag- 1/2-1/2 PTFE 100	4,650	0.23	0.004	0.18	0.002
4	75	25	--	Ag- 1/2-1/2 PTFE 100	3,150	0.19	0.006	0.22	0.003
5	80	15	5	Ag- 1/2-1/2 PTFE 100	3,800	0.13	0.002	0.22	0.005
6	75	20	5	Ag- 1/2-1/2 PTFE 100	2,650	0.14	0.003	0.13	0.003
7	85	15	--	Ag-325 PTFE 100	2,450	0.21	0.008	0.20	0.016
8	80	20	--	Ag-325 PTFE 100	2,100	0.21	0.001	0.26	0.002
9	75	25	--	Ag-325 PTFE 100	1,400	0.23	0.002	0.17	0.002
10	80	15	5	Ag-325 PTFE 100	2,700	0.13	0.006	0.18	0.004
11	75	20	5	Ag-325 PTFE 100	600	0.16	0.003	0.15	0.008
12	85	15	--	Ag- 1/2-1/2 PTFE 1/2-1/2**	7,600	0.21	0.001	0.22	>0.5

*50% 325 mesh-50% sub-micron
**50% 100 mesh-50% sub-micron

TABLE 2. Physical Property Data on Self-Lubricating Retainer

Composition- Vol %	85 Alloy (80 w/o Ag-20 w/o Hg) 15 PTFE
Particle Size Distribution	Silver - 50 w/o 325 mesh 50 w/o sub-micron PTFE - 50 w/o 100 mesh 50 w/o sub-micron
Pressing Conditions	260 C - 60,000 psi - 3 min hold on 1/2" Ø
Tensile - psi	7600
Shear - psi	7325
Flex. Modulus - psi	4.4×10^6
Coef. Thermal Expansion (75° to 300°F)	11.62×10^{-6} inch/inch °F
Friction Coefficient*	
170 psi	0.17
530 psi	0.21
940 psi	0.22
Wear - gm/hr - (30 min run)	
170 psi	0.002
530 psi	0.001
940 psi	.5

*Measured on Westinghouse Hydrostatic Friction-Wear Tester Against 440-C Stainless Steel.

TABLE 3. Composite Outgassing Tests

	Sample Description	Initial Wt. (Grams)	Final Wt. (Grams)
1.	85% AgHg (1/2-1/2)-15% PTFE (100 mesh)	0.6502	0.6500
2.	85% AgHg (1/2-1/2)-15% PTFE (1/2-1/2)	0.6871	0.6870
3.	80% AgHg (1/2-1/2)-20% PTFE (100 mesh)	0.6815	0.6815
3.	80% AgHg (1/2-1/2)-20% PTFE (1/2-1/2)	0.7712	0.7711

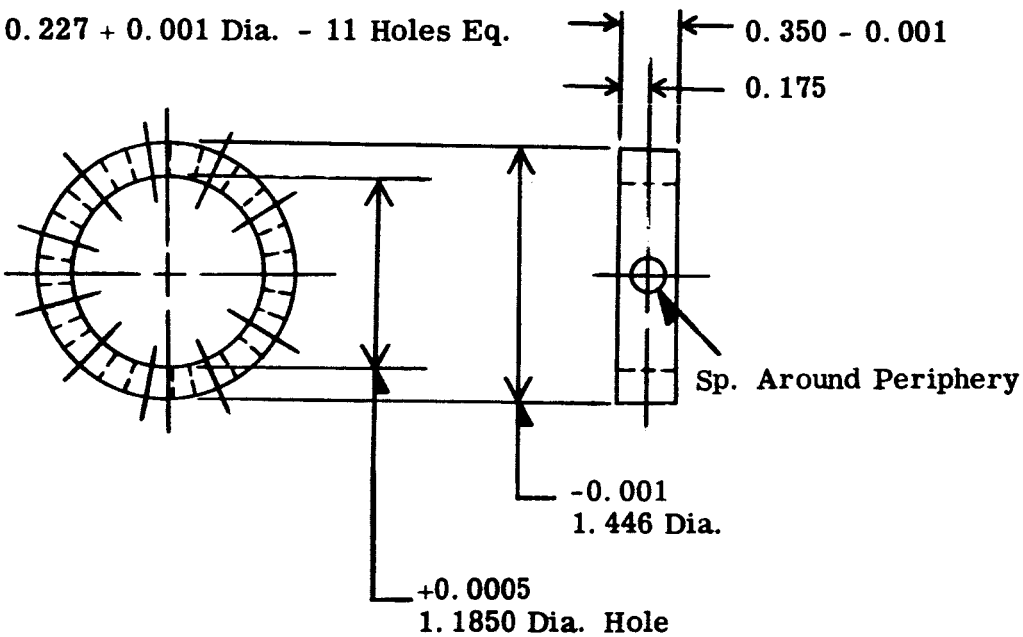

1905 Bearing Dimensions

Outer Race O.D.	= 1.653
Outer Race I.D.	= 1.468
Inner Race O.D.	= 1.180
Inner Race I.D.	= 0.9843
Ball Dia.	= 0.2185
Width	= 0.355

FIGURE 1. Self-Lubricating Cage Design - MRC-1905 Ball Bearing

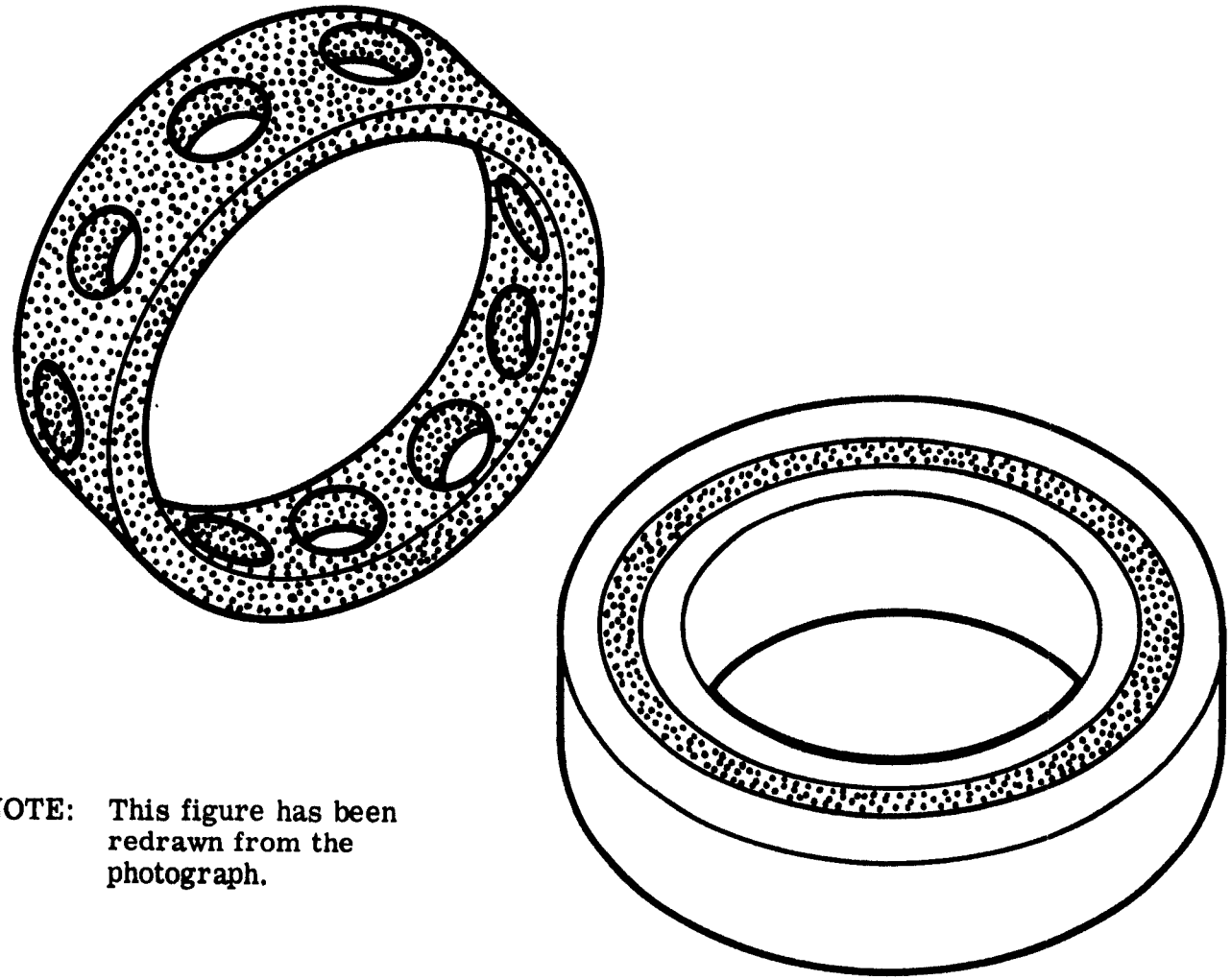

NOTE: This figure has been redrawn from the photograph.

FIGURE 2.